2009

"DESIGN AND SYNTHESIS OF MOLECULAR PROBES FOR THE STUDY OF 5-HT2A AND H1 RECEPTORS"

Jitesh shah
Virginia Commonwealth University

DESIGN AND SYNTHESIS OF MOLECULAR PROBES FOR THE STUDY OF 5-HT_{2A} AND H_1 RECEPTORS

A Dissertation submitted in partial fulfillment of the requirements for the degree of Doctor of Philosophy at Virginia Commonwealth University.

by

JITESH R. SHAH
MS in Pharmaceutical Sciences, University of Mumbai, India, 2003
BS in Pharmacy, University of Mumbai, India, 2001

Director: RICHARD B. WESTKAEMPER
PROFESSOR, DEPARTMENT OF MEDICINAL CHEMISTRY

Virginia Commonwealth University
Richmond, Virginia

Aug 2009

Acknowledgements

First and foremost, I would like to thank my advisor Richard B. Westkaemper for his guidance and support during the entire tenure of my work. He is a great teacher and a brilliant scientist. His broad scientific knowledge and approach towards basic research has been a true inspiration for me. I am grateful to him for his encouragement to apply for the dissertation assistantship in my final semester.

I would also like to thank my committee members, Dr. Richard Glennon, Dr. Glen Kellogg, Dr. Vladimir Sidorov and Dr. Susan Robinson. This committee has greatly contributed to my scientific knowledge and has always been available for suggestions. I would like to thank Professor Glennon for participating in some of our group meetings and giving a valuable insight into the drug design aspects. I am thankful to Dr. Sidorov for his advice in the chemistry related to my project. I am glad to have Dr. Kellogg on my committee, who has always been there for ideas in the molecular modeling work.

I wholeheartedly thank the postdoctoral scholars Dr. Srinivas Peddi, Dr. Gajanan Dewkar and Dr. Philip Mosier in Westkaemper's group. It has been a great experience to work with these talented individuals in my graduate career. Srini and Gajanan have been my mentors in laboratory. They have given me the true guidance and support in my work. Srini was always available for discussions regarding my project. I am gratified to have Gajanan as a chemist in our lab; he has taught me some of the most valuable lessons in

organic chemistry. I am also greatly indebted to Phil. He has guided me throughout my project and shown tremendous patience in teaching me various aspects of molecular modeling. I thank my fellow students Donna McGovern and Justin Pitts for helping me out with my work whenever needed.

Besides Dr. Westkaemper's group, I would like to thank Dr. Umesh Desai, Dr. Keith Ellis and Dr. John Hackett for their support. Dr Desai has always provided moral support and guidance when needed. Dr. Ellis and Dr. Hackett have been kind enough to guide me for the postdoctoral applications. I sincerely appreciate the guidance and support given by Arjun Raghuraman a good friend and a mentor in my graduate studies. I wholeheartedly thank all my friends Jay, Santosh, Parthasarathy, Anil, Sagar, and Jay Patel for their support and care.

Finally, I would like to thank my parents Asha and Rameshchandra Shah for their unwavering support and blessings throughout my career and years ahead. I also thank my brother Rupesh and sister-in-law, Nutan for their love and prayers. This dissertation would not be possible without the help of my friends and well-wishers whom I deeply thank.

Table of Contents

Page

Acknowledgements ii

List of Tables viii

List of Figures ix

List of Schemes xi

List of Abbreviations xii

Abstract xv

Chapter

1 INTRODUCTION 1

1.1 The Discovery of Serotonin 1

1.2 Serotonin Biosynthesis and Metabolism 2

1.3 Classification of Serotonin Receptors 2

1.4 Serotonin Receptors: Clinical Significance 6

1.5 5-HT_2 Receptor Structure, Function and Localization 7

1.5.1 5-HT_2 Receptors in the Development of Novel Antidepressant Drugs 9

1.5.2 5-HT_2 Selective Antagonists as Potential Antipsychotic Drugs 10

1.5.3 5-HT_2 Ligands in the Treatment of Schizophrenia 11

1.5.4 5-HT_2 Ligands in the Treatment of Sleep Disorders 12

1.6 Clinical Relevance for Studying 5-HT_{2A} and H_1 Receptor Binding 14

1.7 5-HT_2 Receptor Ligands 17

1.8 Understanding 5-HT_{2A} Receptor-Ligand Interactions and Development of a Selective GPCR Ligand……...20

1.9 Specific Aims of the Research Project……...21

2 MOLECULAR MODELING OF G PROTEIN-COUPLED RECEPTORS .. 22

2.1 Introduction 22

2.2 Central Role of G Proteins 23

2.3 Common Structural Features of GPCRs 23

2.4 Challenges in GPCR Research 26

2.4.1 Why are there only a Few Experimental Structures of GPCRs?..28

2.5 Homology (Comparative) Modeling as a Workable Solution…….....28

2.5.1 Bovine Rhodopsin and β_2-Adrenergic Receptor Structures as Suitable Templates for Homology Modeling……29

2.6 Construction of Homology Models……....36

2.6.1 Docking and Scoring……36

3 STRUCTURE-AFFINITY RELATIONSHIP STUDIES OF AMDA AND ITS ANALOGS AT 5-HT_{2A} AND H_1 RECEPTORS……38

3.1 Introduction…….....38

3.2 Results and Discussion……...41

3.2.1 Structure-Affinity Relationship Studies…….. ……41

3.2.2 Modeling Receptor-Ligand Interactions: H_1 and 5-HT_{2A} Receptor Models ……45

3.2.3 Binding Mode Analysis……..48

3.2.4 Chemistry……...54

3.3 Synthetic Schemes……56

3.4 Molecular Modeling……59

3.4 Conclusions……...60

4 RING-ANNULATED AND *N*-SUBSTITUTED ANALOGS OF AMDA AS STRUCTURAL PROBES FOR 5-HT_{2A} AND H_1 RECEPTORS……61

4.1 Introduction……..61

4.2 Substituted Phenylalkylamine Analogs of AMDA as Structural Probes….62

4.3 Ring-Annulated Analogs of AMDA as Dimensional Probes ……..63

4.4 Molecular Modeling Studies……65

4.5 Chemistry…….70

4.6 Synthetic Schemes……...70

4.7 Conclusions……72

5 ENGINEERING A SELECTIVE NON-NITROGENOUS AMINERGIC GPCR LIGAND…….73

5.1 Introduction……73

5.2 Hypothesis Based on the Homology Modeling and Reported Site-directed Mutagenesis Studies……74

5.3 Strategy for the Design of a Selective H_1 Ligand……...77

5.4 Results and Discussion……...80

5.4.1 Structure-Affinity Relationship Studies ……....80

5.4.2 Modeling Interactions……....82

5.4.3 Chemistry……..86

5.5 Synthetic Schemes……87

5.6 Conclusions……..90

6 SUMMARY……91

7 EXPERIMENTALS……...93

7.1 Chemistry……..93

7.2 Molecular Modeling……138

RFERENCES……...142

List of Tables

Page

Table 1: Serotonin Receptors Classification. 4

Table 2: Mental Illness where Altered Serotonin Neurotransmission has been Implicated……...6

Table 3: Common Medical Conditions in which 5-HT-Subtype-Selective Drugs have Utility……7

Table 4: Histamine Receptors Classification…….....14

Table 5: Observed Binding Affinities for 9-(aminoalkyl)-9,10-dihydroanthracene (DHA) and Diphenylalkylamine (DPA) Analogs at 5-HT_{2A} and H_1 Receptors……..43

List of Figures

Page

Figure 1: Biosynthesis and Metabolism of Serotonin 3

Figure 2: Scaled Phylogenetic Tree Comparing Human Receptors with Bovine Rhodopsin 5

Figure 3: Distribution of 5-HT_{2A} and 5-HT_{2C} Receptors on GABA-containing and Dopamine Containing Neurons in the Midbrain……10

Figure 4: Serotonergic Regulation of Sleep-Wakefulness Cycle..... 13

Figure 5: Structures of Representative H_1 Antagonists..... 15

Figure 6: Structures of Representative 5-HT_2 Ligands 19

Figure 7: Role of G Proteins 24

Figure 8: GPCRs Structure and Receptor-Ligand Interactions..... 27

Figure 9: Superimposition of the 5-HT_{2A} GPCR Models Based on β_2-AR and Rhodopsin Crystal Structures 33

Figure 10: 3D Bar Graph Showing the Affinities at 5-HT_{2A} and H_1 for the 9-(aminoalkyl)-9,10-dihydroanthracene (DHA) and Diphenylalkylamine (DPA) Analogs... 44

Figure 11: Alignment of the Human β_2-Adrenergic, H_1 and 5-HT_{2A} Receptor Sequences 47

Figure 12: Illustration of the Differences in Binding Site Residue Composition of the H_1 and 5-HT_{2A} Receptors within the Context of the β_2AR-T4L Crystal Structure Docked Receptor-Ligand Complexes……...51

Figure 13: Docked Receptor Ligand Complex 52

Figure 14: HINT Interaction Maps for Compound **9** 53

Figure 15: Binding Affinity Data of AMDA Analogs as Molecular Probes 65

Figure 16: Proposed Binding Mode of Phenylalklyamine analogs of AMDA in 5HT_{2A} and H_1 Receptor……67

Figure 17: Proposed Binding Mode of Quaternary ammonium salt of AMDA in H_1 Receptor……68

Figure 18: Proposed Binding Mode of Isomers of Ring-Annulated AMDA Analogs…...69

Figure 19: Probes for the Design of Selective GPCR Ligands ..... …79

Figure 20: Docked Poses of Olapatadine and Compound **34** 84

Figure 21: HINT Interaction Maps for Compound **34** in H_1 Binding Sites 85

List of Schemes

Scheme 1: 56

Scheme 2: 56

Scheme 3: 56

Scheme 4: 57

Scheme 5: 57

Scheme 6: 57

Scheme 7: 58

Scheme 8: 58

Scheme 9: 58

Scheme 10:……70

Scheme 11:……71

Scheme 12:……71

Scheme 13:……87

Scheme 14:……88

Scheme 15:……88

Scheme 16:……88

Scheme 17:……89

Scheme 18:……89

List of Abbreviations

Å	Angstroms
AC	Adenylate cyclase
AcOH	Acetic acid
$AlCl_3$	Aluminium chloride
AMDA	9-(Aminomethyl)-9,10-dihydroanthracene
ASP	Astex statistical potential
Asp	Aspartate
br	Broad
BH_3	Borane
BRHO	Bovine rhodopsin
°C	Degree Celsius
Calcd	Calculated
CCl_4	Carbon tetrachloride
cAMP	Cyclic 3', 5'-adenosine monophosphate
$CDCl_3$	Duetereted chloroform
$CHCl_3$	Chloroform
CH_3OH	Methanol
CH_3SO_3H	Methanesulfonic acid
CH_2Cl_2	Methylene chloride
CNS	Central nervous system
d	Doublet
DAG	Diacylglycerol
DIBAL-H	Diisobutylaluminium hydride
DMSO-d_6	Deuterated Dimethyl sulfoxide
DA	Dopamine
DHA	Dihydroanthracene
DPA	Diphenyl amines
DMF	Dimethylformamide
Et_2O	Diethyl ether
ESIMS	Electrospray ionization mass spectrometry
EC_{50}	Activation Concentration (half-maximal effect)
EtOH	Ethanol
EtOAC	Ethyl acetate
EL	Extracellular loop
$Fe(NO_3)$	Ferric nitrate
GABA	γ-Aminobutyric acid
GDP	Guanine nucleotide guanosine diphosphate

GTP	Guanine nucleotide guanosine triphosphate
GPCR	G Protein-coupled receptors
GOLD	Genetic optimization for ligand docking
GI	Gastrointestinal
HBr	Hydrobromic acid
HCl	Hydrochloric acid
5-HT	5-Hydroxytryptamine
5-HTP	5-Hydroxy tryptophan
5-HIAA	5-Hydroxyindole acetic acid
HINT	Hydropathic INTeractions
H_1	Histamine
H_2SO_4	Sulfuric acid
HTS	High throughput screening
K_i	Dissociation constant
K	Potassium
KI	Potassium iodide
K_3PO_4	Potassium phosphate
KCN	Potassium cyanide
KOH	Potassium hydroxide
KOR	Kappa-opioid receptor
liq	Liquid
LAH	Lithium aluminium hydride
$LiAlH_4$	Lithium aluminium hydride
LHMDS	Lithium hexamethyldisilazide
LSD	Lysergic acid diethylamide
$MgSO_4$	Magnesium sulfate
MeCN	Acetronitrile
MeOH	Methanol
ml	Milliliter
mmol	Millimolar
mp	Melting Point
$MeNO_2$	Nitromethane
m	Multiplet
MAO	Monoamino oxidase
n-BuLi	n-Butyllithium
NBS	N-bromosuccinimide
nM	Nanomolar
NMR	Nuclear magnetic resonance
Na	Sodium
NaOH	Sodium hydroxide
NaOCl	Sodium hypochlorite
$NaClO_2$	Sodium chlorite
$NaBH_4$	Sodiumborohydride

$NaBH_3CN$	Sodium cyanoborohydride
NEt_3	Triethylamine
NREMS	Non-rapid eye movement sleep
NH_4OH	Ammonium hydroxide
NRD	Nucleus raphe dorsalis
Pd/C	Palladium on carbon
PDB	Protein data bank
$Pd(PPh_3)_4$	Tetrakis (triphenylphosphine) Palladium
PBr_3	Phosphorus tribromide
PET	Positron emission tomography
PI	Phosphatidylinosital
PPA	Polyphosphoric acid
p-TsOH	p-Toluenesulfonic acid
QSAR	Quantitative structure activity relationship
RMSD	Root mean square deviation
rt	Room temperature
s	singlet
SAFIR	Structure affinity relationship
SERT	Serotonin transporter
SN	Substantia niagra
SWS	Slow wave sleep
SAFIR	Structure-affinity-relationships
SAR	Structure activity relationship
$SOCl_2$	Thionyl chloride
t	Triplet
TBAF	Tetra-n-butylammonium fluoride
TBDMS	tert-Butyldimethylsilyl ether
TEMPO	2,2,6,6-Tetramethylpiperidinyloxy
t-BuOK	Potassium *tert*-butoxide
$Ti(O^iPr)_4$	Titanium isopropoxide
THF	Tetrahydrofuran
TLC	Thin-layer chromatography
TM	Transmembrane
TMSCN	Trimethylsilyl cyanide
VTA	Ventral tegmental area
ZnI	Zinc iodide

Abstract

DESIGN AND SYNTHESIS OF MOLECULAR PROBES FOR THE STUDY OF 5-HT_{2A} AND H_1 RECEPTORS

By Jitesh R. Shah, PhD

A Dissertation submitted in partial fulfillment of the requirements for the degree of Doctor of Philosophy at Virginia Commonwealth University.

Virginia Commonwealth University, 2009

Major Director: Richard B. Westkaemper
Professor, Department of Medicinal Chemistry

The serotonin (5-HT) receptors, with seven subtypes and at least fifteen distinct members, mediate a wide range of physiological functions both in the central nervous system and in the periphery.[1,2] All members of the 5-HT family except the 5-HT_3 subtype belong to the family of aminergic G protein-coupled receptors (GPCRs).[3] Over the years, various molecules have been reported which act selectively at 5-HT_2 receptors.[4] However, there are no ligands that exhibit complete selectivity for one subpopulation of 5-HT_2 receptors. Insight into how drugs bind to 5-HT_2 receptors could contribute significantly to the development of subtype-selective agents with enhanced therapeutic effects. We have

begun to address this challenge by the combined approach of chemical synthesis and molecular modeling. 9-(Aminomethyl)-9,10-dihydroanthracene (AMDA) a novel, selective 5-HT_2 antagonist that also has modest affinity for the histamine (H_1) receptor has been reported by Westkaemper et al.[5] A structure-affinity relationships (SAFIR) study of AMDA and its analogs was carried out by studying the effects of *N*-alkylation, variation of the amine-ring system linker chain length and constraint of the aromatic rings on the binding affinities of the compounds for the 5-HT_{2A} and H_1 receptors. The results of the docking studies carried out on the homology models of 5-HT_{2A} and H_1 receptors were consistent with the observed binding affinity data for both receptors. In order to explore the additional binding site interactions of 5-HT_{2A} receptor, synthesis and testing of the ring-annulated analogs of AMDA were carried out. A 3-methoxytetraphen analog of AMDA (**26**) showed high affinity (K_i = 21 nM) and selectivity (126-fold) for 5-HT_{2A} receptor as compared to H_1 receptor (K_i = 2640 nM).

Further, to test the utility of our homology models, and investigate the binding site specific interaction, a compound was synthesized and tested that lacks a basic amine and contains an acidic functionality designed specifically to interact with lysine K191$^{5.39}$ found in H_1 but not in 5-HT_{2A} receptor. This compound would thus be both H_1-selective and demonstrate that a basic amine-D3.32 interaction is not necessary for high affinity. The synthesized compound (**34**) lacking the nitrogen atom showed moderate affinity at the H_1 receptor (K_i = 250 nM), and lacked affinity for 5-HT_{2A} receptors. The modeled ligand orientations in combination with the observed affinity data provide another example of a successful structure-based design strategy.

INTRODUCTION

1.1 The Discovery of Serotonin

5-Hydroxytryptamine (5-HT), commonly known as serotonin, is one of the evolutionarily oldest neurotransmitters.[7] Its discovery and identification as an important monoamine neurotransmitter involved a multidisciplinary approach by several groups.[8] Serotonin was first described as enteramine, which was isolated from the gut in the 1930s by Ersparmer and colleagues and revealed to cause contraction of the uterus. In 1948 5-HT was rediscovered by U. C. Irvine's Page group based on its vasoconstrictor properties, its name being derived from the fact that the substance was produced in the serum ("ser"), and constricted or increased tone ("tonin") in blood vessels.[9,10] The chemical structure of serotonin was proposed to be 5-HT by Rapport[11] which was then confirmed by Erspamer and Asero as identical to enteramine obtained from natural sources.[10,12,13] Following this discovery, in 1953 Twarog and Page reported the presence of serotonin in the central nervous system (CNS),[14] which was considered to be one of the major findings in the field of neuroscience.

1.2 Serotonin Biosynthesis and Metabolism

5-HT is synthesized in the human body from the natural amino acid L-tryptophan. Tryptophan is converted to serotonin via a series of reactions (Figure 1). First, L-tryptophan is hydroxylated to 5-hydroxytryptophan (5-HTP) via the enzyme tryptophan hydroxylase.[15] This reaction constitutes the rate-limiting step in the synthesis of serotonin. 5-HTP is in turn converted to 5-HT via the enzyme amino acid decarboxylase.[16] Serotonin is released into the circulation from the enterochromaffin cells found in the gastrointestinal (GI) tract and rapidly taken up by platelets via the serotonin transporter (SERT).[2] It is then stored in platelet-dense granules which comprise almost all of the circulating serotonin. In the central nervous system, serotonin is stored in secretory granules and released from serotonergic neurons into a synapse. Serotonin is metabolized at the presynaptic terminals by the monoamine oxidase (MAO) enzyme to 5-hydroxyindole acetic acid (5-HIAA) via oxidative deamination. Brain 5-HIAA is actively transported to the periphery where, along with peripheral 5-HIAA, it is excreted in urine.[17]

1.3 Classification of Serotonin Receptors

In 1957 Gaddum and Picarelli started the subdivision of 5-HT receptors by studying the effect of 5-HT blockade in guinea pig ileum in the presence of morphine and dibenzyline. They proposed two receptor classes, 5-HT M and 5-HT D.[18] In 1979 Perouka and Snyder used radioligand binding techniques to describe two classes of serotonin receptors, 5-HT_1 and 5-HT_2.[19]

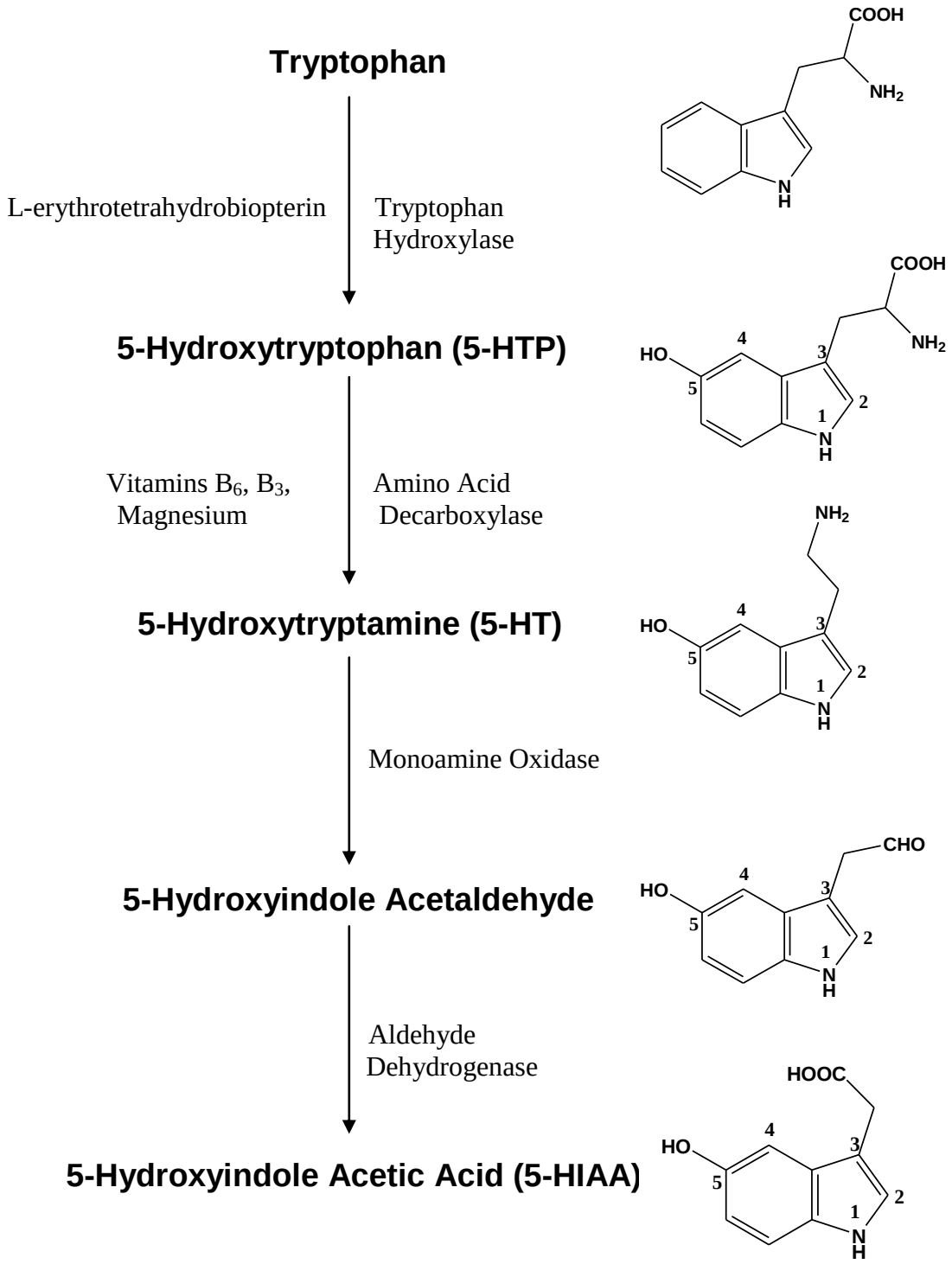

Figure 1. Biosynthesis and metabolism of serotonin. Cofactors are shown left of the arrows; enzymes are shown right of arrows.[2]

Later Bradley *et al.*[20] proposed the existence three families of 5-HT receptors, named 5-HT_1-like, 5-HT_2 and 5-HT_3, the latter corresponding to the M receptor. With the advances in molecular biology techniques 5-HT receptor genes were cloned, which further led to the identification of number of new receptors devoid of physiological counterparts.[1] Based on the new findings and a constantly developing field, the serotonin receptor nomenclature committee proposed a new nomenclature system based on operational, structural and transductional information.[21] To date, 5-HT receptors can be classified into seven families with at least 15 different subtypes. A majority of these receptors are G protein-coupled receptors, with the exception of 5-HT_3 (5-HT_{3A} and 5-HT_{3B}) which are ligand-gated ion-channel receptors [3,22] (Table 1).

Table 1. Serotonin receptor classification.[23]

5-HT_1	**5-HT_2**	**5-HT_3**	**5-HT_4**	**5-HT_5**	**5-HT_6**	**5-HT_7**
5-HT_{1A}	5-HT_{2A}	5-HT_{3A}		5-HT_{5A}		
5-HT_{1B}	5-HT_{2B}	5-HT_{3B}		5-HT_{5B}		
5-HT_{1D}	5-HT_{2C}					
5-HT_{1E}						
5-HT_{1F}						
Coupled AC (-)	Coupled PI	Ion Channel	Coupled AC (+)	Complex	Coupled AC (+)	Coupled AC (+)

Second messenger system: Adenylate cyclase (AC), Phosphatidylinositol (PI)

The 5-HT receptors and a large number of monoamine receptors that belong to the G protein-coupled receptor (GPCR) family are a part of type A family (rhodopsin-like) GPCRs.[24] The presence of highly conserved residues in rhodopsin, β_2-adrenergic receptor and other type A GPCRs suggests the possibility of serotonin receptors sharing certain structural and functional similarities with them.[25] While the overall homology of GPCRs compared to rhodopsin is low (35%) in the transmembrane region, the presence of several highly conserved residues suggests an possible evolutionary relationship.[26] The phylogenetic relationship of each serotonin receptor to others is shown in Figure 2.

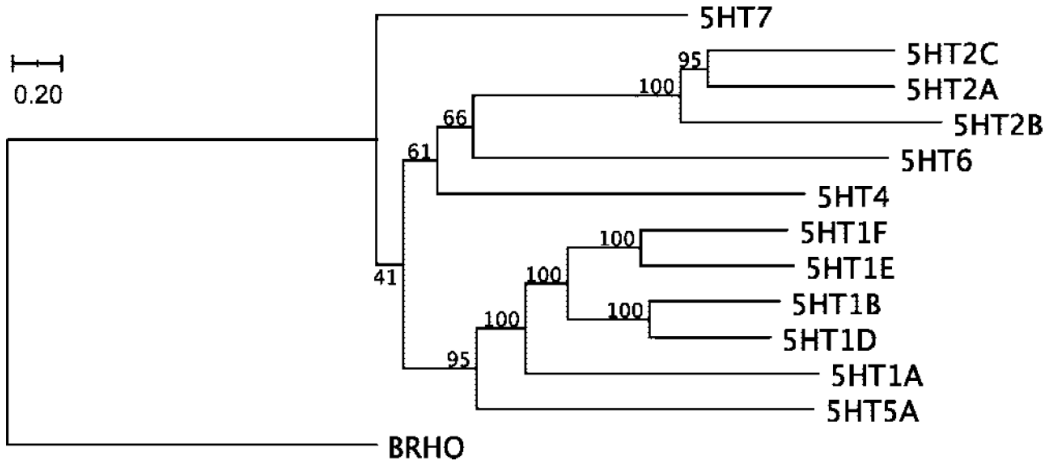

Figure 2. Scaled phylogenetic tree comparing all human serotonin receptors with bovine rhodopsin (BRHO).[3]

1.4 Serotonin Receptors: Clinical Significance

Serotonin is a neurotransmitter that plays a role in large number of physiological processes including regulation of vascular and non-vascular smooth muscle contraction, platelet aggregation and mitogenesis.[27] The greatest concentration of serotonin (90%) is found in enterochromaffin cells of gastrointestinal tract and the effects of 5-HT are seen greatly in the cardiovascular system and central nervous system (CNS). Serotonin receptors contribute to pathological processes related to cardiopulmonary problems,[28,29] irritable bowel syndrome,[30,31] psychiatric illness (i.e., schizophrenia and mood disorders)[32-35] Alzheimer's disease,[36,37] problems involving food and alcohol intake,[38,39] and behavioral problems (i.e. aggression, impulsivity).[40,41] Serotonin exerts its effects on neuronal and non-neuronal tissues by interacting with the various receptor subtype populations (Tables 2 and 3).

Table 2. Mental illness where altered serotonin neurotransmission has been implicated. (Adapted from Roth, B. L. and Shapiro, D. A., *Expert Opin. Ther. Targets*, **2001**, 5, 685-695)[42]

Disease	5-HT receptor	Prototype drug	Agonist/Antagonist
Schizophrenia	5-$HT_{2A/2C}$	Clozapine	5-$HT_{2A/2C/6/7}$ antagonist[43]
Depression	5-$HT_{1A/1B/2A/2B/2C}$	Mianserin	5-$HT_{2A/2B/2C}$ antagonist
Anxiety disorders	5-$HT_{1A/1B/2C}$	Buspirone	5-HT_{1A} partial agonist
Eating disorders/ obesity	5-HT_{2C}	Fenfluramine	5-HT_{2C} agonist[44]

Table 3. Common medical conditions in which 5-HT-subtype-selective drugs have utility. (Adapted from Roth, B. L. and Shapiro, D. A., *Expert Opin. Ther. Targets*, **2001**, 5, 685-695)[42]

Disease	5-HT Receptor	Prototype drug	Agonist/Antagonist
Obesity	5-HT_{2C}	Fenfluramine	Agonist[45]
Irritable bowel syndrome	5-$HT_{3/4/5}$	Tagaserod	5-HT_3 antagonist, 5-HT_4 agonist
Migraine headaches	5-$HT_{1D/1F}$	Sumatriptan	Antagonist
Emesis	5-HT_3	Ondansetron	Antagonist
Pain	5-$HT_{2A/2B}$	Amitryptiline	Antagonist[46]

Over the years, many studies have been reported with reference to the pharmacology, molecular biology and the development of selective ligands for these receptor subtypes.[22,47] However, the following discussion will focus on the 5-HT_2 receptor family due to its relevance to the current work. 5-HT_2 receptors are one of the most extensively studied receptor types within the serotonin family. The structure and function of this group of receptors have been studied in great detail and drugs targeting these receptors have utility for treating large number of diseases[42,48] (Tables 2 and 3).

1.5 5-HT_2 Receptor Structure, Function and Localization

The 5-HT_2 receptor family members comprise a closely related subgroup of G protein-coupled receptors, functionally linked to a phosphatidylinositol hydrolysis pathway and are classified as 5-HT_{2A}, 5-HT_{2B} and 5-HT_{2C} subtypes.[49,50] While the 5-HT_{2A} and 5-HT_{2C} receptors are widely expressed throughout the brain, the 5-HT_{2B} receptor is mostly

expressed in the periphery, with minimal CNS expression. Each 5-HT_2 subtype has a classic G protein-coupled seven-transmembrane helical region connected by extracellular and intracellular loops. Most of the current understanding about the structural features of the 5-HT_2 receptor family is derived from mutagenesis and molecular modeling studies of 5-HT_{2A} receptors.[3,51,52] The general arrangement of residues in the binding pocket is similar to that of rhodopsin and large numbers of studies have identified key residues essential for agonist and antagonist binding to the 5-HT_{2A} receptor.[53-56] The binding pocket of the 5-HT_{2A} receptor is lined with many aromatic residues with the presence of a single charged residue (D155) which acts as an anchor for aminergic drugs binding to the receptor.[57]

The 5-HT_{2A} receptor shares high homology with the 5-HT_{2C} receptor subtype with overall amino acid sequence identity >50% and the sequence identity between transmembrane regions >75%.[21] The 5-HT_{2A} receptor is highly expressed in all layers of the cortex with the highest density in the neocortex.[50] In the basal ganglia and forebrain, 5-HT_{2A} receptor has been localized to medium- and large-sized neurons in the lateral septal nuclei. The 5-HT_{2A} receptor modulates GABAergic and glutaminergic transmission as well as monoaminergic transmission via various mechanisms and interactions.[49] Given the extensive location of this receptor in brain areas that mediate cognitive functions and social interaction, the 5-HT_{2A} receptor is implicated in diseases in which these functions are impaired. Some of the central disorders involving 5-HT_{2A} receptors are schizophrenia, depression and psychosis. In addition, recent studies involving 5-HT_{2A} receptor knockout mice have also implicated its role in sleep disorders.[58]

1.5.1 5-HT$_2$ Receptors in the Development of Novel Antidepressant Drugs

Depression is a common condition that has both emotional and physical aspects.[59,60] It is often accompanied by variety of neurological, psychiatric and other mental illnesses.[59,61] However, no single neurotransmitter abnormality has been identified that fully explains the pathophysiology of depression. Alterations in the serotonergic and noradrenergic function in the CNS have often been implicated in the pathophysiology of depression and the mechanism of action of antidepressant drugs but the specific impairment that underlies depression is unclear.[62,63] The classes of antidepressants drugs that are commonly used include monoamine oxidase (MAO) inhibitors, tricyclic antidepressants (TCAs) and the monoamine reuptake inhibitors.[64] There have been few reports suggesting that the depression is caused by the functional deficiency of the serotonin in the brain.[65,66] Studies involving 5-HT$_2$ receptors have indicated that 5-HT$_{2A}$ antagonism is often associated with significant antidepressant potential[67] and that the long-term administration of tricyclic antidepressants causes a decrease in the cortical density of 5-HT$_{2A}$ receptors.[68] Thus several clinically-effective antidepressants (mianserin,[69] mirtazepine,[70] trazadone and nefazadone[71]) are thought to exert their action by 5-HT$_{2A}$ antagonism in addition to their action at other receptors.[72]

In addition, a study involving the functional interaction between central 5-HT and DA systems has suggested that disinhibition of the mesolimbic DA system might be useful in the treatment of depression.[73] Specifically, the 5-HT$_2$ subtype has been indicated to play a role in the control of central DA activity because of the moderate to dense localization of both mRNA and protein for the 5-HT$_{2A}$ and 5-HT$_{2C}$ receptors in the substantia nigra (SN)

and ventral tegmental area (VTA) in the rat forebrain.[74,75] Further, studies have shown that the 5-HT_{2C} subtype is responsible for the inhibitory influence of 5-HT on the activity of mesolimbic and nigrostriatal dopaminergic pathways[76] (Figure 3) suggesting that 5-HT_2 receptors could act as an potential targets for the development of novel antidepressant drugs.[73]

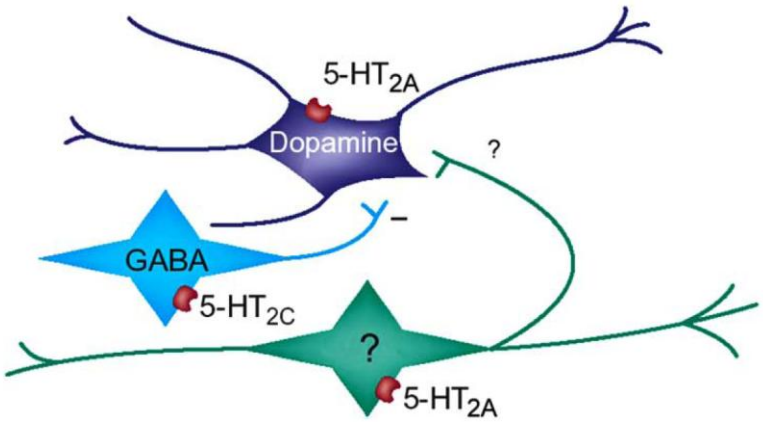

Figure 3. Distribution of 5-HT_{2C} and 5-HT_{2A} receptors on GABA-containing and dopamine-containing neurons in the midbrain. 5-HT_{2A} receptors are expressed on a subpopulation of DA-containing neurons, and on non-DA neurons whose neurochemical identity is yet unknown (indicated by question mark). 5-HT_{2C} receptors are expressed on GABA-containing neurons in both substantia nigra pars reticula (SNr) and the ventral tegmental area (VTA).[73]

1.5.2 5-HT_2-Selective Antagonists as Potential Antipsychotic Drugs

In the past, studies by Meltzer et al.[77] and others have predicted that drugs with high 5-HT_{2A}/D_2 affinity ratios would be effective atypical antipsychotic drugs.[78] Since then, several such atypical antipsychotic drugs (clozapine, olanzapine, risperidone and ziprasidone) have been approved for clinical use. Generally, atypical antipsychotic drugs have a complex pharmacology due to their action at multiple serotonin (5-$HT_{2A,}$ 5-$HT_{2B,}$ 5-

HT_6 and 5-HT_7) receptors.[79] In addition, atypical antipsychotics also interact with dopamine D_4 and muscarinic (M_1-M_5) receptors. It is assumed that 5-HT_{2A} rather than 5-HT_{2C} receptors play a major role in mediating psychosis, which suggests that the variable degree of 5-HT_{2A} vs. 5-HT_{2C} receptor selectivity between atypical antipsychotics may be of clinical relevance. In fact, antagonism of 5-HT_{2A} as well as 5-HT_{2C} receptors has been implicated in the therapeutic effectiveness of atypical antipsychotics.[80] The role of 5-HT_{2A} receptors in psychosis is supported by the report of MDL100907,[81] amperozide, eplivanserin and ritanserin as compounds preferring the 5-HT_{2A} receptor; however, development has been limited.[82] Due to the multiple receptor affinity of the atypical antipsychotics they are often associated with side effects. Thus the development of selective 5-HT_{2A} antagonists might provide an effective therapy for psychosis in addition to acting as pharmacological tools for the study of the 5-HT_{2A} function.

1.5.3 5-HT_2 Ligands in the Treatment of Schizophrenia

Schizophrenia is one of the major neuropsychiatric disorders that involve the 5-HT and DA neurotransmitters.[83] It is diagnosed by its positive symptoms (auditory hallucinations, disorganized thoughts and delusions), negative symptoms (social withdrawal, lack of motivation) and cognitive dysfunction.[84] The first-generation antipsychotics and the newer atypical antipsychotic drugs are the main line of treatment for schizophrenia.[85,86] However, the negative symptoms and cognitive dysfunction are not fully treated by them.[87] Recent studies have shown that the 5-HT_{2A} receptor subtype plays an important role in schizophrenia by modulating dopamine release in the striatum and

cortex.[33,88] In addition, the antiserotonergic properties of atypical antipsychotics decrease the dopamine activity in the frontal cortex that in turn may contribute to improvement in negative symptoms in schizophrenia.[89] Recent studies have also linked the association of the T102C polymorphism in the 5-HT_{2A} receptor gene with schizophrenia.[88,90,91] The 5-HT_{2A} receptor is considered to be a major component of the atypical antipsychotic profile, and atypical antipsychotic drugs used in therapy are known to bind to 5-HT_{2A} receptors.[92,93] However, the use of atypical antipsychotic drugs is often associated with adverse side effects such as metabolic disorders, sedation, movement disorders and weight gain.[84] One of the possible reasons for the side effects of these drugs is their multiple-receptor (serotonin, dopamine, α-adrenergic, muscarinic and histamine) binding profile.[94] Thus the development of newer atypical antipsychotic drugs having selectivity for the 5-HT_{2A} receptor can potentially lead to clinically useful drugs for the treatment of schizophrenia.

1.5.4 5-HT_2 Ligands in the Treatment of Sleep Disorders

It is well established that serotonin plays major role in the regulation of sleep-wakefulness cycles (Figure 4), and that any disruption of serotonergic function induces modification of sleep and waking.[95] Evidence from clinical studies has suggested that 5-HT_2 receptors modulate slow wave sleep (SWS).[96] For example, the 5-HT_2 receptor antagonist ritanserin promotes sleep and enhances slow wave activity in humans and rats.[91] This activity is likely mediated through the 5-HT_{2A} receptor, as similar increases in SWS are observed with more selective 5-HT_{2A} antagonists such as eplivanserin[97] and

MDL100907.[98] In addition, studies involving knock-out mice lacking 5-HT_{2A} receptors have suggested that the 5-HT_{2A} subtype is involved in non-rapid eye movement sleep (NREMS) regulation[58] and that the ligands acting at 5-HT_{2A} receptors might be useful in the treatment of sleep disorders. Thus by improving the quality of sleep and restfulness, 5-HT_{2A} modulators (antagonists/inverse agonists) can offer a significant advancement in the treatment of sleep disorders.

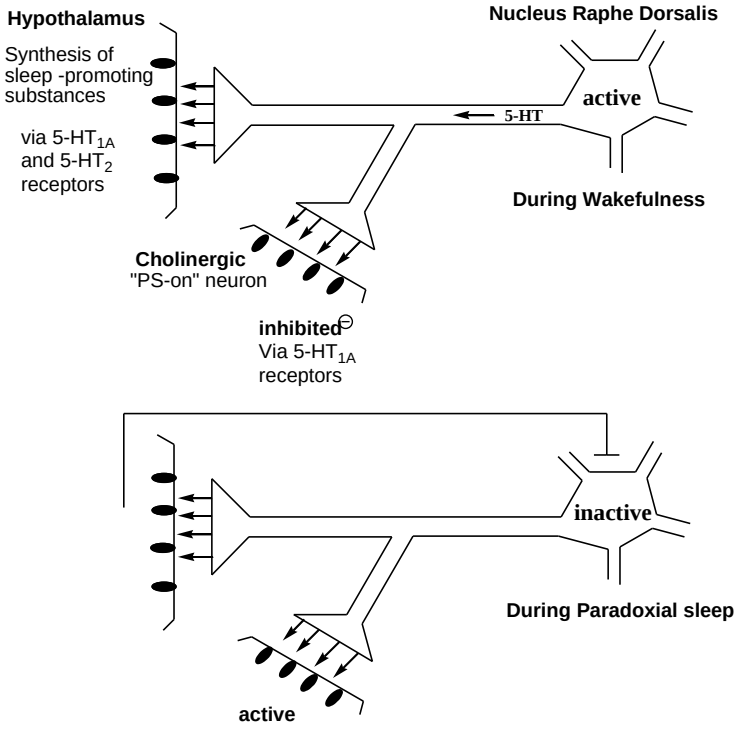

Figure 4. Schematic representation of the serotonergic regulation of sleep-wakefulness cycle. During waking, the serotonergic neurons of nucleus raphe dorsalis (NRD) are active. 5-HT is liberated at the termini and activates postsynaptic serotonin receptors. This activation results in an increase sleep-like condition at the hypothalamic level and inhibition of cholinergic structures responsible for paradoxical sleep (PS) at the pontine level. During sleep, the serotonergic neurons are inactive, possibly due to a negative feedback loop via a sleep-promoting substance. This result in a reduction in both 5-HT_2 influence (facilitating occurrence of SWS) and 5-HT_{1A} inhibitory control of cholinergic "PS-on" neurons, therefore facilitating the occurrence of PS.[99]

1.6 Clinical Relevance for Studying Serotonin (5-HT_{2A}) and Histamine (H_1) Receptors

Histamine is another monoamine which is known to regulate a wide variety of physiological responses.[100] It acts as one of the primary inflammatory mediators released from mast cells following allergic challenges.[101,102] It also acts as a neurotransmitter in the central nervous system (CNS).[103] Histamine exerts its effect by interacting with four different aminergic GPCRs H_1-H_4[104] (Table 4).

Table 4. Histamine receptor classification. (Adapted from Fung-Leung, et al., *Curr. Opin. Invest. Drugs*, **2004**, 5, 1174-1183).[105]

Histamine receptor	**H_1**	**H_2**	**H_3**	**H_4**
Expression	Ubiquitous	Ubiquitous	Neural cells	Mast cells, eosinophils, dendritic cells and T-cells
Gα-protein association	$G\alpha_q$	$G\alpha_s$	$G\alpha_{i/o}$	$G\alpha_{i/o}$
Signaling	$\uparrow Ca^{+2}$	↑cAMP	↓cAMP	$\uparrow Ca^{+2}$
Key function	Bronchoconstriction and vasodilation	Gastric acid secretion	Neurotransmitter release	Mast cell and eosinophil chemotaxis
Agonists	2-Methylhistamine, Histaprodifen	Dimaprit, Anthamine	R-α-methylhistamine, Imetit	Imetit, Immepip
Antagonists	Diphenhydramine Cetrizine Pyrilamine	Burimamide Cimetidine Ranitidine	Thioperamide Clobenpropit	Thioperamide JNJ-7777120

Over the years various classes of H_1 antagonist have been developed and used clinically[106,107] (Figure 5). However, because of CNS penetration and central H_1 receptor blockade their clinical use is hampered by various side effects, most notably sedation.[108,109]

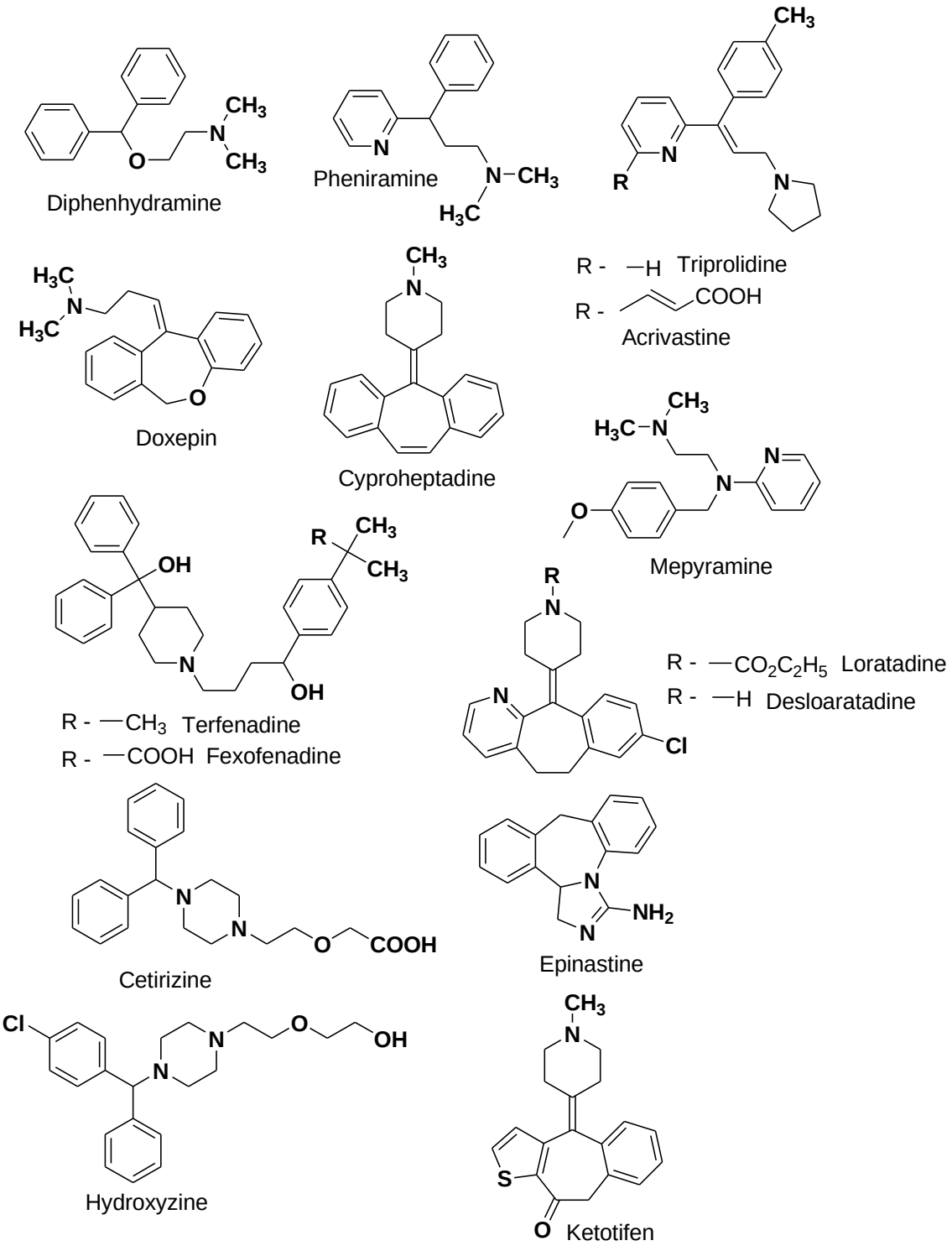

Figure 5. Structures of representative H_1 antagonists.

This led to the development of second-generation antagonists (acrivastine, loratadine, terfenadine, cetirizine, etc.) that exhibited less sedative potential due to the decrease in their ability to penetrate the blood-brain barrier.[107,110,111] Some of these antagonists, such as doxepin, ketotifen, and epinastine that have a tri- or tetracyclic fused ring system also showed affinity at 5-$HT_{2A,}$ adrenaline $\alpha_{1,}$ dopamine D_2 and muscarinic M_1 receptors, indicative of their low selectivity for the H_1 receptor.[112-114] Among the various chemical classes of H_1 antagonist, ligands that are zwitterionic (olopatadine, acrivastine, fexofenadine) showed an improved degree of selectivity for H_1,[115-117] suggesting a specific interaction of the carboxylate group on the ligand with the H_1 receptor. Introduction of a carboxylate moiety thus provides one potential means of designing H_1-selective antagonists with reduced sedative potential.

There have been three reports suggesting that serotonin may be the primary neurotransmitter in the control of sleep states.[95,118,119] However to date, drugs which modulate serotoninergic transmission by stimulating or blocking serotonin receptors have not been used clinically in the treatment of insomnia.[120] Studies related to 5-HT_2 antagonists including the antipsychotics ziprasidone and risperidone have shown that these drugs increased slow wave sleep (SWS) and affect NREM.[96,121] Nevertheless, the study of the clinical role of 5-HT_{2A} receptors in sleep has been hampered by the lack of 5-HT_{2A} selective agents. Thus there is a need for a selective agent for the determination of the role of 5-HT_2 receptors in sleep as a lead to the possible development of a sleep drug based on 5-HT_{2A} antagonism.

In addition to serotonin, histamine has been proposed to be involved in the control of sleep and wakefulness, as mentioned previously.[122] Most common over-the-counter agents used to promote sleep are antihistamines. Development of improved antihistaminic drugs for the treatment of insomnia is hampered by the fact that these drugs have action at multiple targets including serotonergic and muscarinic receptors. There has been a recent report of the use of low-dose of doxepin (an antidepressant agent with high affinity and selectivity for H_1 receptor) in the treatment of insomnia, suggesting a potential role for selective H_1 receptor antagonists in the treatment of sleep disorders.[113] In addition, the latest reports of clinical trial studies[123] have also implicated the role of selective dual-acting 5-HT_{2A}/H_1 ligands in the treatment of sleep disorders. As mentioned earlier, the majority of atypical antipsychotic drugs (clozapine, risperidone, olanzapine, ziprasidone, aripiprazole) used in the treatment of schizophrenia exhibit high affinity for the 5-HT_{2A} receptor. However, they are often associated with the side effects such as weight gain. Results from a recent study have suggested that the histamine H_1 receptor is the most likely molecular target responsible for atypical antipsychotic drug-induced weight gain.[124] Thus, the study of factors relating to the selectivity between H_1 and 5-HT_{2A} receptors could also help in the design of next-generation atypical antipsychotic drugs with fewer side effects.

1.7 5-HT_2 Receptor Ligands

The 5-HT_2 family of serotonin receptors represents major target for drugs used in the treatment of a variety of diseases as mentioned earlier. As the 5-HT_2 family of receptors has three members (5-HT_{2A}, 5-HT_{2B} and 5-HT_{2C}), the development of subtype-

selective compounds will be needed in order to avoid side effects and to enhance therapeutic value. Unfortunately not many ligands are available which exhibit subtype selectivity.[125] Some of the ligands that act at 5-HT_2 receptors are shown in Figure 6. The indolealkylamine ligands act as 5-HT_{2A} agonists but are less selective as compared to phenylalkylamines such as DOB and DOI that exhibit low affinity at non-5-HT_2 sites. However, phenylalkylamines also cannot differentiate among 5-HT_2 subpopulations.[126] One of the most selective antagonist classes of 5-HT_{2A} ligands are the *N*-alkylpiperidines,[4] (e.g. ketanserin); although ketanserin only shows about 10- to 15- fold selectivity for 5-HT_{2A} versus 5-HT_{2C} receptors. Various analogs of ketanserin have been made, but not much selectivity has been achieved. The other 5-HT_{2A} antagonists such as ritanserin, MDL 100907,[81] spiperone,[127] risperidone and olanzapine demonstrate increased selectivity for 5-HT_{2A}.[82,120] Various nonspecific tricyclic agents (tricyclic neuroleptics and antidepressants) bind at 5-HT_{2A} receptors.[128] A range of new compounds reported to have activity at 5-HT_{2A} receptors is under clinical development.[129]

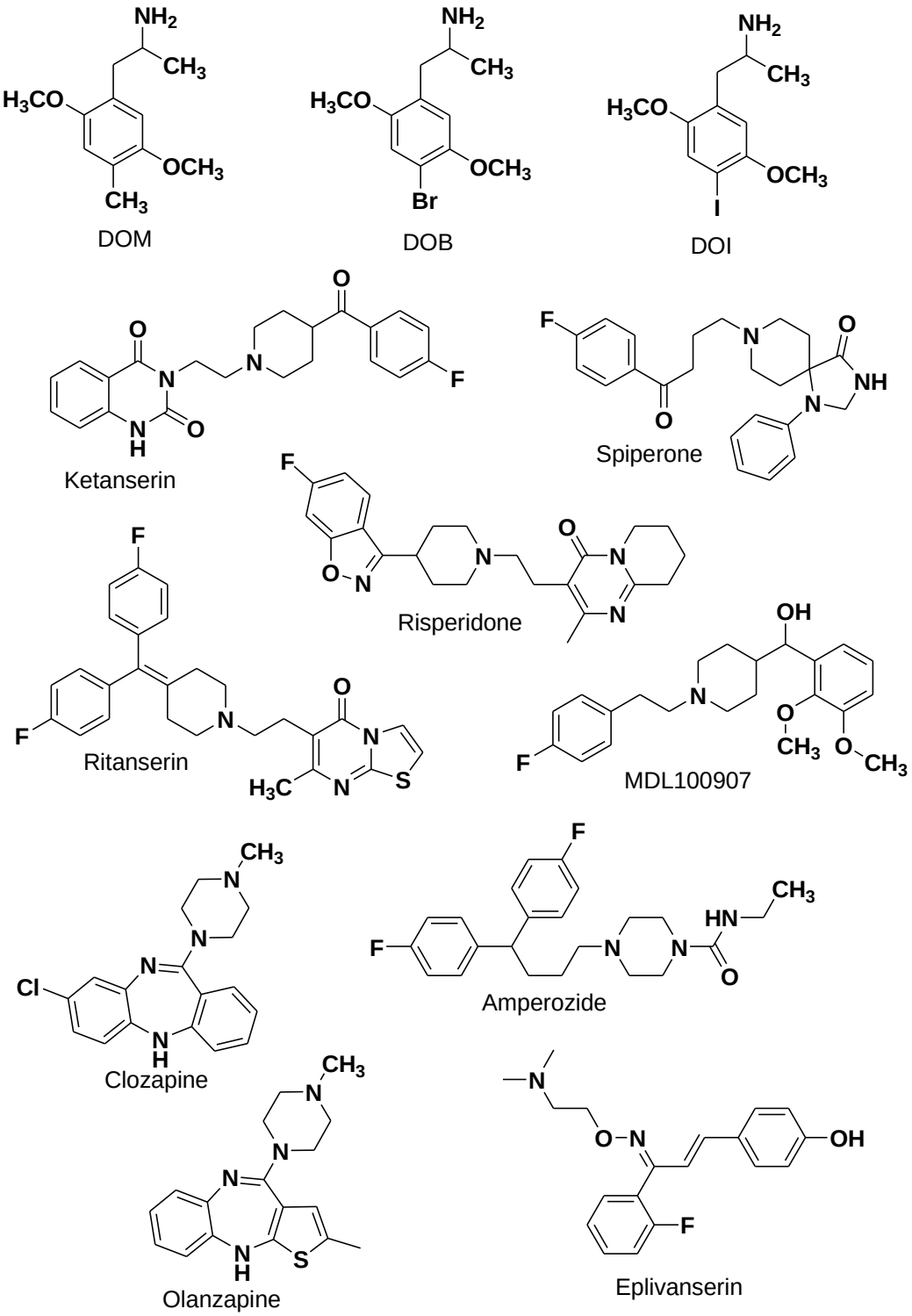

Figure 6. Structures of representative 5-HT_2 ligands.

1.8 Understanding 5-HT_{2A} Receptor-Ligand Interactions and Development of a Selective GPCR Ligand

The 5-HT_2 family of receptors has three members (5-HT_{2A}, 5-HT_{2B} and 5-HT_{2C}) and development of 5-HT_2-selective compounds is expected to lead to drugs with better therapeutic indices. To date, very few truly selective 5-HT_2 receptor ligands have been discovered and found to have clinical application. One of the challenges in the development of a subtype-selective ligand is the possible interaction with the multiple serotonin receptor subpopulations (5-HT_1 through 5-HT_7) and the serotonin transporter (SERT). In an attempt to develop a selective 5-HT_2 ligand and understand how the molecules bind at these receptors, we decided to use receptor structure-based drug design. Integrating data from molecular models, site-directed mutagenesis studies and traditional SAR studies makes it possible to generate new and interesting leads. With the introduction of a structure of a true aminergic (β_2-adrenergic) GPCR[130,131] in addition to existing bovine rhodopsin structures, homology modeling techniques are better-equipped to produce biologically relevant GPCR models.

In an effort to develop a 5-HT_2-selective ligand, we started with a simple nonselective structural template (phenylethylamine) having low affinity for the 5-HT_{2A} receptor (K_i = 16,800 nM) and modified its structure so as to enhance affinity and selectivity. Initial investigations[5,51] in our laboratory have led to the development of AMDA (9-aminoalkyl-9,10-dihydroanthracene; K_i = 20 nM), a novel 5-HT_2 antagonist having moderate affinity at histamine H_1 (K_i = 197 nM) receptors. Using structure-based

drug design methods and AMDA as a lead compound, testable hypotheses were generated and compounds were designed to test these hypotheses.

1.9 Specific Aims of the Research Project

Taking into account the lack of the experimentally derived 5-HT_2 receptor structure and the need to understand the 5-HT_{2A} receptor-ligand interactions, a set of specific aims were devised as follows:

Aim 1) To design and synthesize ligands based on AMDA (9-aminoalkyl-9,10-dihydroanthracene) and its pharmacophore as molecular probes for the study of the 5-HT_{2A} and H_1 receptor binding sites.

Aim 2) To test hypotheses relevant to the affinity/selectivity of the compounds at the 5-HT_{2A} and the H_1 receptor using ligand SAR, homology modeling and existing site-directed mutagenesis studies.

Aim 3) To use the information acquired in the above investigations for the refinement of homology models and test the utility of our models for the design of new H_1- and/or 5-HT_2 -selective compounds.

MOLECULAR MODELING OF G PROTEIN-COUPLED RECEPTORS

2.1 Introduction

G protein-coupled receptors (GPCRs) are vital components of biological signaling processes in higher animals and humans, which constitute one of the most important set of targets for pharmaceutical industry.[132] More than 1000 genes encoding GPCRs have been identified from the human genome sequencing effort. This represents a substantial part of human genome (~3%). On the basis of structural and sequence similarities, GPCRs are generally classified into 5 families: Class A (rhodopsin-like) is the largest group and contains receptors for classical neurotransmitters (biogenic amines and nucleotides) and a large variety of peptides and lipids, with class B (secretin), class C (glutamate), class D (fungal hormone), class E (cAMP)[133,134] and class F (frizzled) comprising the remaining classes. The physiological function of a large fraction of these GPCRs is unknown; these receptors are referred to as orphan GPCRs.[135]

2.2 Central Role of G Proteins

On activation, GPCR's trigger a cascade of intracellular responses through interactions with their associated heterotrimeric G proteins.[136] The G proteins are a family of closely related membrane-linked polypeptides. By acting as a carrier they form central elements for the signal transduction between the receptors and the effector components (enzymes or ion channels) in the cytoplasm. At rest, they consist of a heterotrimer possessing a guanine nucleotide-binding α subunit (40 - 52 kDa), a β subunit (35 kDa) and a γ subunit (98 - 100 kDa). The β-γ complexes are presumed to be exchangeable from one G protein to another.[137] G proteins are peripheral membrane proteins, in contrast to integral membrane proteins which span the entire membrane (e.g. GPCRs). Activation of the receptor promotes the exchange of a molecule of GDP with a molecule of GTP within the active site of the α-subunit. The binding of GTP causes the dissociation of the heterotrimeric complex, and both the GTP-bound α subunit and the released β-γ complex are then able to interact with intracellular or membrane effectors. The intrinsic GTPase activity of the α-subunit hydrolyses GTP to GDP, restoring its initial inactive conformation as well as its affinity for the β-γ complex (Figure 7).

2.3 Common Structural Features of GPCRs

GPCRs share a common structural motif of seven hydrophobic transmembrane (TM) segments, three extracellular loops (EL), an extracellular amino terminus, three cytoplasmic loops and an intracellular carboxyl terminus. They share the greatest

homology within the TM segments. Each of the TM regions is composed of approximately 20-30 amino acids.

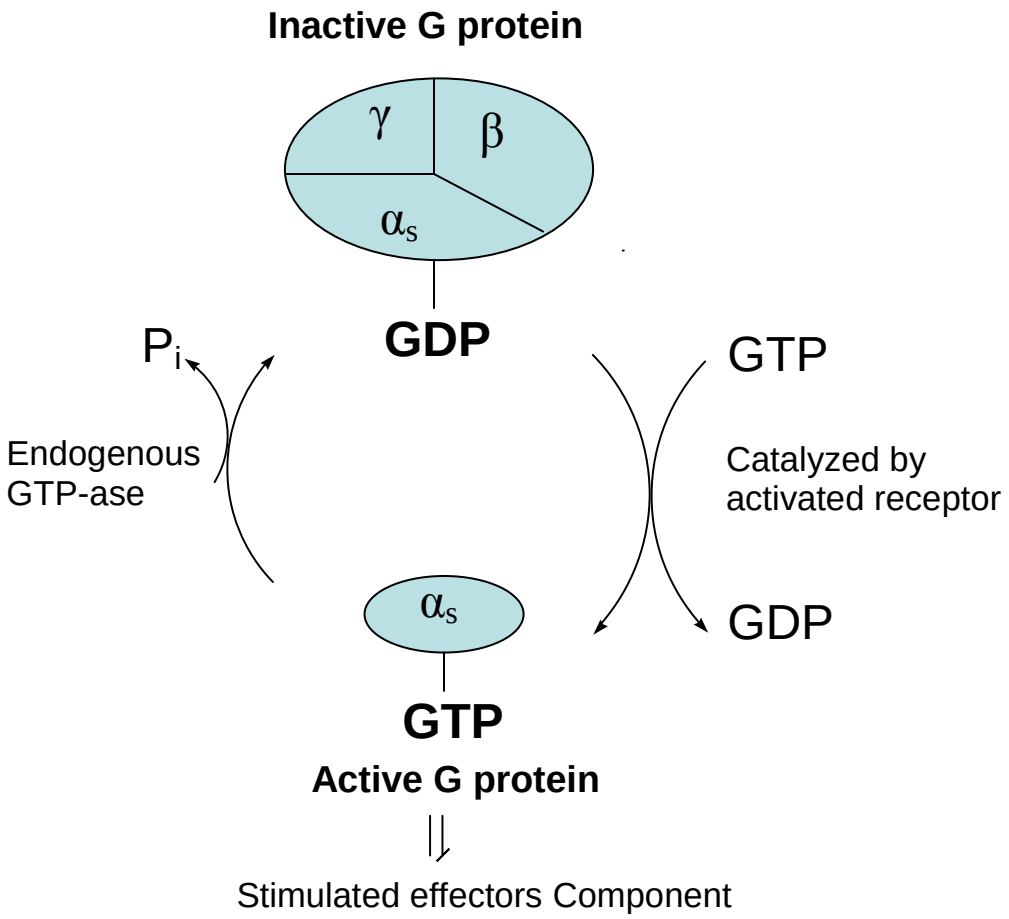

Figure 7. Role of G Proteins.[137]

The most variable structures among the family of GPCRs are the carboxyl terminus (12 - 360 amino acids) the third intracellular loop (5 - 230 amino acids) and the amino terminus (7 - 595 amino acids). Amongst these the greatest diversity is observed in the amino terminus. This sequence is relatively short (10 - 50 amino acids) for the

monoamine and peptide receptors, and much larger (350 - 600 amino acids) for glycoprotein hormone receptors and the glutamate family receptors.[137]

The 7TM structure of GPCRs has certain structural and functional merits as noted by Ji et. al.[138] The odd number of TMs places the N- and C-terminal segments at opposite membrane surfaces that allows glycosylation and ligand binding at the N-terminal segment (for non-aminergic GPCR's), and phosphorylation and palmitoylation at the C-terminal segment for desensitization and internalization. Also, seven TMs may be the minimum necessary to form six loops and a TM core with a sufficient size and versatility to offer an unusual number of specificities, regulatory mechanisms, and contact sites for G protein and other signal molecules. TM α-helices vary in sequence length and can extend beyond the lipid bilayer.[139] Therefore, the boundaries between TMs and loops are likely to be uneven and may be dynamic. TMs 1, 4, and 7 are significantly more hydrophobic than TMs 2, 3, 5, and 6 that contain several ionic and/or neutral residues that are hydrophilic. Proline residues frequently found in TM α-helices kink the helix backbone by ~26° and impact the global structure. The seven TMs are arranged as a closed loop in the counterclockwise direction from TM 1 to TM 7 when viewed from the extracellular surface (Figure 8A). The orientation of the TMs imposes a steric and geometric specificity on a ligand's entry into and binding to the TM core.[140] In this arrangement, the core is primarily comprised of TMs 2, 3, 5, 6, and perhaps 7, whereas TMs 1 and 4 are peripherally sequestered. This arrangement is consistent with the view that the more hydrophobic TMs 1, 4, and 7 are exposed more to the lipid bilayer than the less hydrophobic TMs 2, 3, 5, and 6. The high resolution 3D structure of

bacteriorhodopsin[141,142] suggest that the TM core is tightly packed by hydrogen bonds and salt bridges between the residues of same TMs as well as other TMs. Disulfides linkages often play a major role in the structure and stability of proteins. Among numerous cysteine residues found in eukaryotic GPCRs, two conserved cysteine residues in EL2 are known to be linked by a disulfide bond in bovine rhodopsin and other GPCRs. This disulfide constrains the EL2 loop, preventing it from moving too far away from the TM helical bundle.[143,144]

In contrast to the structural and functional similarity of GPCRs, the types of natural GPCR ligands interacting with them are structurally wide-ranging. The diverse set of ligands is comprised of small organic molecules, subatomic particles (e.g. photons), ions, peptides and proteins. The location of ligand binding domains for a few GPCRs has been determined and has been postulated for many others. While many small molecule agonists bind within the TM segments, peptide hormones and proteins often bind to the amino terminus and extracellular loop regions [138,145] (Figure 8B-F).

2.4 Challenges in GPCR Research

In spite of remarkable advances in the biology and pharmacology of GPCRs, progress in the area of protein structure has been more limited. Until the recent reports of the crystal structure of human β_2-adrenergic receptor[130,146] the only high resolution structure of a GPCR was that of the bovine rhodopsin.[142]

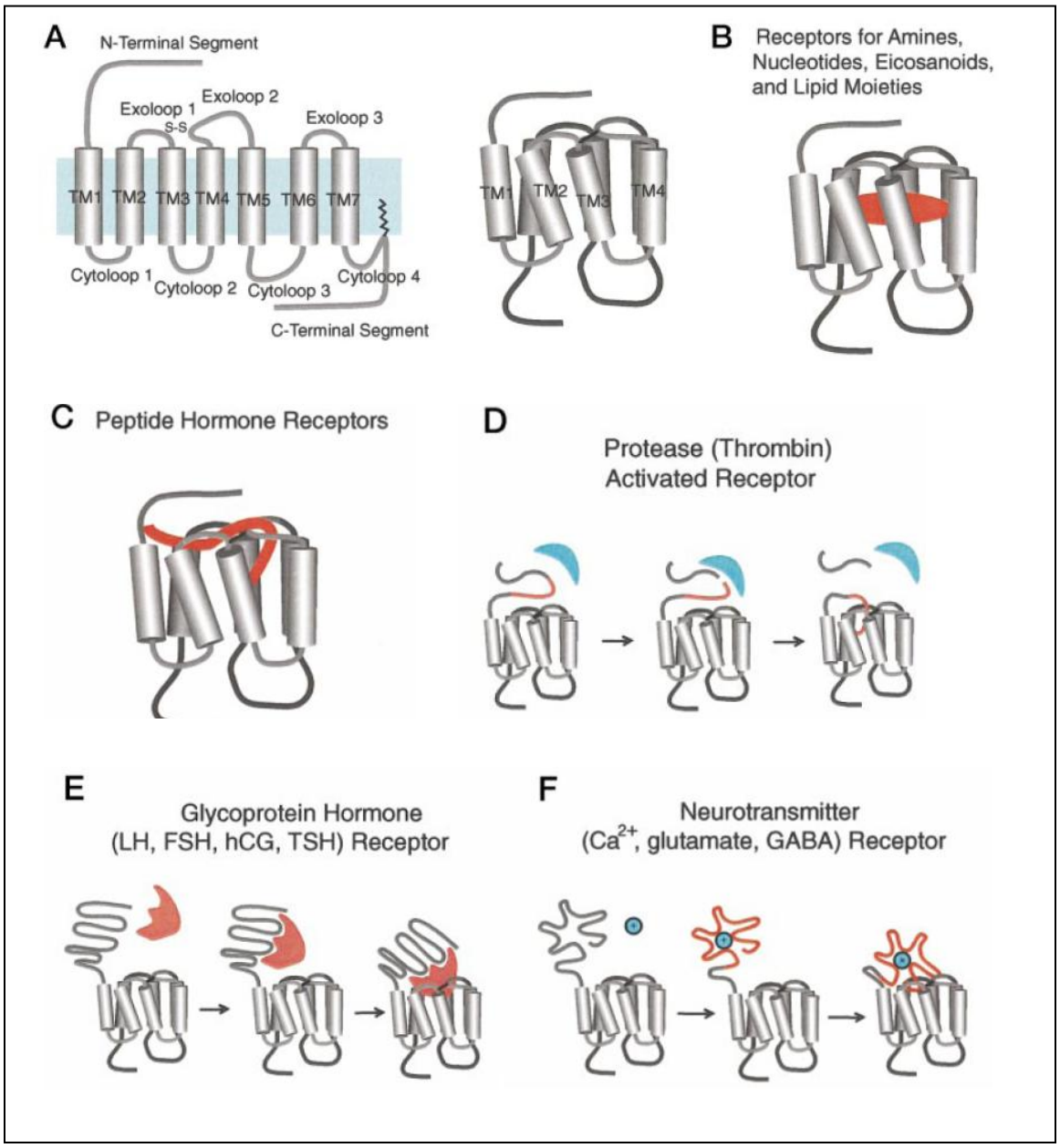

Figure 8. GPCRs structure and receptor-ligand interactions.[138]

2.4.1 Why are there only a few Experimental Structures of GPCRs?

Some of the major obstacles to obtaining structures of GPCRs include protein expression, purification, and protein stability.[147] Crystallization of membrane protein is often a very difficult and time consuming process. With the exception of rhodopsin, which is present in abundant amounts in rod outer segments, membrane proteins occur at relatively low concentration in cell membranes. Another problem associated with crystallization of these receptors is their conformational flexibility. To orchestrate the complex signaling pathways the helical bundle of GPCRs adopt various conformations (active and inactive states) leading to conformational heterogeneity. In addition, the polar surface area available for crystal contacts is limited because of the receptor residues that are predominantly nonpolar being buried in the membrane bilayer. Purified GPCRs are not stable in detergent compatible with crystallography.[148] They tend to be more stable in non-ionic detergents with relatively long alkyl chains. These detergents may form large micelles that prevent the formation of crystal contacts.[149] The successful addressing of these problems, with the recent advances in crystallographic techniques is accelerating the progress in this area of research. Meanwhile, to keep up with the rate of newly discovered GPCR sequences, one may rely on alternate solutions such as generation of 3D models based on the available crystal structure data of a few GPCRs.

2.5 Homology (Comparative) Modeling as a Workable Solution

Given the scarcity of crystal structures for GPCRs, the study of this family of proteins has been greatly advanced through the use of structural models.[150] These models,

combined with experimental testing, have proven to be successful tools to obtain a structural understanding of the GPCR function, and the characteristics of the ligand binding sites.[151] Homology modeling is a method for constructing a three dimensional model of a protein sequence based on the structure of homologous proteins. Steps involved in building a homology model are 1) Identifying the homologous protein(s) and determining their sequence similarity with the unknown; 2) Alignment of the receptor sequence to be modeled with those of the template(s); 3) Identification and mutation of residues in the structurally conserved regions; 4) Generation of conformations for the structurally variable regions (primarily extracellular and intracellular loops); 5) Building and optimization of the side-chain conformation; 6) Evaluation and refinement of the generated model.

2.5.1 Bovine Rhodopsin and β_2-Adrenergic Receptor Structures as Suitable Templates for Homology Modeling

The general observation that evolutionarily related proteins share a similar 3D structure inspite of the fact that they have different amino acid sequences has led to protein models from structurally different templates. By far the most common way the inactive state of a GPCR is modeled is based on the crystal structure of bovine rhodopsin.[142,152] All rhodopsin-like GPCRs are likely to share a common topography with 7TMs bundled together in a similar manner. Sequence comparison has revealed specific amino acid patterns characteristic of each TM that are highly conserved in class A GPCRs. These conserved amino acid residues are also the basis of a commonly used

GPCR residue indexing system introduced by Ballesteroes and Weinstein.[153] (Briefly, the most conserved residue in a given TM is assigned the index X.50, where X is the TM number. The remaining residues are numbered relative to position 50). These specific conserved residues are 1) N1.50, D2.50, N7.50. They contribute to the stabilization of 3D structures of TM1, TM2, and TM7 and their mutation produces serious effects in function of the receptor.[154] 2) The D/ERY motif in TM3 and E6.30 in TM6. The central arginine (R3.50) of the D/ERY motif makes a hydrogen bond with the adjacent D3.49 and a highly conserved glutamic acid in TM6 (E6.30). For a number of GPCRs, mutations in this motif induce a constitutively active phenotype, and thus it is assumed that this motif holds the receptor constrained in the ground state.[52,155] 3) The aromatic cluster including highly conserved F6.44, W6.48, F6.51, and F6.52. UV absorbance studies and site directed mutagenesis have shown a conformational change of W6.48 upon rhodopsin activation, consistent with a change in the relative orientation of helices of TM3 and TM6.[156] Computational studies have shown that the conformation of W6.48 and F6.52 are highly correlated, and may constitute a rotamer "toggle switch" that may modulate the TM6 proline kink. W6.48 and P6.50 are likely to share a common functional role enabling the activation of receptor.[157] 4) The NPXXY motif in TM7. The crystal structure of rhodopsin reveals that this motif induces a large distortion in TM7 which is stabilized by hydrogen bond between polar N7.49 and a network of waters that connect it with D2.50. Studies have demonstrated that NPXXY motif and helix 8 play an important role in the activation process, binding of the G-proteins and may act as a conformational switch domain involved in activation.[158]

Recently a crystal structure of the β_2-adrenergic receptor (3.4 Å) was reported as a receptor-antibody complex with carazolol (inverse agonist) bound in the helical region.[130] Although the β_2AR structure represents the truncated versions, the overall topology of rhodopsin and β_2AR are quite similar. The root mean square deviation (RMSD), which is measure of structural similarity between protein's structures for alpha carbon backbone of TM region between the two is 1.56 Å which indicates similar arrangement of TM helices. Also, a high resolution (2.4 Å) crystal structure of engineered β_2-adrenergic receptor-lysozyme T4 fusion protein has been reported that is similar to the antibody- β_2-AR complex.[131,146] Among the major differences which exist between rhodopsin and β_2-AR relevant to the ligand binding site are the disposition of the helical segments and the second extracellular loop (Figure 9). In case of β_2AR the EL2 loop contains a short helix. This helix contains two disulfide bonds which appear to maintain the loop in a constrained state presumably providing space for diffusion of ligands into the binding site of the receptor, whereas in rhodopsin the second extracellular loop contains a buried β-hairpin which forms a cap-like structure that isolates the retinal-binding site in a hydrophobic pocket. Another difference between two structures is in the state of "ionic lock" defined as the network of hydrogen bonding and charge interactions between R131 in TM3 and E268 in TM6 for β_2AR and R135 and E247 in rhodopsin. The ionic lock is proposed to maintain rhodopsin and other class A GPCRs in an inactive conformation. Disruption of this interaction is thought to allow formation of the active conformation. The crystal structure of inactive rhodopsin displays an ionic lock with a distance of 2.9 Å between E247 and R135. However in both β_2AR structures the ionic lock is broken with

a R131-E268 distance of >6.0 Å. Evaluation of the ligand binding site, carazolol (in β_2AR) and cis-retinal (in rhodopsin) reveals difference in their interaction with the highly conserved "rotamer toggle" (W265 in rhodopsin and W268 in β_2AR). It has been proposed that a change in the rotameric state of this tryptophan in class A GPCRs serves as a second activation switch. Although carazolol does not directly interact with W286 in β_2AR it appears to control the rotameric state of W286 indirectly via interaction with F289 and F290.

In the absence of an experimentally-determined structure for either 5-HT_{2A} or H_1 receptors, rhodopsin and β_2-adrenergic receptor crystal structures were used to create homology models of these receptors. Each template has certain advantages and disadvantages which justifies its selection. For example it is not clear if the β_2AR/T4 lysozyme fusion protein is in the inactive or active state while the rhodopsin structure has been extensively studied (biophysical characterization) and crystal structures for both active and inactive states have been determined. On the other hand, β_2AR is an aminergic GPCR that reversibly binds ligands whereas the rhodopsin ligand, retinal, is covalently linked to the receptor. Moreover the sequence homology is higher between 5-HT_{2A} /H_1 and β_2AR than between 5-HT_{2A}/H_1 and rhodopsin. The overall goal of this project was to determine ligand-receptor interactions for the serotonin 5-HT_{2A} receptor for selected target compounds. 5-HT_{2A} is a typical rhodopsin-like aminergic GPCRs consisting of two soluble domains (extracellular N-terminal, intracellular C-terminal) and seven hydrophobic regions corresponding to seven transmembrane-spanning (7TM) helices. In order to determine the receptor-structure based affinity and selectivity of ligands for the

5-HT_{2A} and H_1 receptors, homology models of the 5-HT_{2A} and H_1 receptors were built using both bovine rhodopsin and the recently reported structure of the human β_2-adrenergic receptor as templates.

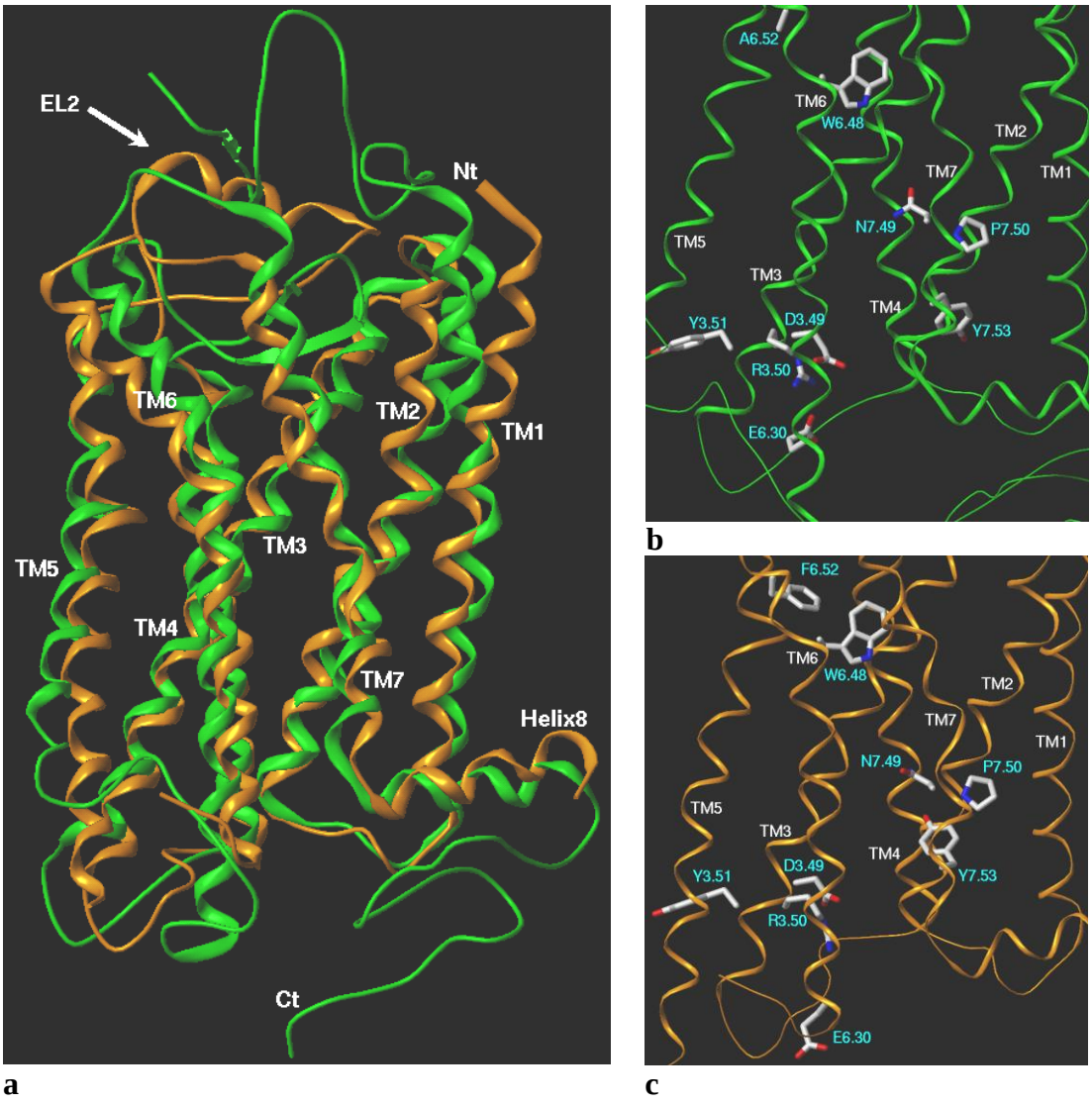

Figure 9. a) Superimposition of the 5-HT_{2A} GPCR models based on β_2-AR (orange: PDB 2RH1) and rhodopsin (green: PDB 1U19) crystal structures. b) Conserved residues in rhodopsin based model and c) β_2-AR based model.

2.6 Construction of Homology Models

Models of the 5-HT_{2A} and H_1 receptors were built using two primary homology modeling techniques.

1) **Manual approach**. An alignment of the primary amino acid sequences was carried out using the ClustalX program.[159] The adjustments to the alignments were made wherever necessary. In the structurally conserved regions (primarily TMs) there was a high degree of sequence similarity and no insertions or deletions. Hence the amino acids were directly mutated from bovine rhodopsin to the corresponding residues in the template receptor (5-HT_{2A} and H_1). Most of the loop regions connecting the TM helices were of varied length and low in sequence homology, so they were modeled using a loop search facility (selection of loops from a database of high resolution protein structures found in the PDB) in the SYBYL molecular modeling package.

The N-terminal region of the 5-HT_{2A} receptor is of different length and showed little sequence similarity to the templates. Deletion of N-terminus from the 5-HT_{2A} receptor does not appear to affect receptor function[160] so explicit consideration of the N-terminal segment was not given for the generation of 5-HT_{2A} and H_1 models. The rhodopsin crystal structure consisted of only the first 18 residues in the C-terminus. A short α-helical segment (Helix 8) is present at the beginning of C-terminus following TM7. Helix 8 is perpendicular to the TM helix aggregate and is preceeded by the NPXXY motif of TM7 that is common to 5-HT receptor sequences. The side chains were then placed in the final model and checked for stereochemical integrity using the

PROCHECK[161] and ProTable feature within the SYBYL. The final receptor model was then energy-minimized.

2) MODELLER-generated models. Based on ligand binding studies and generation of constitutively active receptors, it has been implied that the rhodopsin can exist in two receptor states. Thus a ligand can bind to and stabilize the receptor, which can exist in various different conformations. In order to consider this conformational flexibility of the receptor, MODELLER[162] program was used in the generation of a population of receptor models, each with a slightly different conformation. MODELLER builds models of 3D structures of proteins by satisfaction of the spatial restraints. These restraints include the positions of the atoms in the template structures, distances and dihedral angles in the template structures. Stereochemical restraints such as bond length and bond angle are obtained from the CHARMM forcefield, and statistical preferences of dihedral angles and non-bonded atomic distances were obtained from a representative set of protein structures.

The 5-HT_{2A} (P28233) receptor sequence was aligned with a profile of several related class A GPCRs using the ClustalX program. Manual adjustment of the ClustalX alignment was required to properly align the disulfide-forming cysteine residues in the e2 loop. The result was an unambiguous alignment in the transmembrane (TM) helical regions of both the H_1 and 5-HT_{2A} sequences with that of the bovine rhodopsin. This alignment, along with a file containing the atomic coordinates of the inactive form of rhodopsin receptor (PDB ID = 1U19) or β_2-AR receptor (PDB ID = 2RH1), was used as input to the MODELLER software package to generate a population of 100 different

5-HT_{2A} homology models. Each of these receptor models was subsequently energy-minimized. The selection of the best fit model was done based on the observed interactions of the docked pose of the set of high affinity ligands (see experimental section), the reported site directed mutagenesis data for the respective receptors (H_1 and 5-HT_{2A}) and the observed GOLD scores. In addition to using the GOLD score, HINT (Hydropathy Interaction)[163] score was also used to characterize the nature of the binding site. An attempt was made to correlate the experimentally obtained binding affinity data with the GOLD scores and the HINT scores; however a very modest correlation was obtained.

2.6.1 Docking and Scoring methods for ligands

Following the generation of final models, the automated docking program GOLD[164] (Genetic Optimization for Ligand Docking) was then used to optimally place the ligands in the binding site of receptor models. The GOLD program uses a genetic algorithm to sample the complete range of ligand conformational flexibility with partial flexibility of the protein, and satisfies the basic requirement that the ligand must displace loosely bound water on binding. It works as follows: A population of potential solutions (i.e. possible docked orientations and conformations of the ligand) is set up at random. Each member of the population is encoded as a chromosome, which contains information about the mapping of protein ligand interactions. Each chromosome is assigned a fitness score based on its scoring function and the chromosomes within the population are ranked according to fitness. The population of chromosomes is iteratively optimized. At

each step, a point mutation may occur in a chromosome, or two chromosomes may mate to give two children chromosomes. The selection of chromosomes is inclined towards fitter members of the population, i.e. chromosomes corresponding to ligand dockings with good fitness scores. The fittest chromosomes are then used as the starting point of the next iteration. The GOLD program provides three different scoring functions 1) **Gold Score**. The original scoring function provided with GOLD, which has been optimized for the prediction of ligand binding positions and takes into account factors such as H-bonding energy (intra/inter molecular), van der Waals energy and ligand torsion strain. 2) **ChemScore**. It estimates the total free energy change that occurs on ligand binding and is trained by regression against binding affinity data. As the fitness scores are dimensionless, they cannot be used explicitly as values for binding energy or binding affinity 3) **ASP** (Astex Statistical Potential)[165] is an atom-atom potential derived from a database of protein-ligand complexes. Assessment of the docking and scoring methods indicated that reasonable results were obtained with ChemScore function of GOLD. This docking/scoring combination was used in most of the studies.

STRUCTURE-AFFINITY RELATIONSHIP STUDIES OF AMDA AND ITS ANALOGS AT 5-HT_{2A} AND H_1 RECEPTORS

3.1 Introduction

The serotonin 5-HT_2 and histamine H_1 receptors have been implicated in various central nervous system (CNS) related disorders.[42,109,166] In the absence of an experimentally-determined structure of a 5-HT family receptor, most structure-based drug design and optimization have relied on the information gained by structure-activity relationship (SAR) studies. Many SAR studies [51,125,167] for the 5-HT_2 ligands and their potential therapeutic uses [82,120,168] have been reported which stress the importance for the development of subtype selective ligands. In addition, the recent reports of the role of 5-HT_{2A} receptors in non-rapid eye movement sleep (NREMS) regulation and respiratory control,[58] suggest that selective antagonism of the 5-HT_{2A} receptor may be a promising new mechanism for the treatment of sleep disorders.[169] Thus, study of the 5-HT_2

receptor's binding site and generation of 5-HT_2 subtype-selective agents have been of considerable interest.

Molecular modeling studies based on the 5-HT_{2A} receptor sequence and high-resolution crystal structure of bovine rhodopsin have been reported by Westkaemper et al. and others to envision ways in which the existing and new compounds may interact with the residues in the ligand binding site.[170,171] Some of these studies suggested that the affinity of structures containing a phenylethylamine skeleton for the 5-HT_{2A} receptor could be enhanced by a second aromatic moiety, perhaps by participating in the additional aromatic-aromatic interactions between the ligand and the receptor.[172] This ultimately led to the design of 9-(aminomethyl)-9,10-dihydroanthracene (AMDA), which has proven to be a unique 5-HT_2 antagonist.[5] Although AMDA was structurally unique and simple, it became apparent that the AMDA structure bears general similarity to two classes of known drugs- tricyclic antidepressants and antipsychotic agents. Both of these classes are tricyclic amines consisting of two aromatic groups and a central non-aromatic ring that bears an alkylamine linker chain as in AMDA. Also, most clinically useful tricyclic amines are conformationally flexible. Since alkylamine chain length and *N*-alkylation are two major structural features that distinguish AMDA from conformationally flexible classical tricyclic amines, our group investigated the influence of chain length and *N*-alkylation in a series of AMDA analogs and compared to imipramine.[173,174] Also, a series of AMDA analogues were tested to determine the importance of the tricyclic ring system, and the effect of restricting the conformational freedom of the ammonium ion on 5-HT_{2A} receptor affinity. This resulted in the synthesis

of spiro[9,10-dihydroanthracene]-9,3'-pyrrolidine (SpAMDA), a conformationally constrained analog of AMDA.[175] Both AMDA and SpAMDA proved to be high-affinity antagonists for 5-$HT_{2A/2C}$ receptors with better selectivity for these receptors as compared to the D_2 receptor and serotonin and norepinephrine transporters, unlike the tricyclic antidepressants.

Histamine released by tissue mast cells, basophils and histaminergic neurons is also known to impact the ability to fall asleep and stay asleep.[176] Research and development of H_1 ligands have focused largely on antagonists that are used for their antiallergic effects in the periphery. However, the first-generation H_1 receptor antagonists (e.g. diphenhydramine, mepyramine, chlorpheniramine) also exhibit high H_1 receptor occupancy in the CNS due in part to their lipophilicity, leading to sedative effects.[177,178] Recent reports of the clinical trial studies have indicated that compound acting at both 5-HT_{2A} and H_1 receptor enhances sleep and should have low abuse potential.[123] Thus the study of ligands acting at both 5-HT_{2A} and H_1 receptors could be therapeutically relevant. Binding studies conducted for the selectivity profile of AMDA and its analogues showed that SpAMDA had high affinity for H_1 receptors (K_i = 4 nM), while AMDA showed moderate affinity (K_i = 197 nM). Given the potential therapeutic use of dual 5-HT_{2A}/H_1 ligands in the treatment of sleep disorders we decided to continue our studies on the AMDA structure and carried out the systematic structure-affinity relationship (SAFIR) studies of AMDA and its analogs.

3.2 Results and Discussion

3.2.1 Structure-Affinity Relationship Studies

Several reviews describing structure-activity relationship studies of diphenhydramine-like antihistamines have been reported.[178-180] The features that have been systematically varied include the nature of the two required aromatic groups, the terminal basic amine and the aliphatic linker between these two features. We have examined similar structural variations with AMDA as the parent structure. Note that replacement of the ether oxygen of diphenhydramine by a methylene unit results in compound **18** (Table 5). Replacement of the pyridin-2-yl group of the H_1 antagonist pheniramine with phenyl results in **15**. Binding affinities of the compounds for the 5-HT_{2A} and H_1 receptors are shown in Table 5 and displayed graphically in Figure 10. The most significant differences in affinity for both 5-HT_{2A} and H_1 receptors were observed between the 9-(aminoalkyl)-9,10-dihydroanthracene (DHA) compounds and their corresponding diphenylalkylamine (DPA) congeners. Ring-opening of the tricyclic system uniformly produced decreases in affinity for both 5-HT_{2A} and H_1 receptors. No DPA compound exhibited high affinity at 5-HT_{2A} (K_i <100 nM) and only three showed high affinity for H_1 receptors (**14**, K_i = 64 nM; **15**, K_i = 75 nM; **18**, K_i = 70 nM). In contrast, many of the DHA analogs were found to have high affinity at both receptors, demonstrating that rigid dihydroanthracene is a privileged structure.[181]

For compounds interacting with the H_1 receptor, progressively increasing either the number of methylene units in the linker or the number of *N*-methyl groups consistently retained or enhanced affinity in both the DHA and the DPA series. The H_1

receptor affinity was insensitive to chain length for the unsubstituted amine analogs of AMDA (**1**, K_i = 197 nM; **4**, K_i = 137 nM; **7**, K_i = 175 nM). In contrast, H_1 affinity increased with increasing chain length for both *N*-methylated (**2**, K_i = 189 nM; **5**, K_i = 47.5 nM; **8**, K_i = 3 nM) and *N*,*N*-dimethylated analogs (**3**, K_i = 25 nM; **6**, K_i = 6 nM; **9**, K_i = 0.5 nM). For the DHA analogs, *N*,*N*-dimethylation and a three-methylene linker was optimum for H_1 affinity (**9**, K_i = 0.5 nM). The trends in affinity at 5-HT_{2A} are less uniform. However, increasing the linker length for the *N*,*N*-dimethylated DHA analogs did produce a successive increase in affinity (**3,** K_i = 540 nM; **6**, K_i = 84 nM; **9**, K_i = 22 nM).

Like the H_1 receptor, the affinity of the DPA compounds for 5-HT_{2A} generally increased with increasing linker size or degree of *N*-methylation though, as noted above, no DPA compound was found to have substantial affinity (K_i < 700 nM) for 5-HT_{2A}. As observed previously[174] for DHA compounds with a one-methylene linker, 5-HT_{2A} affinity decreased as the degree of *N*-methylation increased (**1**, K_i = 20 nM; **2**, K_i = 52 nM; **3**, K_i = 540 nM). This trend was not observed for the other linker lengths where *N*-methylation showed the tendency to increase affinity. Affinities were more uniform for compounds with one *N*-methyl group (**2**, K_i = 52 nM; **5** K_i = 92 nM; **8**, K_i = 13 nM), and for those with two *N*-methyl groups, affinity increased with linker length by 25-fold (**3**, K_i = 540 nM; **6,** K_i = 84 nM; **9**, K_i = 22 nM). In general, binding affinity for the 5-HT_{2A} receptor is less sensitive to *N*-methylation and chain length variation than the H_1 receptor.

Table 5. Observed binding affinities for 9-(aminoalkyl)-9,10-dihydroanthracene (DHA) and diphenylalkylamine (DPA) analogs at 5-HT_{2A} and H_1 receptors.

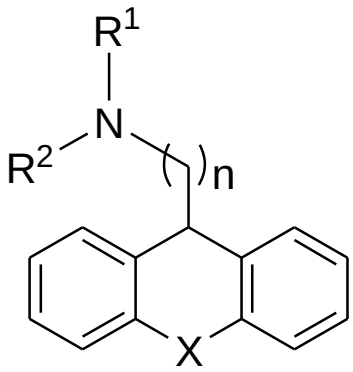

					K_i (nM)[a]	
Cpd	**X**	**n**	**R^1**	**R^2**	**5-HT_{2A}**	**H_1**
1	—CH_2—	1	—H	—H	20[b]	197 ± 67
2	—CH_2—	1	—H	—CH_3	52[b]	189 ± 28
3	—CH_2—	1	—CH_3	—CH_3	540[b]	25 ± 4
4	—CH_2—	2	—H	—H	480[b]	137 ± 47
5	—CH_2—	2	—H	—CH_3	92 ± 2.8	48 ± 7
6	—CH_2—	2	—CH_3	—CH_3	84 ± 9	6 ± 0.5
7	—CH_2—	3	—H	—H	32[b]	175 ± 59
8	—CH_2—	3	—H	—CH_3	13[b]	3 ± 0.3
9	—CH_2—	3	—CH_3	—CH_3	22[b]	0.5 ± 0.07
10	—H, —H	1	—H	—H	4480 ± 300	>10,000
11	—H, —H	1	—H	—CH_3	>10,000	>10,000
12	—H, —H	1	—CH_3	—CH_3	7360 ± 1691	5170 ± 750
13	—H, —H	2	—H	—H	>10,000	2760 ± 310
14	—H, —H	2	—H	—CH_3	1500 ± 163	60 ± 5
15	—H, —H	2	—CH_3	—CH_3	1640 ± 172	75 ± 6
16	—H, —H	3	—H	—H	2590 ± 632	1670 ± 180
17	—H, —H	3	—H	—CH_3	750 ± 79	390 ± 29
18	—H, —H	3	—CH_3	—CH_3	1150 ± 120	70 ± 5

. [a]Standard errors typically range between 15-25% of the K_i value. [b]From Runyon, et al., 2001.[174]

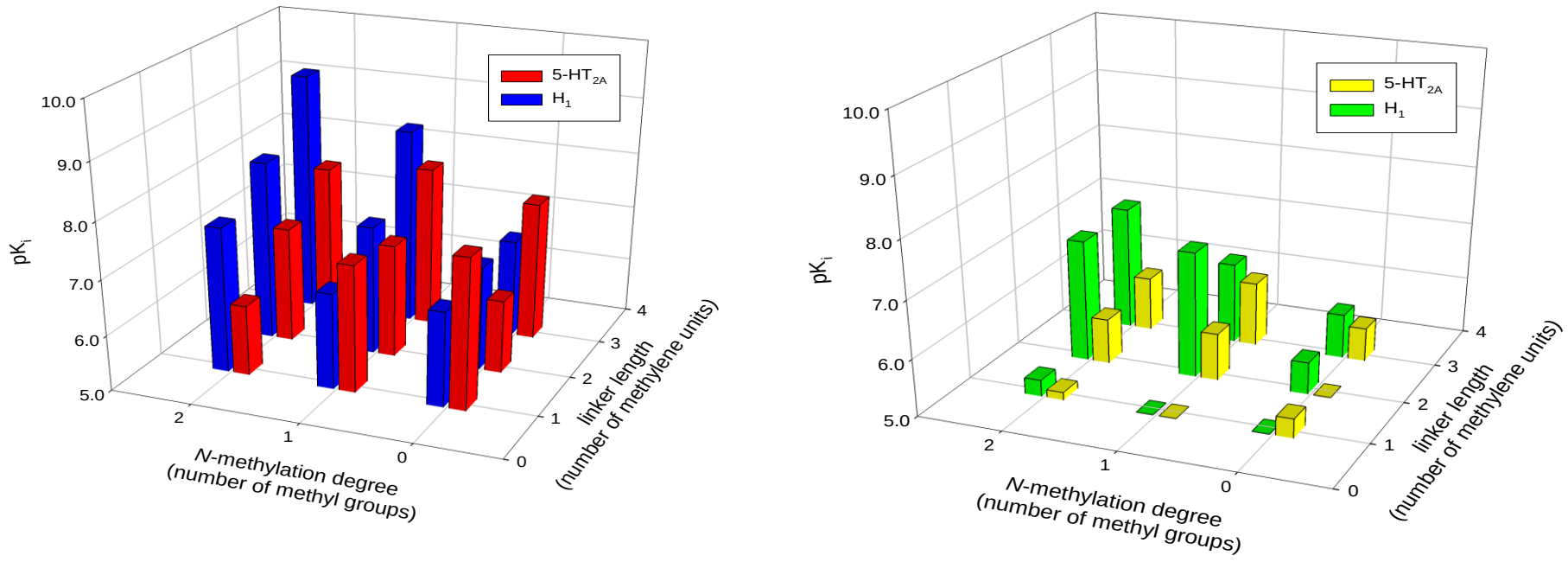

Figure 10. 3D bar graphs showing the affinities at 5-HT_{2A} and H_1 for the **a**) 9-(aminoalkyl)-9,10-dihydroanthracene (DHA) and **b**) diphenylalkylamine (DPA) analogs shown in table 5.

3.2.2 Modeling Receptor-Ligand Interactions: H_1 and 5-HT_{2A} Receptor Models

When considering the selectivity of a particular ligand for one receptor versus another, it is useful to analyze the differences in amino acids that comprise the binding sites of the two receptors. The alignment of the human H_1 and 5-HT_{2A} receptor sequences with that of human β_2-AR is presented in Figure 11. The H_1 receptor is phylogenetically related to the 5-HT_2 receptor subtypes, with high sequence homology specifically in the transmembrane region.[182] Based on the primary sequences, binding site analysis of both 5-HT_{2A} and H_1 receptors indicates that the major variations in amino acid constitution occur at positions 3.33, xl2.52, xl2.54, 5.39, 5.42, 6.55 and 7.35 (Figure 11). Differences in steric and electrostatic side chain properties at these and other positions are likely responsible for ligand selectivity of the two receptors. The H_1 receptor amino acid residue K191$^{5.39}$, not commonly found at this position among aminergic GPCRs, could be potentially exploited for the design of highly selective H_1 ligands. The three-dimensional arrangement of these residues is shown in Figure 12. The residues that are conserved between H_1 and 5-HT_{2A} are those that tend to be highly conserved among all aminergic GPCRs. These residues, primarily located in the inner region of the binding cavity, include W$^{3.28}$, the amine counter-ion D$^{3.32}$, S$^{3.36}$ and T$^{3.37}$, the 'aromatic cluster' residues W$^{6.48}$, F$^{6.52}$, and Y$^{7.43}$ (an H-bonding partner for D$^{3.32}$).

Models of human H_1 and 5-HT_{2A} receptors were generated with the MODELLER program using a high-resolution crystal structure of the human β_2-adrenergic receptor as a template. Inspection of putative receptor binding sites and ligand binding modes in our homology models (Figure 13) indicate two common interactions that occur for each of

the compounds at both 5-HT_{2A} and H_1 receptors: 1) The highly conserved aspartic acid residue at position[183] 3.32 (H_1, $D107^{3.32}$; 5-HT_{2A}, $D155^{3.32}$) is able to interact with the protonated amine of the docked ligand; and 2) Hydrophobic residues present in TM6 comprising the aromatic cluster[184] are able to interact with the aromatic rings of ligand. In other binding site locations, variability of amino acid residues at equivalent positions in the H_1 and 5-HT_{2A} influence the way the aromatic rings are oriented in the receptor, which in turn provide an explanation for the observed differences in affinity for AMDA and its analogs with varying chain lengths. The presence of hydrophobic residues surrounding the conserved $D^{3.32}$ in H_1 and in 5-HT_{2A}, together with the aromatic cluster region in H_1 and in 5-HT_{2A}, provide sites of favorable interaction with the ligands for each receptor.

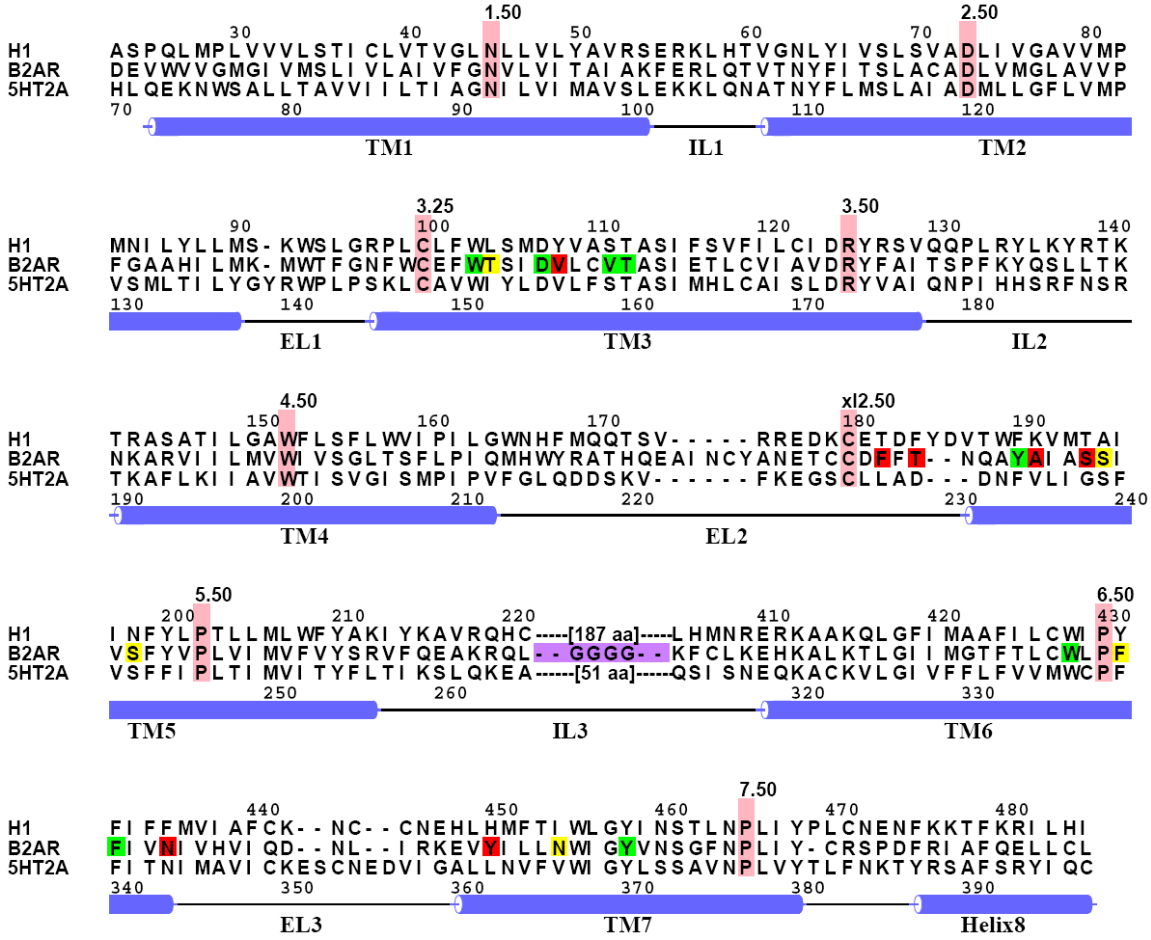

Figure 11. Alignment of the human β_2-adrenergic, H_1 and 5-HT_{2A} receptor sequences. Sequence positions highlighted in pink indicate highly conserved amino acids among the Class A GPCR family which serve as reference positions in the Ballesteros-Weinstein[153]numbering system. The traditional numbering shown corresponds to the H_1 (top) and 5-HT_{2A} (bottom) sequences. β_2-Adrenergic residues highlighted in purple indicate positions in the third intracellular loop that were mutated to glycine in the H_1 and 5-HT_{2A} sequences; these were retained in subsequent H_1 and 5-HT_{2A} models. Other residues highlighted in the β_2-AR sequence represent the binding site and are those which are within 5.0 Å of the carazolol ligand bound in the β_2AR. The residue color indicates the degree of similarity at a particular position as defined by the Gonnet PAM250 similarity matrix (green = identical; yellow = strong or weak conservation; red = no conservation). The figure was created using ALSCRIPT.[185]

3.2.3 Binding Mode Analysis

Compounds listed in Table 5 were docked into the receptor binding sites of the H_1 and 5-HT_{2A} receptor models using an automated docking routine GOLD. The GOLD scoring function (steric and electronic interactions) was used to select the favored ligand conformation. In addition, we carried out HINT[163] (Hydropathic INTeraction) analysis to characterize the nature of the binding site interactions. HINT is a free-energy-based method that considers atom-atom interactions in a bimolecular complex using a parameter set derived from octanol/water partition coefficients.[186] Modeling observations indicate that the compounds prefer to be oriented within the binding pockets of the two receptor models in similar but distinct binding modes (Figure 13). The well-known aspartate $D^{3.32}$ residue was found to interact with the basic amine in both receptors for each docked ligand, and the ligand aromatic rings were consistently oriented in the binding site surrounded by TM4, TM5 and TM6. In general, for the short-chain linker ligands there is a relatively small amount of ligand surface area that may interact with the surrounding hydrophobic environment in the binding pocket, accounting for the observed decreased affinity of these compounds at both 5-HT_{2A} and H_1. However, for AMDA (**1**), the observed high affinity could be due to the presence of an alternate binding mode.[170]

The tricyclic DHA ring system in **9** showed strong hydrophobic interactions ($Y108^{3.33}$, $L163^{4.61}$, $F168^{xl2.38}$, $F190^{5.38}$ and $F435^{6.55}$), with the phenyl rings oriented toward TM5 and the aliphatic linker located deep in the H_1 binding pocket. In contrast, in the 5-HT_{2A} model, **9** is oriented such that the phenyl rings are facing TM6 ($F339^{6.51}$, $F340^{6.52}$ and $N343^{6.55}$) and the aliphatic linker is positioned closer to EL2 (Figure 13a and

13d). For both H_1 and 5-HT_{2A}, the compound with the longest linker and highest degree of methylation (**9**) was found to have the greatest (H_1) or one of the highest (5-HT_{2A}) affinities among the compounds tested. The methylene linkers in the H_1 receptor are able to interact with residues $L104^{3.29}$ and $Y431^{6.51}$ which may explain the comparatively higher affinity of **9** for H_1 than for 5-HT_{2A}. Further, the observed differences in ligand orientation within the receptor binding site can account for the preference for *N*-methylation at H_1, with the methyl groups more closely surrounded by hydrophobic residues as compared to 5-HT_{2A} (Figure 13a and 13d).

For the unbridged DPA analogs, the increased conformational flexibility (as compared to DHA) and intramolecular steric repulsion produce a twisted ring orientation. This results in more unfavorable receptor-ligand interactions (steric clashes and polar-nonpolar interactions) involving the ring system and the surrounding residues (Figure 13b and 13e) which may explain the generally low affinity of compound in DPA series as compared to DHA series.

HINT hydropathy interaction analysis provided additional support for the proposed orientation of the ligands in the binding pocket. Figure 14 shows the HINT maps generated for compound **9** (which has highest affinity for both receptors) in the binding sites of the H_1 and 5-HT_{2A} receptors. In each case the tricyclic ring system fits into the hydrophobic 'aromatic cluster' while the amine group faces $D107^{3.32}$ and is stabilized by both ionic and hydrogen bonding interactions. However, both the aliphatic linker region and the *N*-methyl groups engage in more extensive hydrophobic interactions in H_1 than in 5-HT_{2A}.

In addition, the receptor-ligand complexes described here are in general agreement with other studies that have implicated residues that contribute to an antagonist binding site in H_1 and 5-HT_{2A}.[170,187,188] Besides the several key residues that have been reported by site-directed mutagenesis studies in H_1 receptor models[189] (W158$^{4.56}$, F424$^{6.44}$, W428$^{6.48}$, F432$^{6.52}$ and F435$^{6.55}$) and 5-HT_{2A} receptor models[190] (F243$^{5.47}$, W336$^{6.48}$, F339$^{6.51}$, F340$^{6.52}$), we found that Y108$^{3.33}$ was oriented to favorably interact with ligands in the binding pocket of the H_1 receptor, and the cognate residue V156$^{3.33}$ for the 5-HT_{2A} receptor. The differences in the stereoelectronic character of these residues likely contribute to the differences in the way the ligand binds to these receptors, and consequently the observed differences in binding affinity.

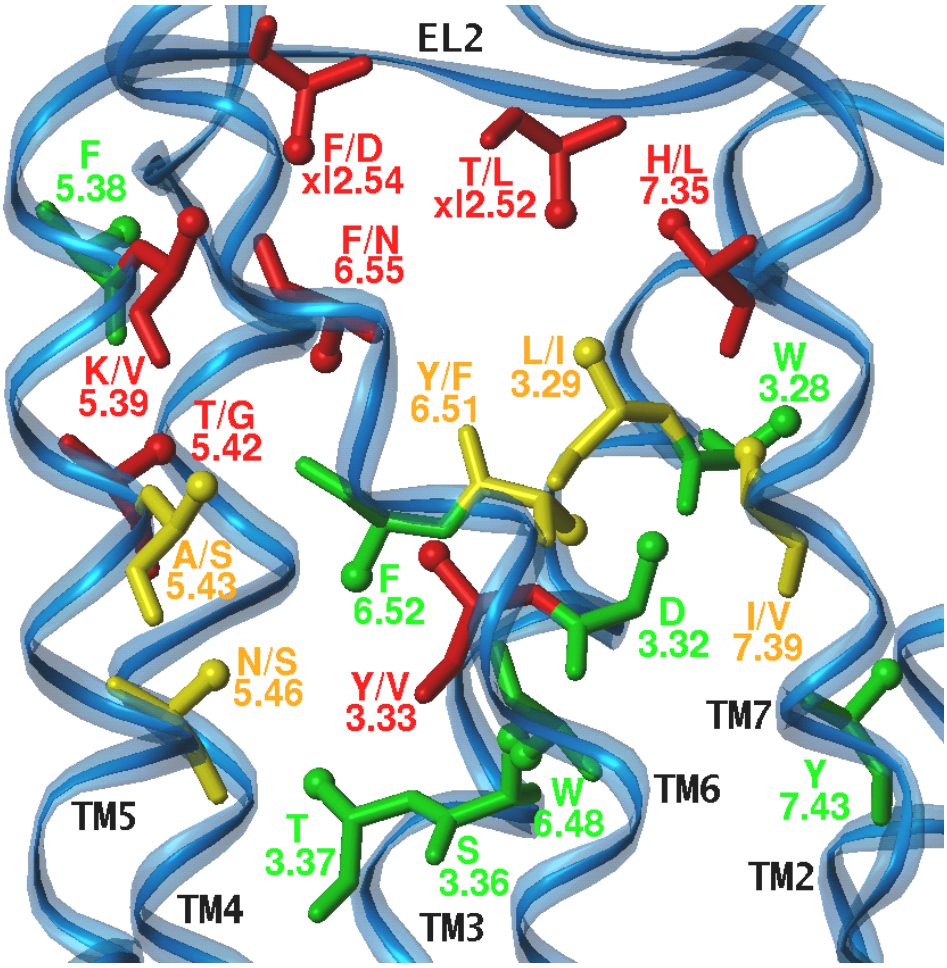

Figure 12. Illustration of the differences in binding site residue composition of the H_1 and 5-HT_{2A} receptors. Residues are truncated at the C^{β} carbon atom (ball-and-stick representation) and are colored based on residue similarity as described in figure 11. For those positions whose residue identity differs, the H_1 residue is listed first, followed by the 5-HT_{2A} residue.

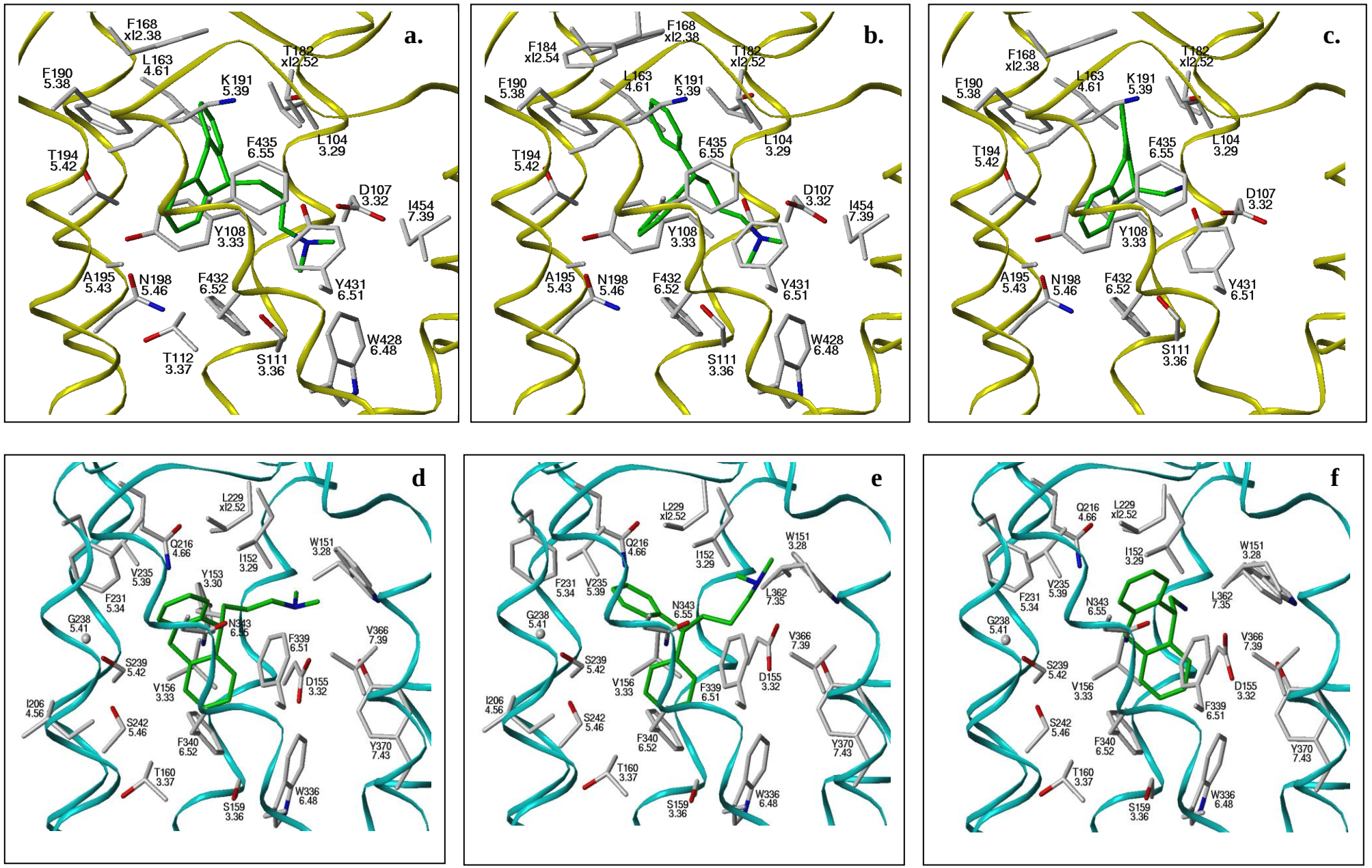

Figure 13. Docked receptor-ligand complexes. The H_1 receptor model with compounds a) **9**, b) **18** and c) **1**. The 5-HT_{2A} receptor model with compounds d) **9**, e) **18** and f) **1**. Residues within 5 Å of the bound ligand are displayed.

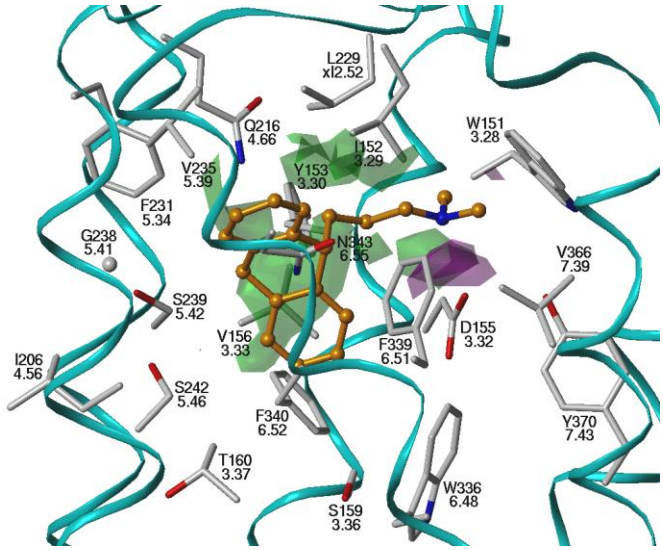

a.

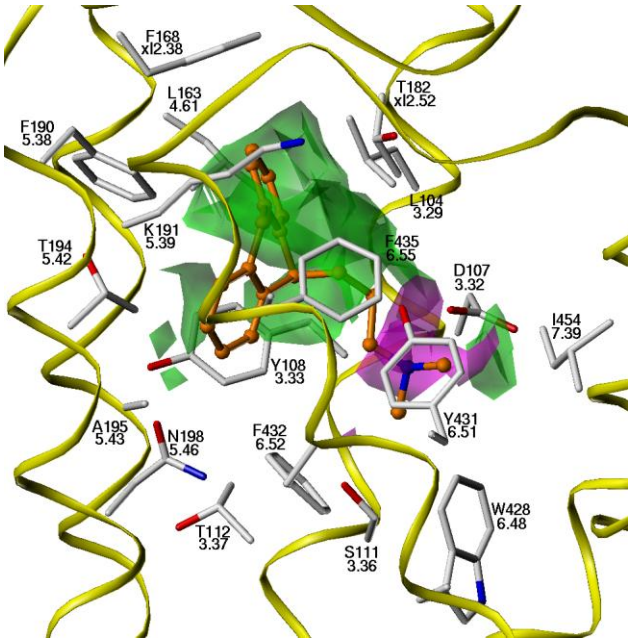

b.

Figure 14. HINT interaction maps for compound **9** in a) 5-HT_{2A} and b) H_1 binding sites. Regions of favorable hydrophobic (green) and polar (magenta) interactions are shown as contours.

3.2.4 Chemistry

9-Aminomethyl-9,10-dihydroanthracene (**1**) was reported by our group in the past.[173] (9,10-Dihydroanthracen-10-yl)-*N*-methylmethanamine (**2**) and (9,10-dihydroanthracen-10-yl)-*N*,*N*-dimethylmethanamine (**3**) were prepared by reduction (BH_3•THF) of amides **44** and **45** obtained by the treatment of the acid chloride of **43** with methyl or dimethylamine[174] (Scheme 1). 2-(9,10-Dihydroanthracen-9-yl)ethanamine (**4**) was prepared from 2-(anthracen-9-yl)ethanamine (**48**). The condensation of 9-anthraldehyde (**46**) with nitromethane in methylene chloride gave 9-(2-nitrovinyl)anthracene (**47**)[191] which was reduced to 2-(anthracen-9-yl)ethanamine (**48**) using $LiAlH_4$/THF. The target molecule i.e., **4** was then prepared through middle ring reduction using sodium metal in liquid ammonia[192] (Scheme 2). 2-(9,10-Dihydroanthracen-9-yl)-*N*-methylethanamine (**5**) was synthesized using 9-hydroxymethylanthracene (**49)** as the starting material. Bromination[193] followed by cyanation[194] of the alcohol gave 2-(anthracen-9-yl)acetonitrile (**51**) which was further hydrolyzed to the corresponding acid **52**. Anthracene ring reduction using sodium metal in 1-pentanol gave 2-(9,10-dihydroanthracen-9-yl)acetic acid (**53**). Sequential conversion of the acid **53** to its amide **54** via the chloride, followed by reduction gave the target molecule **5** (Scheme 3). 2-(9,10-Dihydroanthracen-9-yl)-*N*,*N*-dimethylethanamine (**6**) was prepared by reductive amination[195] of 2-(9,10-dihydroanthracen-9-yl)acetaldehyde (**57**) obtained by the oxidation of 2-(9,10-dihydroanthracen-9-yl)ethanol (**56**)[196] (Scheme 4). 3-(9,10-Dihydroanthracen-9-yl)propan-1-amine (**7**), 3-(9,10-dihydroanthracen-9-yl)-*N*-methylpropan-1-amine (**8**), 3-(9,10-dihydroanthracen-9-yl)-*N*,*N*-dimethylpropan-1-

amine (**9**) were prepared by reduction (BH_3•THF) of amides **63, 64** and **65** obtained by treatment of the acid chloride of 3-(9,10-dihydroanthracen-9-yl)propanoic acid (**62**)[197] with ammonia gas, methylamine and dimethylamine, respectively (Scheme 5). 2,2-Diphenylethanamine (**10**) was commercially obtained. *N*-methyl-2,2-diphenylethanamine (**11**) was obtained by the *N*-methylation of the respective amine **66** as reported[198] (Scheme 6). Compounds *N*,*N*-dimethyl-2,2-diphenylethanamine (**12**) and *N*-methyl-3,3-diphenylpropan-1-amine (**14**) were obtained commercially. 3,3-Diphenylpropan-1-amine hydrochloride (**13**) was obtained in salt form from commercially available 3,3-diphenylpropan-1-amine. *N*,*N*-Dimethyl-3,3-diphenylpropan-1-amine (**15**)[199] was synthesized by reductive amination of 3,3-diphenylpropanal (**68**) obtained by the oxidation of commercially available 3,3-diphenylpropanol (**67)** using Dess-Martin reagent (Scheme 7). 4,4-Diphenylbutan-1-amine (**16**)[200] was prepared by the BH_3•THF reduction of 4,4-diphenylbutyronitrile (**71**) that was obtained from potassium amide/liquid ammonia solution of diphenylmethane (**69**) by alkylation with bromopropionitrile[201] (Scheme 8). *N*-Methyl-4,4-diphenylbutan-1-amine (**17**) and *N*,*N*-dimethyl-4,4-diphenylbutan-1-amine (**18**) were prepared by reduction (BH_3•THF) of amides **75** and **76** obtained by treatment of the acid chloride of 4,4-diphenylbutyric acid (**73**)[202] with methylamine and dimethylamine, respectively. The intermediate compound **73** was obtained from treatment of commercially available lactone **72** with benzene in the presence of anhydrous aluminum chloride (Scheme 9).

3.3 Synthetic Schemes

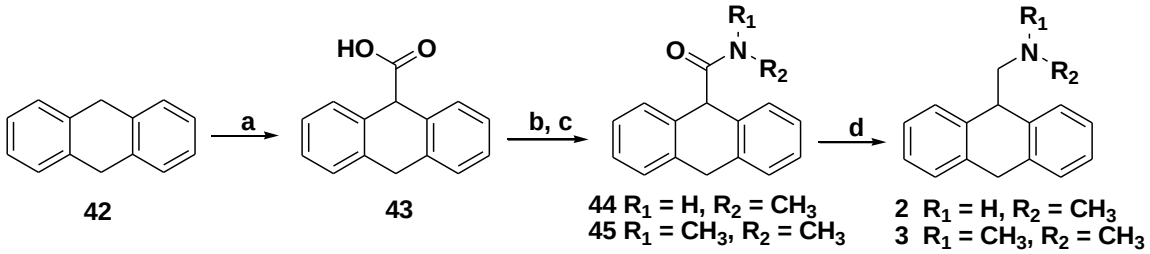

Scheme 1. a) *n*-BuLi, diethyl ether, dry ice; b) $SOCl_2$, reflux; c) methyl or dimethyl amine, THF, 25 ºC; d) BH_3•THF, reflux.

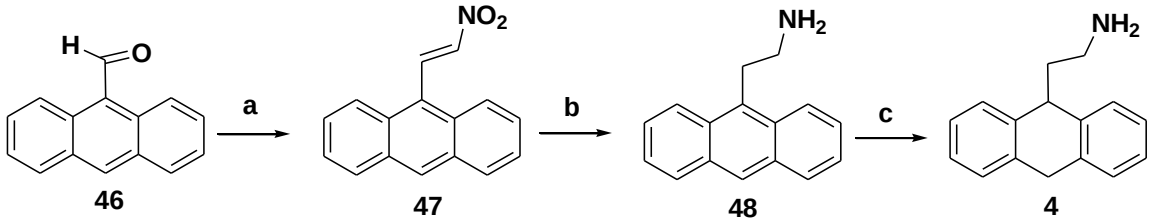

Scheme 2. (a) CH_3NO_2; (b) $LiAlH_4$, THF; (c) Na, liquid ammonia.

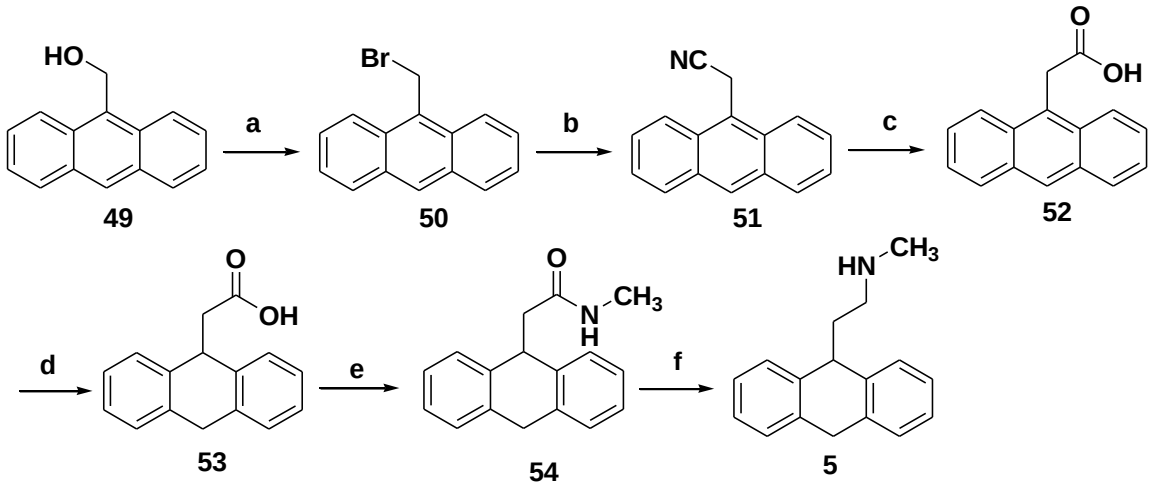

Scheme 3. (a) PBr_3 , toluene; (b) KCN, DMSO; (c) ethylene glycol, KOH; (d) Na, 1-pentanol; (e) $SOCl_2$, benzene, methylamine (2M) THF; (f) BH_3•THF, reflux.

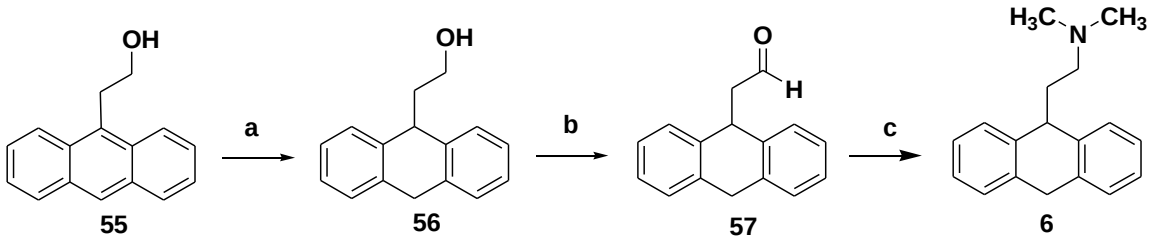

Scheme 4. (a) Na_2K silica gel, THF; (b) Dess-Martin (periodinane) reagent, CH_2Cl_2; (c) dimethylamine hydrochloride, $Ti(O^iPr)_4$, NEt_3, abs EtOH, $NaBH_4$.

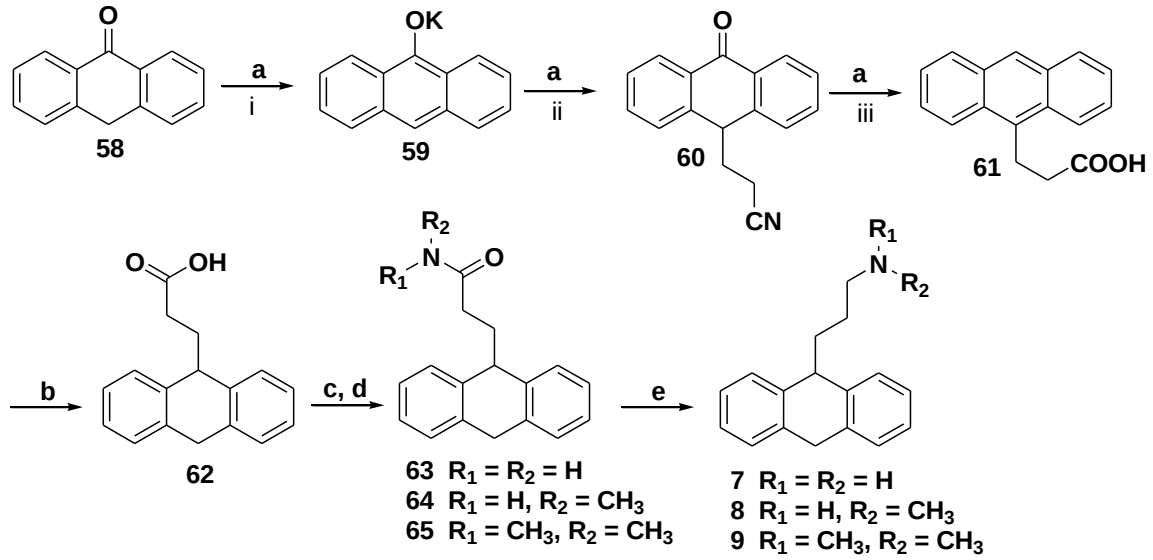

Scheme 5. (a) i. $KOC(CH_3)_3$ ii. acrylonitrile, *t*-butyl alcohol, iii. NH_4OH, Zn dust, hydrochloric acid reflux; (b) Na, 1-pentanol, reflux, 10 min; (c) $SOCl_2$, reflux, 2 hr; (d) NH_3 or methylamine or dimethylamine, THF, 25 ºC; (e) BH_3•THF, reflux, 6 hr.

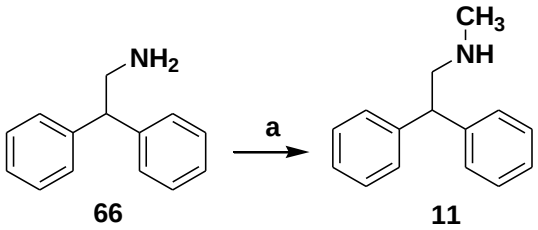

Scheme 6. (a) aqueous (37%) formaldehyde, CH_3CN, $NaBH_3CN$, glacial acetic acid, (2N) KOH, Et_2O.

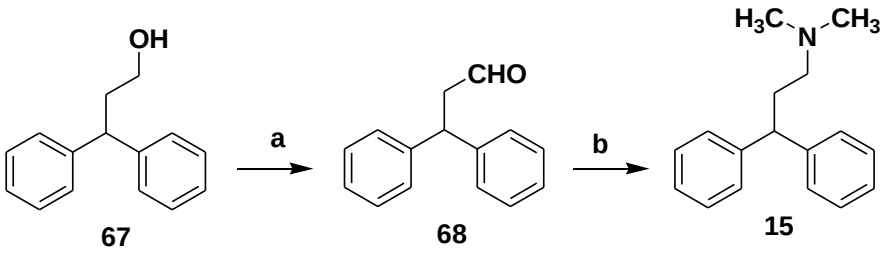

Scheme 7. a) Dess-Martin (periodinane) reagent, anhydrous CH_2Cl_2; (b) dimethylamine hydrochloride, $Ti(O^iPr)_4$, NEt_3, abs EtOH, $NaBH_4$.

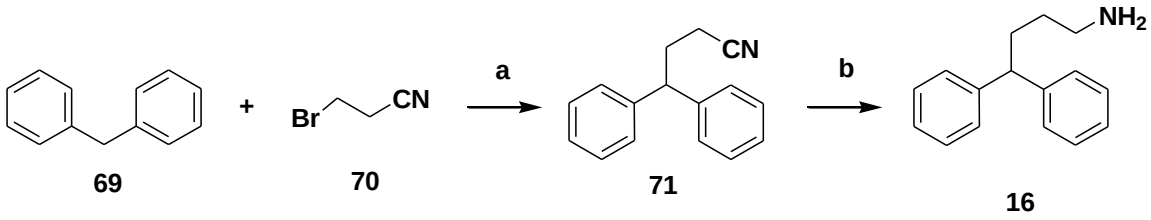

Scheme 8. a) K metal, $Fe(NO_3)_3$, liq NH_3, Et_2O; (b) BH_3•THF.

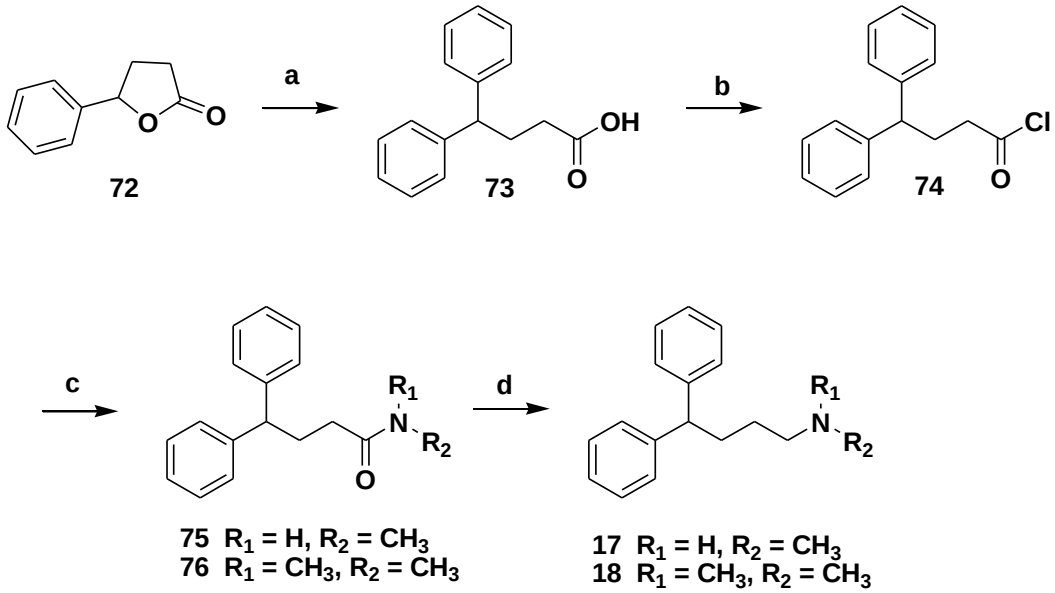

Scheme 9. a) anhydrous benzene, $AlCl_3$; (b) $SOCl_2$, benzene; (c) methylamine or dimethylamine (2M) THF; (d) BH_3•THF.

3.4 Molecular modeling

Homology models were built using the automated software MODELLER (details in experimental section). The populations of 100 different H_1 and 5-HT_{2A} homology models were generated and subsequently energy minimized. The β_2-adrenergic receptor was used as the template for the generation of models. The selection of the best fit model in each (H_1 and 5-HT_{2A}) case was based on the fitness function values obtained as a result of docking studies conducted using the automated docking program GOLD details in experimental). In addition to consistently observed GOLD score, steric and electronic interactions of the docked poses and reported site-directed mutagenesis data was considered for the selection of the best fit model. Further, HINT scoring function was used to characterize the nature of the binding site interactions (details in experimental section).

3.5 Conclusions

Within the matrix of compounds synthesized and tested, the *N*,*N*-dimethylated chain lengthened propylene analog of AMDA shows the highest affinity at both 5-HT_{2A} and H_1 receptors (**9**; 5-HT_{2A}, K_i = 22 nM; H_1, K_i = 0.5 nM) and the highest selectivity for the H_1 receptor (44-fold). In addition, removing the conformational restriction of the dihydroanthracene tricyclic system is detrimental to the ligand affinity for both 5-HT_{2A} and H_1 receptors. Structure-affinity relationships among these compounds show that *N*-alkylation either decreases or has little effect on 5-HT_{2A} affinity. In the case of compounds with propylene linker (**7**, **8** and **9**), all have relatively high affinity for the 5-HT_{2A} receptor and are less sensitive to the degree of *N*-alkylation. In addition, the ring-opening of the dihydroanthracene system to diphenyl system is generally unfavorable for the affinity at both 5-HT_{2A} and H_1 receptors. Hydropathic analysis of the modeled complexes supports the proposed role of the TM6 aromatic cluster in directing binding. The proposed differences in the binding pocket of H_1 ($Y108^{3.33}$) and 5-HT_{2A} ($V156^{3.33}$) may determine the way ligands bind, which in turn determine the selectivity of the ligands for each of two receptors. These preliminary modeling results provide a qualitative understanding of how AMDA analogs might interact with the 5-HT_{2A} and H_1 receptors. This study also provides potential insight into the mechanisms by which differences in the structures of the receptor and ligand determine the receptor selectivity.

RING-ANNULATED AND *N*-SUBSTITUTED ANALOGS OF AMDA AS STRUCTURAL PROBES FOR 5-HT_{2A} AND H_1 RECEPTORS

4.1 Introduction

In the past few years, much information has been generated about the 5-HT_2 receptor and its subtypes.[3,49] However, it is still not completely clear how serotonergic ligands (agonists, partial agonists and antagonists) including 5-HT itself interact with the receptors. In the absence of a crystal structure for the 5-HT_2 receptor family, models generated from a representative GPCR such as rhodopsin or a β-adrenoceptor are used to study possible drug-receptor interactions.[51,171,203] We have previously synthesized and tested many analogs of the selective 5-HT_2 antagonist 9-aminomethyl-9,10-dihydranthracene (AMDA). Modeling investigations of AMDA and its analogues have provided some insight into the possible ligand-receptor interactions responsible for their affinities at the 5-HT_{2A} and H_1 receptors.[170,204,205] Literature studies involving H_1 antagonists show that diphenhydramine-like structures are the most investigated series of anti-H_1 active structures.[107] The results of the quantitative structure-activity relationship (QSAR)[206] studies of these series of compounds suggest that the major characteristics for

H_1 activity are high lipophilicity of an aromatic group, a given distance between a hydrophobic region and observed ammonium ion and a region of relatively large "bulk acceptance" around the ammonium ion. In order to further explore receptor binding site dimensions, we synthesized and tested *N*-substituted and ring-homologated analogues of AMDA which can in turn also serve as structural probes to determine the preferred ligand orientations, ligand-receptor interactions and predict the dimensions of the binding site.

4.2 Substituted Phenylalkylamine Analogs of AMDA as Structural Probes

Molecular modeling studies conducted by us suggested that, all the AMDA analogs are oriented in a similar fashion but exhibit a different binding mode for 5-HT_{2A} and H_1 receptors.[205] In both cases, the tricyclic ring system prefers a hydrophobic core surrounded by TM 4, 5, and 6 whereas the basic amine-bearing end is oriented toward TM3. In accordance with the existing trend for various class of antihistamines,[107] it was observed that *N*-alkylation is favorable for the H_1 receptor affinity among AMDA analogs. However, in case of 5-HT_{2A} receptor an opposite trend was observed in which *N*-alkylation led to decreases in the binding affinity. As mentioned above, we synthesized and tested *N*-phenylalkylamine analogs of AMDA (**19-22,** Figure 15) to further explore the bulk tolerance at this portion of the binding site. Compound **19** was previously synthesized in our group. The observed affinity data for these compounds showed that these compounds had low affinity (K_i = 365 to 710 nM) at 5-HT_{2A} and H_1 (K_i = 223 to 964 nM) receptors. The slight variation in the binding affinity values for the 5-HT_{2A} receptor corresponded to the previously observed trend. However, it was

surprising that phenylalkyl substitution at the basic amine greatly reduces affinity at the H_1 receptor (**20**, K_i = 242 nM, **21**, K_i = 223 nM, **22**, K_i = 964 nM), since both classical and tricyclic antihistamines often have very bulky amine substituents.[107] The results obtained suggest the possibility that the basic amine in the *N*-phenylalkyl AMDA analogs bind in a different environment as compared to the diphenhydramine series and tricyclic antihistamines. The proposed orientation of the *N*-phenylalkyl substituent within the 5-HT_{2A} and H_1 receptor binding site is shown in Figure 16a and 16b.

In addition, the synthesis and testing of the quaternary ammonium salt of AMDA (**23**) showed substantially higher affinity for H_1 receptor (K_i = 70 nM) as compared to 5-HT_{2A} receptor (K_i = 4000 nM). The observed affinity for the H_1 receptor could be due to the presence of Y6.51 in the binding site that forms a π-cation bond[207] with the quaternary ammonium ion in the H_1 receptor but not in the 5-HT_{2A} receptor (Figure 17), further suggesting the possibility of a more hydrophobic binding site environment in H_1 as compared to 5-HT_{2A}

4.3 Ring-annulated Analogs of AMDA as Dimensional Probes

The concept of using ring-annulated or so called "stretched-out" analogues of high affinity ligands as dimensional probes has been reported but not widely employed.[208] By carrying out systematic ring annulation and substitution one can infer information about the dimensions of the binding site.[209-211] AMDA and its analogs contain a rigid tricycyclic scaffold. Previously conducted SAR studies[170] of substituted AMDA analogs by us have indicated that there may be a great deal of steric tolerance

around this tricyclic ring system. However, the large substituents examined to date have a high degree of rotational freedom due to alkyl chain flexibility. In order to construct a rigid and elongated structure we decided to expand the tricyclic ring system with fused aromatic rings (Figure 15). The expansion of the AMDA pharmacophore by benzene fusion will provide dimensional probes which can extend beyond the existing site and may permit interactions with additional binding site residues. The initial compound that we attempted to synthesize and test was tetracene **25**. However, the synthetic methodology chosen for **25** gave a mixture (75:25) of isomers of tetraphene **24** and tetracene **25** respectively (Scheme 12). The binding affinity data obtained for this mixture had the K_i value of 10 nM (5-HT_{2A}). Thus it was concluded that at least one of the isomers binds with high affinity. Based on our previous SAR study experience we synthesized the ring substituted methoxy-analogue **26** of the expanded AMDA structure with a similar procedure. The attempted synthesis (Scheme 12) gave a mixture of two isomers **26** and **27**. Due to the challenges faced in the final cyclization step and difficulty in the separation of products, the reaction gave a very low yield of the final product. The purification of the reaction mixture resulted in the separation of only the major isomer i.e., (**26**) whose binding affinity was determined. The binding affinity data showed that methoxy-substituted isomer **26** had reasonable affinity (K_i = 21 nM) for the 5-HT_{2A} receptor while possessing very low affinity for H_1 receptor (K_i = 2640 nM). In order to further confirm the possibility that a single isomer is responsible for high affinity at 5-HT_{2A}, the synthesis of compound **25** was carried out by another group member (S. Peddi) via an unambiguous cyclization route. The binding studies of compound **25** indicated that

it had no affinity for 5-HT_{2A} receptor (K_i = >10,000 nM). These results indicate the possibility of an isomer having a pharmacophore features similar to **26** to be responsible for the affinity of the ligand.

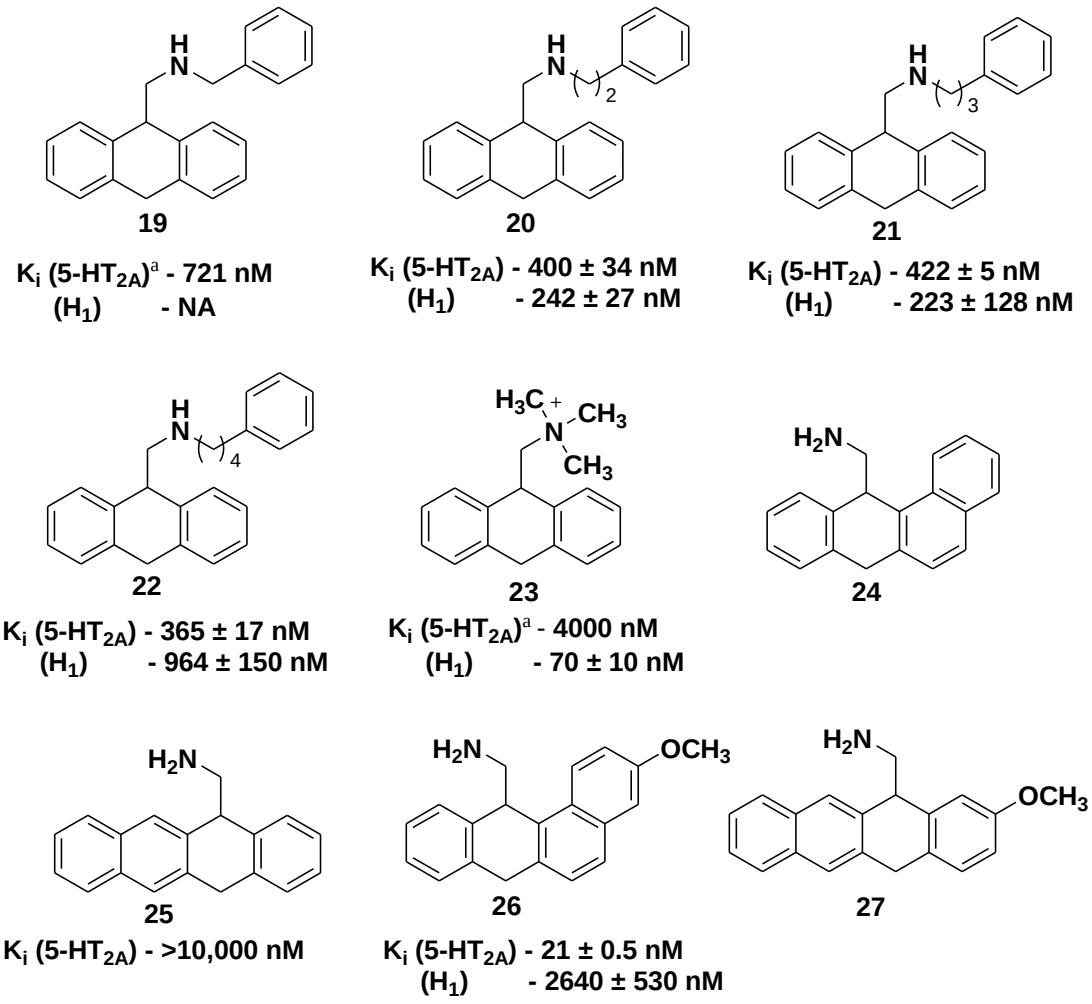

Figure 15. Binding affinity data of AMDA analogs as molecular probes. [a]From Runyon, et al., *Biorg. Med. Chem. Lett.* **2001**, 11, 655-688.[174]

4.4 Molecular Modeling studies

The generation and refinement of the 5-HT_{2A} and H_1 receptor homology models used in the docking studies is described in the experimental section. A virtual library of

compounds shown in Figure 15 with explicit consideration of stereoisomers was built and energy-minimized. The structures were then docked into the receptor binding site using the automated docking program GOLD (experimental section). To begin with, the structures were docked into the homology model built using β_2-adrenergic receptor as the template. However, the docked poses failed to show the optimum interactions between the ligand and the binding site residues hence we used the homology models built using bovine rhodopsin as the template. Visual inspection of docking poses in conjunction with the ChemScore fitness function was used to select the final solution for each isomer. The GOLD program used for docking was able to place all the ligands in the previously predicted binding site (Figures 16-18). In each solution, the ligand ammonium ion interacts with the D155$^{3.32}$ residue in the binding site. The tetraphene isomer (**24)** showed lipophilic interactions with the hydrophobic residues in the binding pocket (Figure 18). In the case of the methoxy substituted analog **26**, docked pose of both the (*R*)- and (*S*)-stereoisomer showed additional interactions with hydrogen-bond donating S159$^{3.36}$ and S77$^{1.35}$ residues respectively, in the 5-HT$_{2A}$ binding site. The vast difference in the affinity value of compound **25** (>10,000 nM) and mixture of **24** and **25** (K_i = 10 nM), combined with the observation that methoxy-substituted compound (**26**) showed higher affinity (K_i = 21 nM) suggest that the non-linear tetraphene analogs are responsible for the observed affinity.

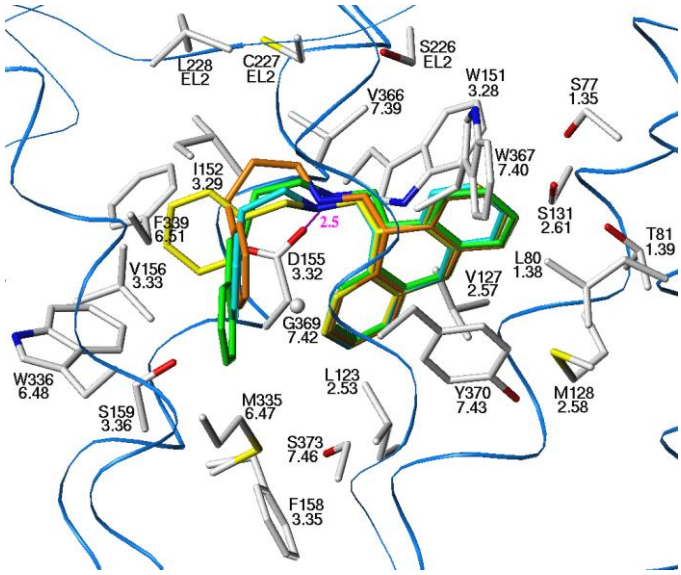

a.

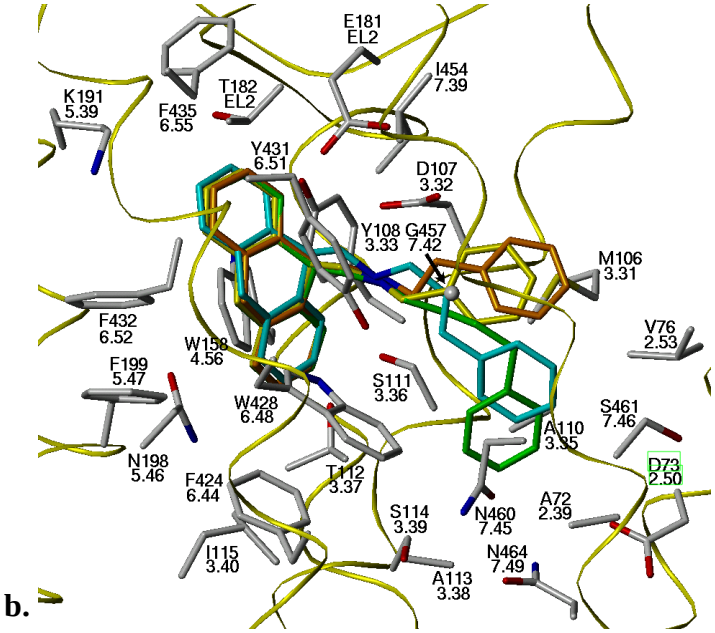

b.

Figure 16. Proposed binding mode of phenylalkylamine analogs of AMDA in the binding site of the a) 5-HT_{2A} and b) H_1 receptors. Ligands are represented as capped stick model with compounds **19** (yellow), **20** (orange), **21** (cyan) and **22** (green) respectively. Residues within 4 Å of the bound ligands are displayed.

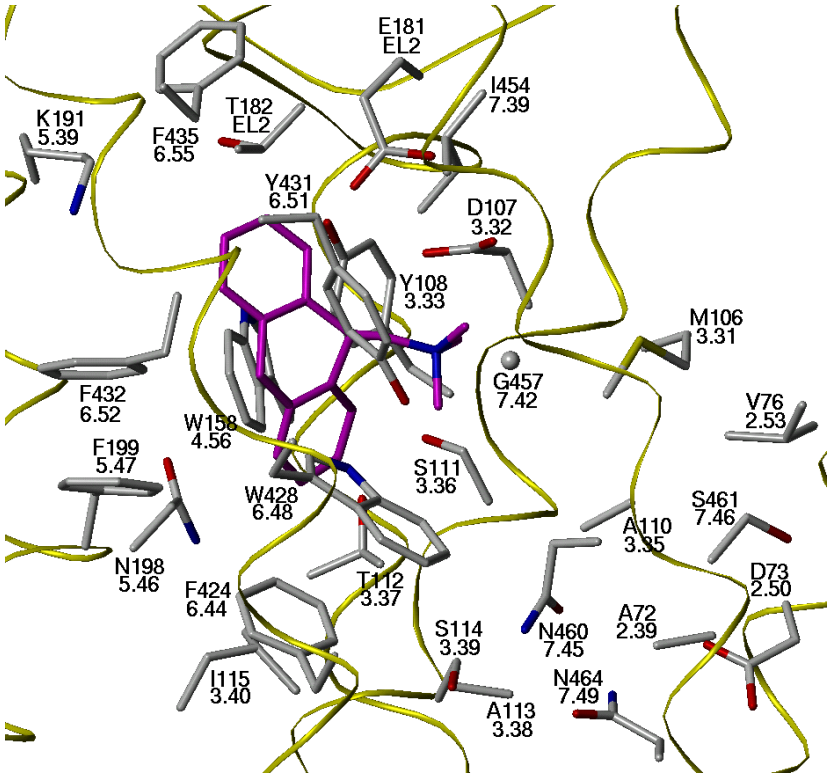

Figure 17. Proposed binding mode of quaternary ammonium salt of AMDA in the binding site of the H_1 receptor. Compound **23 (**magenta) is represented as capped stick model. Residues within 4 Å of the bound ligands are displayed.

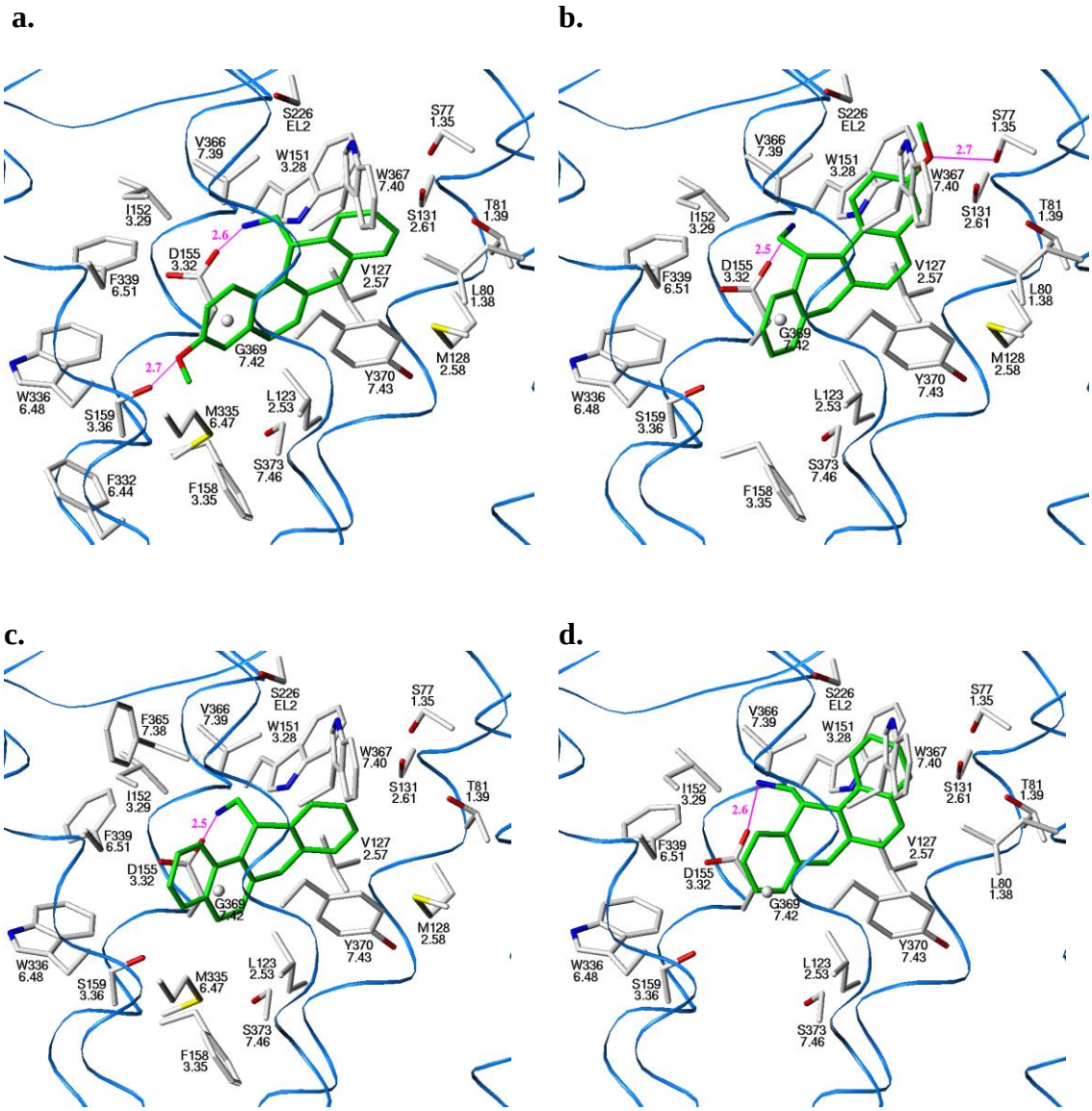

.

Figure 18. Proposed binding mode of isomers of ring-homologated AMDA analogs a) (*R*)-**26** b) (*S*)-**26** c) (*R*)-**24** d) (*S*)-**24** within the binding site of the 5-HT_{2A} receptor. Residues within 4 Å of the bound ligands are displayed.

4.5 Chemistry

Compound 9-(*N*-benzylaminomethyl)-9,10-dihydroanthracene (**19**) was reported by our group earlier.[174] The phenylalkyl amines **20, 21** and **22** were prepared by reduction (BH_3•THF) of amides obtained by the treatment of the acid chloride with phenylethyl-, phenylpropyl and phenylbutyl amine respectively (Scheme 10). Compound **23** was obtained by the *N*-methylation of previously synthesized compound **3** using iodomethane (Scheme 11). In case of ring-annulated analogs, commercially available α-bromo-o-tolunitrile (**80**) on treatment with DIBAL-H in anhydrous CH_2Cl_2 and work up using aqueous HBr gave the aldehyde **81** in quantitative yields.[212] Palladium catalyzed cross-coupling of 2-naphthylboronic acid and 6-methoxy-2-naphthylboronic acid with the aldehyde **81** gave the respective coupled aldehydes **82** and **83**. Cyanosilylation of the aldehydes **82** and **83** using TMSCN gave the cyano trimethylsilyl ether as intermediates, which were reduced with $LiAlH_4$ to give the respective amino alcohols **84** and **85**. Cyclodehydration of aminoalcohols using methanesulfonic acid gave the isomers of cyclized products **24, 25** and **26, 27** respectively (Scheme 12).

4.6 Synthetic Schemes

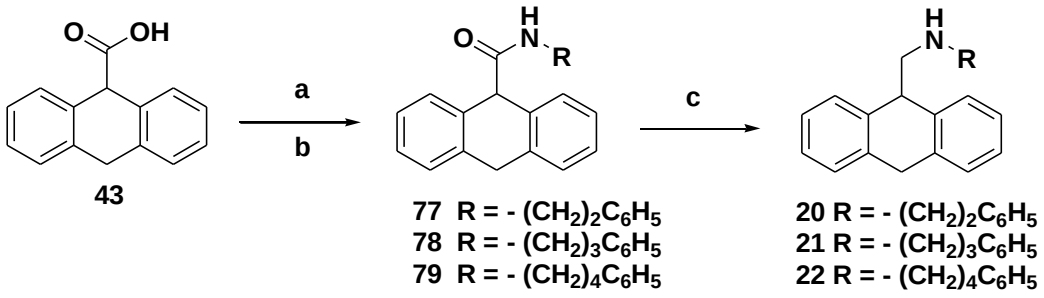

Scheme 10. (a) $SOCl_2$, benzene; (b) phenylethylamine or phenylpropylamine or phenylbutylamine; (c) BH_3•THF.

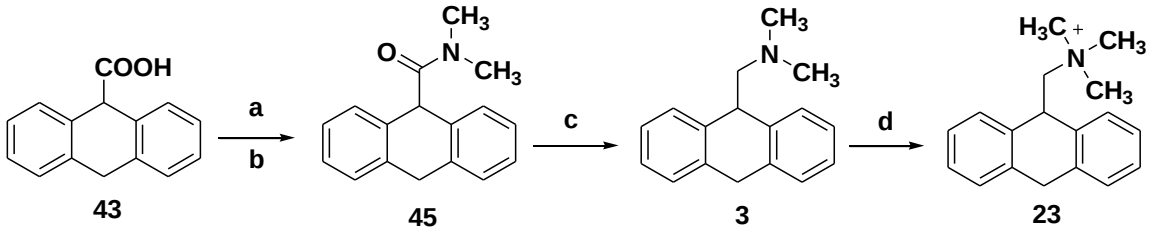

Scheme 11. (a) $SOCl_2$, reflux; (b) dimethylamine, THF, 25 ºC; (c) BH_3•THF, reflux; (d) iodomethane, CH_2Cl_2.

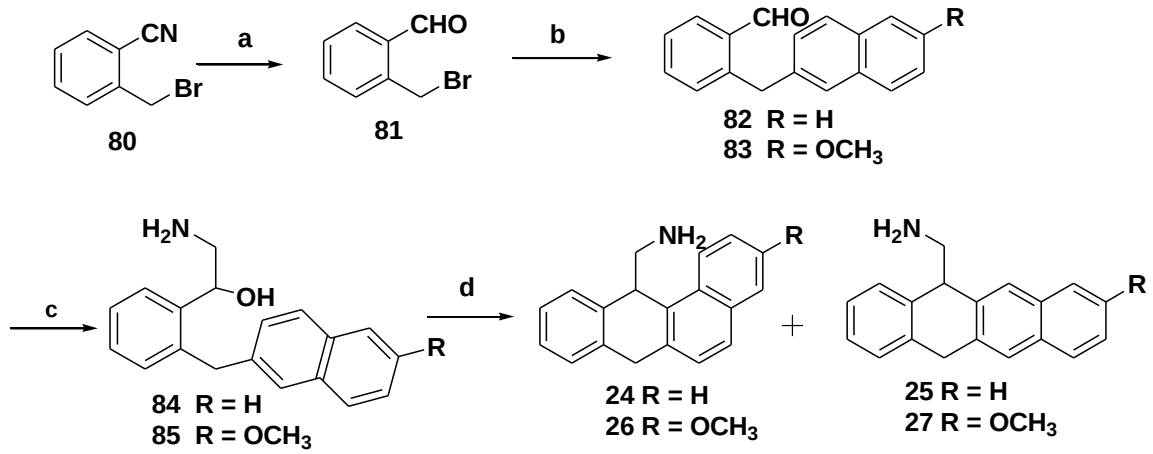

Scheme 12. (a) DIBAL-H, CH_2Cl_2; (b) $Pd(PPh_3)_4$, K_3PO_4, 2-naphthylboronic acid/6-methoxy-2-naphthylboronic acid; (c) TMSCN, ZnI_2, CH_2Cl_2, $LiAlH_4$, THF; (d) CH_3SO_3H.

4.7 Conclusions

Overall, our results imply that large rigid ring-annulated AMDA analogs can be sterically accommodated within the proposed 5-HT_{2A} binding site. It is rather remarkable that compounds of the dimensions of **24** and **26** bind at all and in fact have very high 5-HT_{2A} affinity and a low H_1 affinity. There are currently no known rigid ligands that show the affinity for 5-HT_{2A} receptors and exceed the dimensions of these AMDA analogs. For example, in case of of tricyclic antidepressants, ergot alkaloids and apomorphine the longest dimension is equivalent to 3 linearly fused rings. We have chosen to carefully examine the dimensions of the binding site by elaboration of the tricyclic system with successive aromatic ring fusions which present a rigid obstacle. Further elaboration of the AMDA skeleton by benzfusion will create dimensional probes which will extend beyond AMDA itself and allow access to additional sets of binding site residues. Since both the tetracene and tetraphene isomers of the unsubstituted ring-annulated AMDA analog show remarkable differences in binding affinities, we would attempt synthesis of substituted tetraphen analogs of AMDA by a different synthetic method in the future. Based on the results obtained, we would also attempt the resolution of enantiomers by HPLC using chiral column supports. The dimensional probe concept can be exploited further by the design, synthesis of various substituted benzene fused AMDA analogs. Due to their large rigid structures these ligands can interact with subtype specific residues which can help to generate selective agents.

ENGINEERING A SELECTIVE NON-NITROGENOUS AMINERGIC GPCR LIGAND

5.1 Introduction.

Over the years, significant progress has been made in the development of novel, high-affinity ligands for several aminergic GPCRs including those activated by histamine,[107] serotonin[213] and dopamine.[214] However, there is a lack of truly selective agonists and/or antagonists for most of these receptors. Development of a selective ligand in the case of aminergic GPCRs is especially challenging due to the presence of highly conserved structural features among the members of this class of receptors.[134,215,216] In addition, it is also assumed that due to the presence of these common structural features the various subtypes exhibit a common mechanism of interaction with their ligands. Since most aminergic GPCR ligands have a basic amine moiety, this feature was identified as a crucial component for high-affinity receptor-ligand interaction.[57] Systematic mutagenesis studies by various groups have identified negatively charged Asp$^{3.32}$ as a counter ion for the basic amine in both agonists and antagonists.[217-219]

In the past Glennon et al.[213] have reported several successful strategies for the development of selective serotonergic ligands. However, to-date very few cases are reported for the receptor structure-based design of a selective ligand. Recently, our group has reported[220] homology modeling studies of the kappa-opioid receptor (KOR) with salvinorin A, a selective non-nitrogenous KOR agonist. The result of our modeling study suggests that one of the possible reasons for the salvinorin A's high KOR selectivity could be the absence of the highly conserved $Asp^{3.32}$-amine interaction that is conserved among all GPCRs. In addition, the models also indicate the presence of a KOR specific interaction in the binding site. Also, there have been reports of the binding of some antagonists with reduced, but still significant, affinity at the Asp-mutated 5-HT_{1A},[221] 5-HT_{2A}[54] and muscarinic acetycholine receptors[222] suggesting that it may be possibile to design a GPCR ligand that does not interact with this aspartate.

As mentioned in our earlier studies, in order to understand how molecules bind at 5-HT_{2A} and the H_1 receptors, we conducted docking studies for AMDA and its analogs with the homology models of receptors. Continuing our efforts to understand the binding site interactions and test the utility of our models, we generated a testable hypothesis about the necessity of the interaction involving the highly conserved $Asp^{3.32}$ and the basic amine containing ligands that could possibly lead to a selective GPCR ligand.

5.2 Hypothesis based on the Homology Modeling and Reported Site-Directed Mutagenesis Studies

Most of the second-generation H_1 antagonists penetrate poorly into the CNS, and have an improved selectivity profile as compared to first-generation H_1 antagonists. It is observed that the addition of a chemical group that is ionized at physiological pH will convert a potent sedating H_1-antagonist into a less sedating one.[223] For example the oxidation of the terminal alcohol group in hydroxyzine to a carboxylic acid group results in cetrizine, which is less sedating than the parent compound. However, the precise structural requirements that contribute to receptor selectivity and affinity are unknown.[224-226] Site-directed mutagenesis studies have revealed that Asp $107^{3.32}$ in TM3 is crucial for binding of histamine and nearly all H_1 receptor antagonists.[6,219] In addition, mutation analysis of the H_1 receptor binding pocket has revealed several residues that are essential for agonist and antagonist interactions.[187,188,227] Of these, $Lys191^{5.39}$ appears to be unique to the H_1 receptor.[189,228]

A multiple sequence alignment of TM5 for a set of aminergic GPCRs indicates that Lys191 is found in the histamine H_1 receptor at a position (5.39) near the extracellular end of the TM5 domain where no charged residue is observed in other aminergic GPCRs.[229] Lys191 is thought to interact with the proximal nitrogen (N^{π}) of the imidazole ring of histamine.[229] In addition, it may act as a specific anchor point for second-generation H_1 antagonists containing a carboxylate moiety.[187,230] Mutation of $Lys191^{5.39}$ (human) and its counterpart $Lys200^{5.39}$ (guinea pig) to alanine leads to decreased affinity for histamine (5-fold) and an even higher decrease in functional EC_{50} value (50-fold). In addition, mutational analysis of the antagonist binding site reveals that the Lys200Ala mutation results in a 10- to 50-fold loss of affinity for zwitterionic

antagonists such as acrivastine and cetrizine. The affinities of structural analogs of these compounds lacking carboxylate group were unaffected by the mutation[189] (Figure 19).

Studies involving tricyclic rigid analog olopatadine and its structural analog doxepin that lacks the carboxylic acid substituent, has shown that the presence of the carboxylic substituent has no significant effect on wild-type H_1 receptor affinity (increases by ~ 2-fold). However, in the case of the mutant D107A H_1 receptor, the affinity of doxepin deceases significantly (~ 60-fold) as compared to olopatadine (~ 12-fold), suggesting that a cationic interaction exists in the binding site in addition to the hydrophobic interactions. Taking into consideration these findings, we carried out docking studies of a series of known first and second generation H_1 antagonists and AMDA analogs synthesized in our lab. Binding site analysis from the docked poses of ligands reveal that AMDA and its analogs may bind in a similar manner to H_1 antagonists. The basic amine in each bound ligand is able to interact with the conserved Asp107.$^{3.32}$ In addition, the carboxylic acid moiety present on the zwitterionic compounds (acrivastine and olopatadine) was in a favorable position to interact with Lys191$^{5.39}$ in H_1 receptor. Based on our docking observations and reported[228] mutation study of Lys$^{5.39}$, we predicted that in addition to the conserved Asp$^{3.32}$ interaction and the overall fit of the ligand in the binding pocket, one of the key interactions for the observed affinities of the zwitterionic compounds could be the ionic interactions involving the Lys191$^{5.39}$ that is unique to the binding site of H_1 receptor. Thus we generated a hypothesis that either one of these two ionic interactions might be sufficient for ligand affinity. Further, the binding study results[6] involving the mutant D107A H_1 receptor and

the drug olopatadine suggested that inspite of mutating the highly conserved D107 residue, olopatadine retains its affinity (Figure 19). Thus in order to test our hypothesis of possibly substituting the highly conserved $Asp^{3.32}$ ionic interaction with an equivalent $Lys^{5.39}$ interaction we decided to synthesize a compound without the basic amine but incorporate a carboxylic acid substituent in the compound.

5.3 Strategy for the Design of a Selective H_1 Ligand

Taking into consideration our predicted anionic interaction of the carboxyclic acid substitution on the ligand with the specific $Lys191^{5.39}$ residue in the binding site of H_1 receptor, we decided to synthesize the analog of our earlier obtained lead compound AMDA. Previously conducted SAR studies[170,204] on the AMDA analogs had suggested that the C-3 position of the DHA core showed high stereo-electronic tolerance. Thus, initially 3-carboxy-AMDA (**28**) was synthesized in our laboratory by G. Dewkar and tested. Given the challenges faced in the cyclization and purification of compound **28**, a parallel effort was made to synthesize carboxylic acid-substituted diarylalkyamine analog **29** (Figure 19). Further in accordance with the affinity data obtained (SAR discussion below) we attempted the synthesis of the 3-carboxy-AMDA analog **30**. In addition, we intended to synthesize a non-nitrogenous, carboxylic acid-containing analog **34** that could not interact with the conserved $Asp^{3.32}$. It was also anticipated that such a compound would be highly selective for the H_1 receptor having removed the one ligand-receptor interaction common to all aminergic GPCRs. Taking into consideration the difficulties faced in the synthesis of acid-substituted AMDA, we decided to use a different approach

for the design of high affinity and selective ligands. We used the "deconstruction" approach that is similar to the previously reported "deconstruction-reconstruction-elaboration" approach for the design of selective 5-HT_2 ligands.[213] In our approach, we started with the structure of a lead compound olopatadine (**35**) and deconstructed its structure to determine the structural requirements for binding. Then we reintroduced each structural feature in a rational manner to determine how they influence affinity and selectivity. In doing so, we first synthesized and tested the tricyclic core of olopatadine with an acetic acid substitution at C-2 position i.e., compound **31**. We then synthesized compound **32** by the reduction of the ketone functionality. Further, we replaced the ketone with an olefinic bond to obtain **33**. However, we found that none of these compounds i.e., **31**, **32** and **33** bind at 5-HT_{2A} and H_1 receptors. Comparing the structure and binding data of **33** (Figure 19) with lead compound olopatadine (**35**) and its analog doxepin (**36**), we concluded that an alkylamine chain is needed for high affinity at both receptor types and acid substitution might determine selectivity. Hence in the final step, we synthesized compound **34** that was structurally analogous to olopatadine with the exception of basic nitrogen atom.

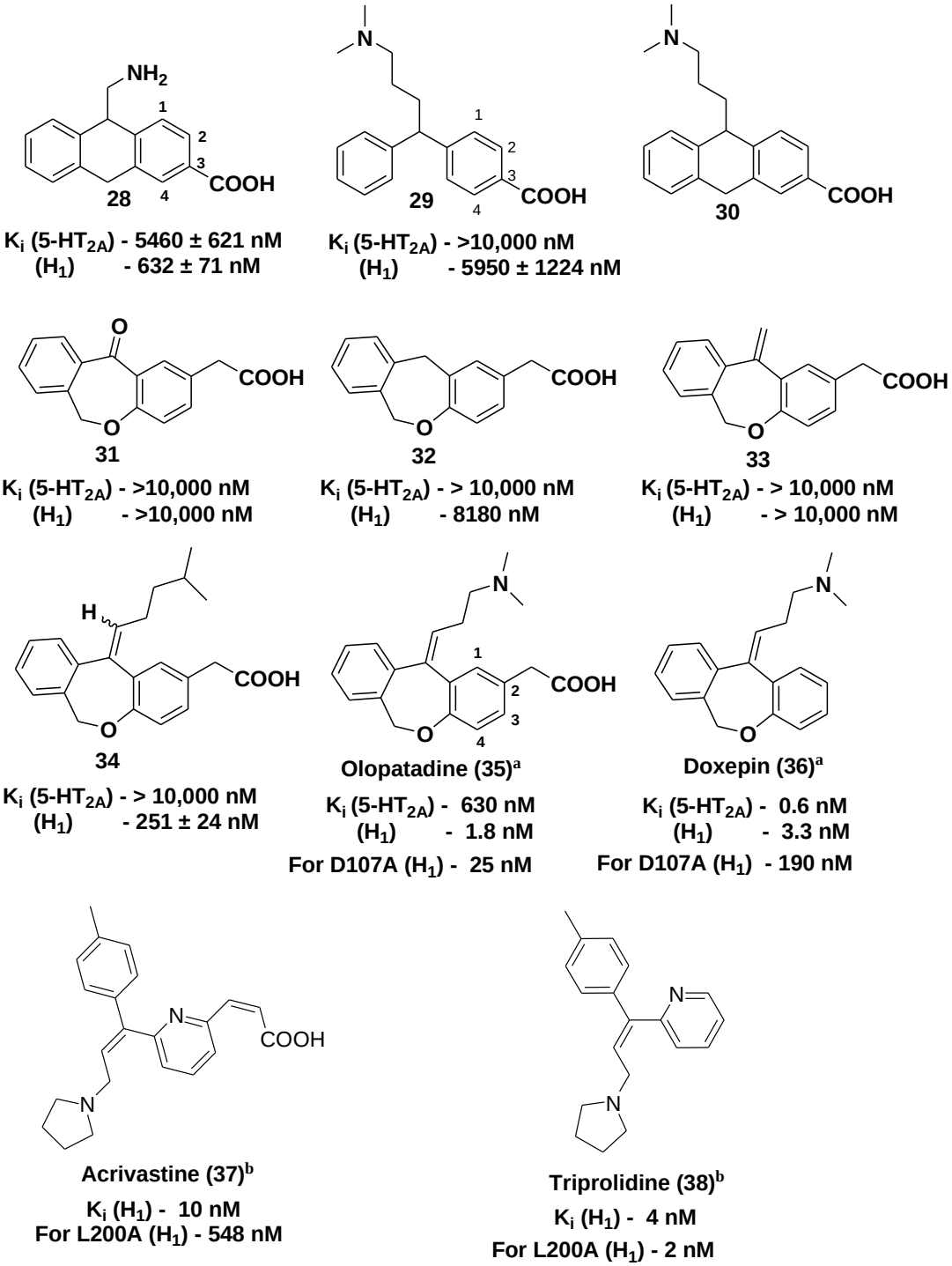

Figure 19. Probes for the design of a selective H_1 ligand. [a]From Nonaka, et al., *Eur. J. Pharmacol.* **1998**, 345, 111-117.[6] [b]From Weiland, et al., *J. Biol. Chem.***1999**, 274, 29994-30000.[189]

5.4 Results and discussion

5.4.1 Structure-Affinity Relationship Studies

The modeled orientation of the ligand within the predicted binding site and the associated receptor-ligand interactions were consistent with the binding affinity data in Figure 19. The 3-carboxy-AMDA (**28**) exhibited some affinity for the H_1 receptor, suggesting a possible interaction of the carboxylate substituent with a cationic residue Lys191$^{5.39}$ in the H_1 binding site. However, the affinity was very low (K_i = 632 nM). Observation of docked poses indicates that the relatively low affinity of **28** as compared to AMDA (K_i = 197 nM) could be due to the length of the short linker connecting the amine with the biaryl moiety, which would prevent compound **28** from adopting a high-affinity conformation in the binding pocket so as to interact with both D(3.32) and K(5.39). The studies[189] involving the H_1 antagonist triprolidine (**38**) and its acid-substituted analog acrivastine (**37**) suggest that the presence of a carboxylic group substituent has little effect on H_1 affinity (decreases by 2.5-fold). However, the mutant K200A H_1 receptor showed a decrease in affinity (~ 55-fold), suggesting the possible cationic interaction of K200$^{5.39}$ with the carboxylate group of the ligand. Thus, in comparison to the acrivastine structure to test the possible effect of a larger amine linker length, we synthesized and tested diarylamine analog **29**. Interestingly**,** it exhibited very low affinity (K_i = 5950 nM) for the H_1 receptor.

From our initial modeling studies, it was rationalized that one possible reason for the observed lack of affinity could be that the presence of the highly charged carboxylate group prevents the parent aromatic ring from taking full advantage of the aromatic cluster

located on and around the TM5 and 6. In addition, comparison of the docked poses of compound **29** with acrivastine (**37**) in our model suggests that in order to take advantage of the cationic interaction of K(5.39), the carboxylic group substituent should be located at the 4-position (**29**, Figure 19) with an extended ethylene linker as in acrivastine. As stated in our strategy, we then synthesized and tested structural analog of olopatadine lacking the nitrogen atom. None of the non-nitrogenous carboxylic acid-substituted analogs **31**, **32** and **33** showed affinity for the 5-HT_{2A} receptor, suggesting the importance of other pharmacophoric features (basic amine) on the molecule for the favorable interaction in the binding site. Among all of the tested non-nitrogenous compounds with a rigid tricyclic core, only compound **34** showed moderate affinity at the H_1 receptor (K_i = 250 nM) providing support for our proposed hypothesis. In accordance with a previously reported study[6] investigating the binding site interactions of H_1 receptor antagonists, one of the possible reasons for the observed binding affinity of **34** at the H_1 receptor is that the conserved ammonium ion interaction is not essential for the binding. The anionic interaction of the carboxylate group with K191$^{5.39}$ on TM5 likely provides an equivalent electrostatic interaction to that of D107$^{3.32}$ on TM3. The modest affinity values for compound **34** can be due to multiple reasons, one of them being the replacement of the functionally relevant nitrogen atom. Studies relating functional group contributions to drug-receptor interactions have shown that replacement of a critical charged nitrogen atom with a neutral carbon atom would result in an average decrease in the actual binding energy of 11.5 kcal/mol, suggesting that the charged nitrogen group shows a stronger interaction than the neutral group[231] or even a carboxylate group (8.2 kcal/mol) and

providing a partial explanation for the modest observed affinity of **34**. Furthermore, the proposed K191$^{5.39}$ residue in the binding site possesses a flexible butylene side-chain linker providing more rotational degrees of freedom than D107$^{3.32}$ or most other naturally occurring amino acids. Thus its interaction with a flexible carboxyl group substituent on **34** is entropically disfavored, leading to decrease in binding affinity.

5.4.2 Modeling interactions

The histamine H_1 receptor model was generated by using a β_2-adrenergic receptor crystal structure (β_2AR) as the homology modeling template and used to study the ligand-receptor interactions involving acid substituted ligands. The lead compound olopatadine and its non-nitrogenous analog **34** with precise consideration of stereoisomers, was sketched, energy-minimized and docked into the receptor binding site (see Experimental Methods). Visual inspection of docked poses, the GoldScore fitness function and information from site-directed mutagenesis studies were used to select a solution for each isomer. The GOLD[232] program used for docking was able to place all the ligands in the previously predicted binding site (Figure 20). In case of olopatadine, both *E* and *Z* isomers show a similar binding mode in the binding site of H_1 receptor. The protonated amine exhibits strong ionic interaction with the D107$^{3.32}$, while the carboxylate group simultaneously showed extensive hydrogen bonding/ionic interaction with K191$^{5.39}$. Binding site residues T194$^{5.42}$ and Y108$^{3.33}$ also form putative hydrogen bonds with the ligand carboxylate moiety. Both isomers of compound **34** bind in a similar fashion to olopatadine in the binding cavity with the exception of the ammonium ion interaction.

The HINT (Hydropathic INTeraction) scoring function was used to further support the receptor-ligand interactions predicted by the generated conformations of the ligand using the GOLD docking program. A HINT map was generated (details in experimental). Figure 21 illustrates the interactions with a HINT map, where the size of the displayed contour represents the extent of the interaction, and the color represents the type of interaction between the molecule **34** and the histamine binding site. The tricyclic ring system of compound **34** with the aliphatic linker fits in the predominantly hydrophobic pocket formed by $Y108^{3.33}$, $F190^{3.38}$, $N198^{5.46}$, $S111^{3.36}$ and $Y458^{7.43}$. In addition, there is a region of favorable polar interactions surrounding the carboxylate substituent on the aromatic ring. This carboxylate group engages in favorable polar interaction with the residue $K191^{5.39}$ and the neighboring residues $Y108^{3.33}$ and $T194^{5.42}$. The relatively large number of favorable polar and nonpolar interactions could be responsible for the significant observed affinity of compound **34** for the H_1 receptor, despite the absence of a basic amine moiety.

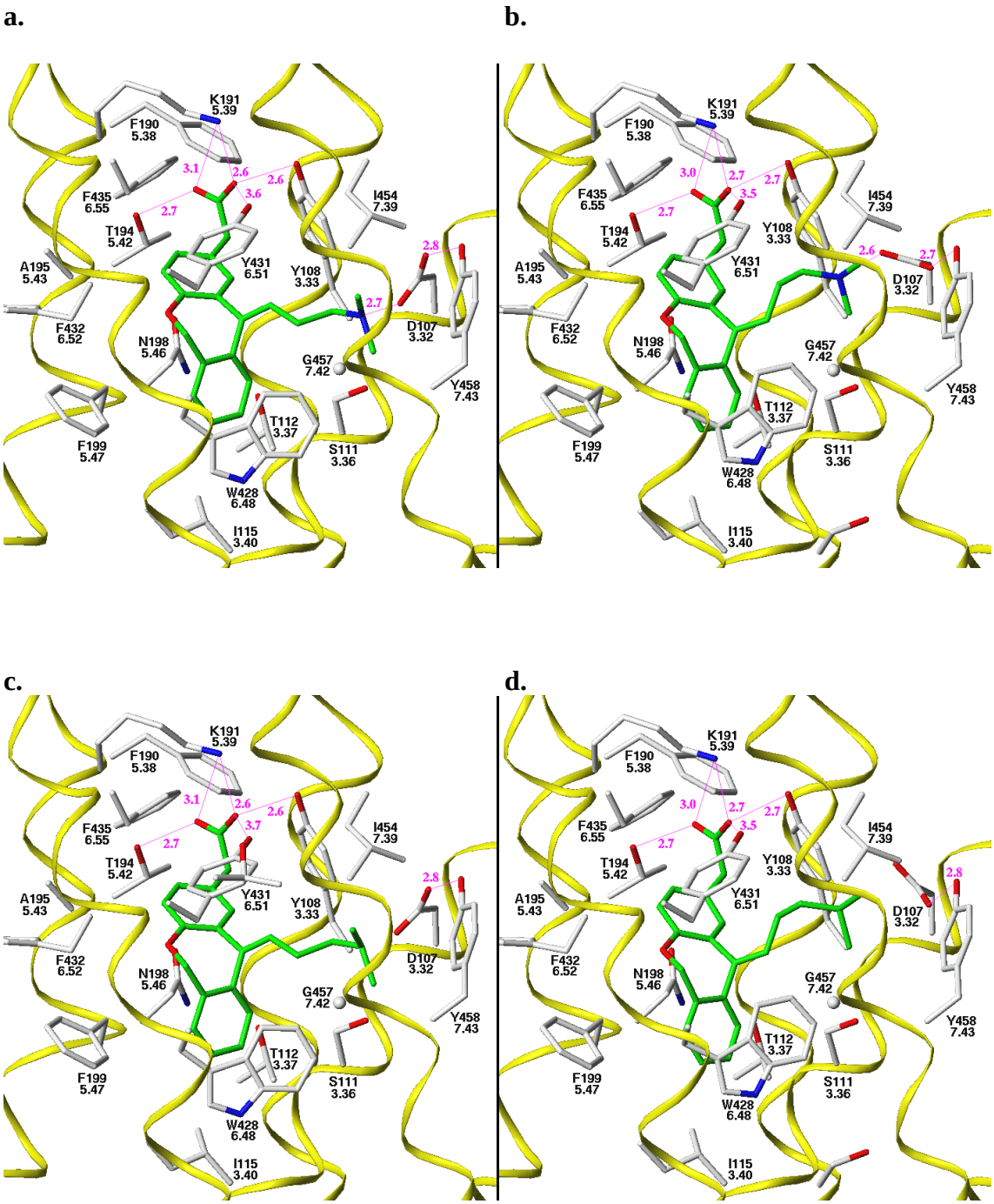

Figure 20. Docked poses of **a.** (*E*)-olopatadine, **b.** (*Z*)-olopatidine, **c.** (*E*)-**34**, **d.** (*Z*)-**34** in H_1 model.

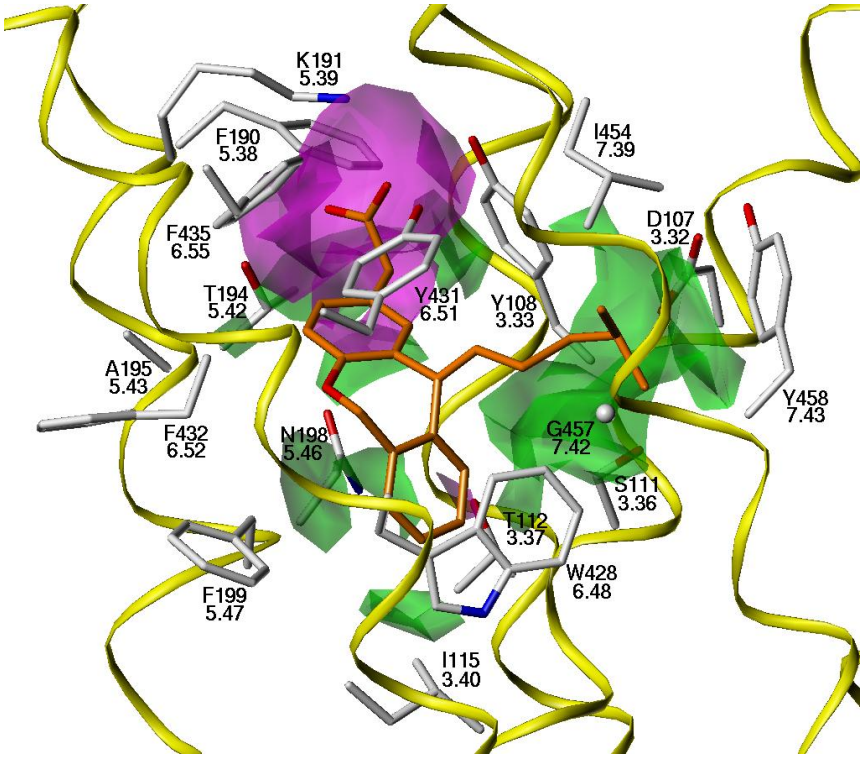

Figure 21. HINT interaction maps for compound **34** in H_1 binding sites. Regions of favorable hydrophobic (green) and polar (magenta) interactions are shown as contours.

5.4.3 Chemistry

Compound **28** was synthesized by G. Dewkar in our laboratory. Synthesis of compound **29** was carried out by standard Wittig reaction following the reported procedure[233] (Scheme 13). The keto ester **87** obtained by the esterification of 4-benzoylbenzoic acid (**86**) was reacted with phosphonium salt followed by the hydrolysis of the ester side-chain to give intermediate **89**. This was further subjected to hydrogenation to give the final product **29**. We were not able to synthesize compound **30** (Figure 19). To begin, an attempt was made to synthesize **34** from dibenz[b,e]oxepin-2-acetic acid (**31**) and the corresponding phosphonium salt prepared from 1-bromo-4-methylpenatane and triphenylphosphine.[234] A substituted ethyl *o*-toluate (**90**) was brominated with *N*-bromosuccinimide to provide **91**. This intermediate was then condensed with ethyl 2-(4-hydroxyphenyl)acetate to give crude ester **92** which was hydrolyzed to the diacid **93**. The diacid obtained was cyclized using polyphosphoric acid-acetic acid mixture to obtain the product **31** (Scheme 14). Compound **32**[235] was obtained by the reduction of ketoacid **31** using Zn-AcOH (Scheme 15). Compound **33** was obtained by the hydrolysis of **94**[236], which was obtained by the Wittig reaction using the reported method[236] (Scheme 16). Synthesis of compound **34** turned out to be much more challenging than expected. As shown in Scheme 18, initial attempts of carrying out Wittig reaction on the keto acid **31**[237] and the corresponding ester **35**[235] failed. Further attempts to use the Wittig reaction with the oxazoline-protected compound failed due to the low yield of compound **36**[236] obtained utilizing 2-methyl-2-aminopropanol for the formation of oxazole.[238] The *in situ* esterification of the keto acid **31** following the Wittig

reaction resulted in compound **37**; however, the yield was drastically low. The synthetic Scheme utilized in the preparation of the desired (*E,Z*)-(11-[4-methylpentylidene]-6,11-dihydrobenz[*b,e*]oxepin-2-acetic acid (**34**) is illustrated in Scheme 17. In this method, using 4-(2-hydroxyethyl)phenol instead of 4-hydroxyphenylacetate as the starting material, the alcohol substituted ketone (**98**)[239] was obtained. The alcohol was protected using TBDMS[240] to give **99** which was then subjected to the Wittig reaction using LHMDS as a base.[241] The deprotection of the compound **100** by TBAF[234] followed by the TEMPO[242] oxidation of the alcohol side-chain gave the final product **34**.

5.5 Synthetic Schemes

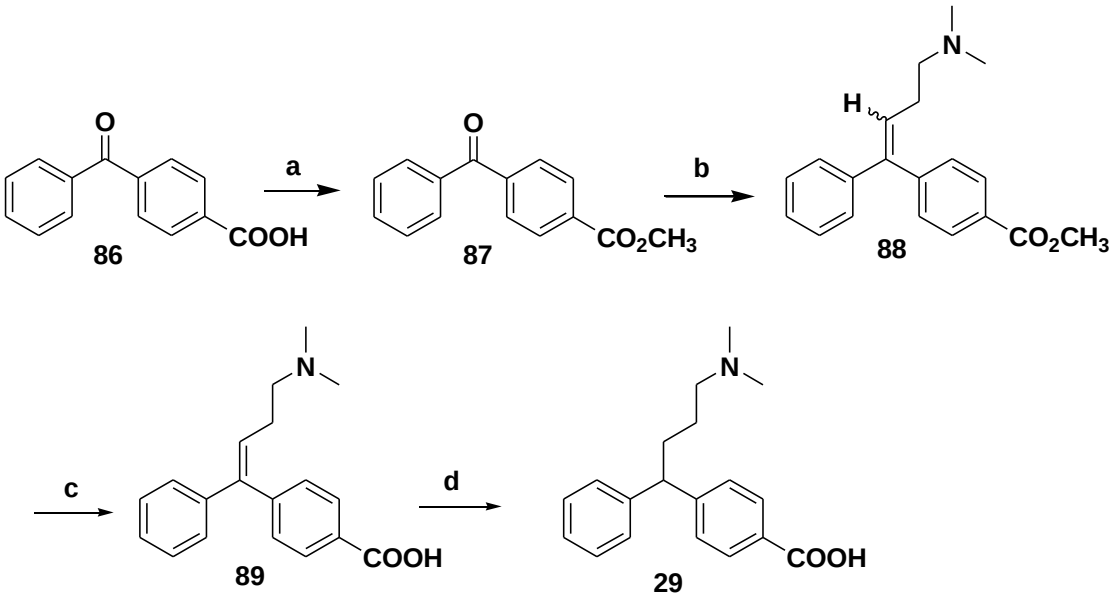

Scheme 13. (a) CH_3OH, H_2SO_4; (b) Ph_3P^+-$CH_2(CH_2)_2$-$N(CH_3)_2Br^-$, THF, 1.6M *n*-BuLi; (c) 1N NaOH, CH_3OH; (d) 10% Pd/C, HCl, CH_3OH.

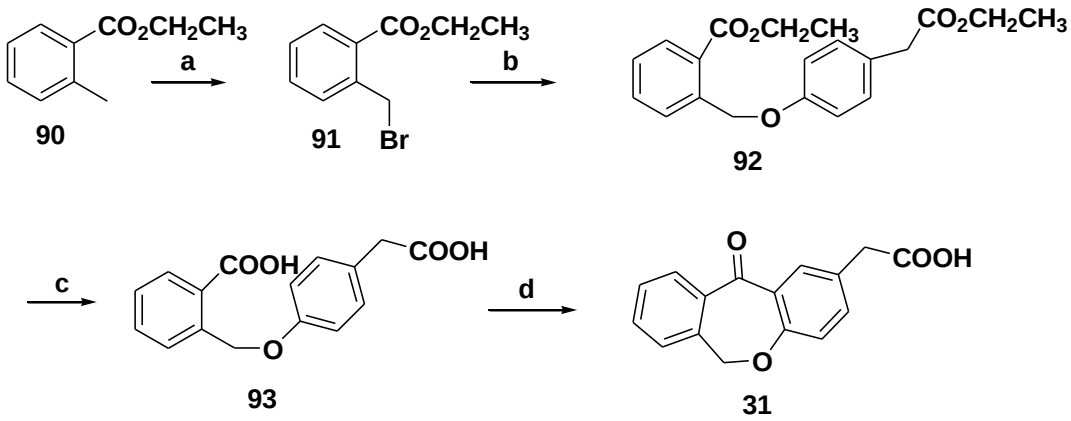

Scheme 14. (a) NBS, benzoyl peroxide, CCl_4; (b) K_2CO_3, KI, ethyl 2-(4-hydroxyphenyl)acetate, butanone; (c) aq NaOH, MeOH; (d) PPA, acetic acid.

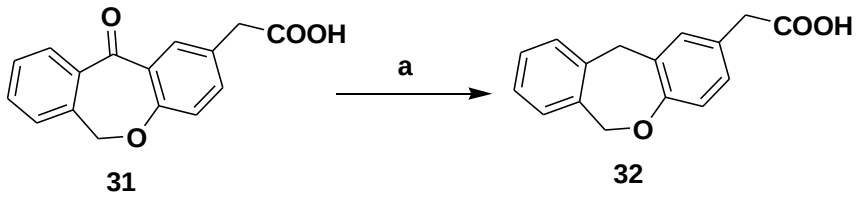

Scheme 15. (a) Zn-AcOH.

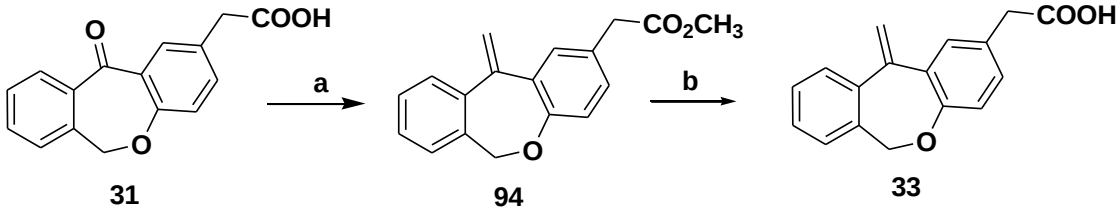

Scheme 16. (a) Ph_3P^+-CH_3Br, *n*-BuLi, THF, p-TsOH, MeOH; (b) 10% NaOH, MeOH.

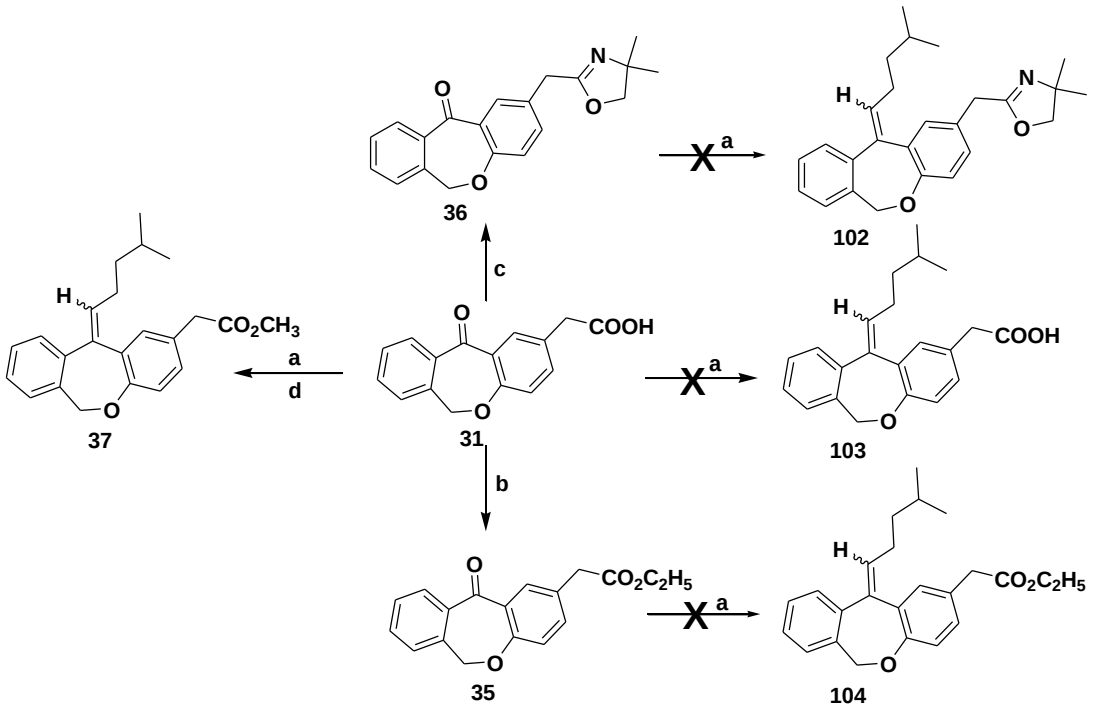

Scheme 17. (a) *n*-BuLi, THF, Ph_3P^+-$CH_2(CH_2)_3$-$CH(CH_3)_2$ Br^-; (b) abs ethanol, H_2SO_4; (c) (i) Pyridine, $SOCl_2$, CH_2Cl_2; (ii) $NH_2C(Me)_2CH_2OH$, toluene; (iii) $SOCl_2$, CH_2Cl_2; (d) *p*-TsOH, MeOH.

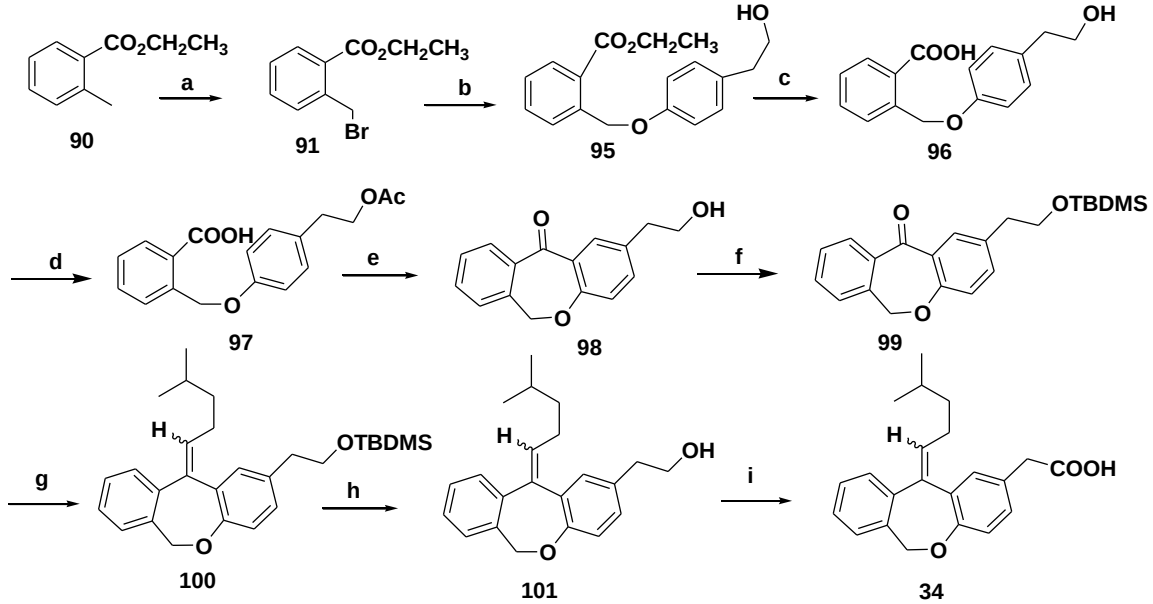

Scheme 18. (a) NBS, benzoyl peroxide, CCl_4; (b) K_2CO_3, KI, 4-(2-hydroxyethyl)phenol butanone; (c) aq NaOH, MeOH; (d) acetyl chloride; (e) TFAA, $BF_3{\cdot}OEt_2$, DCM, NaOH;(f) TBDMS, imidazole, DMF; (g) LHMDS, Ph_3P^+-$CH_2(CH_2)_3$-$CH(CH_3)_2$ Br^-, THF; (h) TBAF, THF; (i) $NaClO_2$/TEMPO, NaOCl, MeCN.

5.6 Conclusions

The results obtained from the binding data and site-directed mutagenesis studies, supported by the homology modeling studies show that the compound (*E*,*Z*)-(11-[4-methylpentylidene]-6,11-dihydrobenz[*b*,*e*]oxepin-2-acetic acid (**34**) is a lead for the design of selective H_1 receptor antagonists. The moderate affinity (K_i = 250 nM) and high selectivity for the H_1 vs. 5-HT_{2A} receptor without a basic amine moiety in the ligand structure imply that the presence of an ionizable functional group (e.g. carboxylate) as a substituent can replace the basic nitrogen atom essential for the interaction with D3.32 in H_1, and these results may be used in the further development of selective high-affinity H_1 ligands. Further, the general approach reported here can be used in the design of selective GPCR ligands. In continuation of our work, we also would attempt the synthesis of analog of compound **34** without the carboxylic acid substituent which could serve as a reference for our proposed hypothesis and also study the effect of $Lys^{5.39}$ mutation on our tested ligands.

SUMMARY

Based on our investigation of the binding site interactions of serotonin 5-HT_{2A} and histamine H_1 receptors with various ligands, we conclude that homology modeling and ligand docking studies, supported by binding affinity and site-directed mutagenesis data, can be used to understand the possible ligand-receptor interactions and to generate reasonable leads for the development of selective high-affinity ligands. Rational SAFIR studies around the early lead compound AMDA (9-aminomethyl-9,10-dihydroanthacene) led us to identify a molecule 3-(9,10-dihydroanthrace-9-yl)-*N*, *N*-dimethylpropan-1-amine (**9**) with high affinity at both 5-HT_{2A} (K_i = 22 nM) and H_1 K_i = 0.5 nM) receptors.. However, the selectivity of this compound with respect to other 5-HT subtypes (5-$HT_{2B,}$ 5-HT_{4-7}) remains to be tested. Further, the molecular modeling indicates the presence of differing residues at position 3.33 within the binding site of 5-HT_{2A} ($V156^{3.33}$) and H_1 ($Y108^{3.33}$) receptors and that this difference could play a role in determining the affinity and selectivity of ligands among these two receptors. SAFIR and modeling observations suggest that AMDA and its chain-lengthened analogs can serve as effective probes to investigate the 5-HT_{2A} and H_1receptor binding sites.

The modeling investigations supported by the binding data show that ring-annulated AMDA analogs with a methoxy substituent can be used as dimensional probes to explore the additional binding site interactions. Using this technique (7, 12-dihydro-3-methoxytetraphen-12-yl)methanamine (**26**), a compound with high affinity and selectivity was identified (5-HT_{2A} K_i = 21 nM; H_1 K_i = 2640 nM). In addition, comparison of the binding site residues between 5-HT_{2A} and H_1 receptors and the reported sequence alignment studies among aminergic GPCRs show that $Lys191^{5.39}$ is unique to the H_1 receptor. $Lys191^{5.39}$ is proposed to be able to form an ionic interaction with the carboxylate group of zwitterionic H_1 antagonists (acrivastine and olopatadine) and the designed compound (*E*,*Z*)-(11-[4-methylpentylidene]-6,11-dihydrobenz[*b*,*e*]oxepin-2-acetic acid (**34**). Our compound **34** could act as a lead for the development of non-nitrogenous H_1-selective receptor ligands. However, the selectivity of this compound with respect to other 5-HT subtypes (5-$HT_{2B/2C}$ and 5-HT_{4-7}) remains to be tested.

EXPERIMENTALS

7.1 Chemistry

Melting points were determined using a Thomas-Hoover melting point apparatus and are uncorrected. Nuclear magnetic resonance (^{1}H NMR and ^{13}C NMR) spectra were obtained with a Varian Gemini 300 MHz spectrometer and chemical shifts are reported in parts per million (δ), using tetramethylsilane (TMS) as an internal standard. Unless otherwise mentioned the spectral data corresponds to the free amine using chloroform as the internal standard. In case of the salt form the respective solvent is mentioned. The oxalate salts were prepared by dissolving the respective amine in anhydrous acetone; this mixture was then added to a solution of oxalic acid in anhydrous acetone. Hydrochloride salts were prepared similarly by addition of anhydrous HCl solution. Elemental analysis was performed by Atlantic Microlab Inc. (Norcross, GA), and determined values are within 0.4% of theory (except where indicated). Column chromatography was performed on silica gel, grade 62, 60-200 mesh, 150 Å (Sigma-Aldrich, MO). Routine thin-layer chromatography (TLC) was performed on silica gel GHFL (250 microns, 2.5 × 10 cm; Analtech Inc., Newark, DE). Unless otherwise mentioned, all the reagents and chemicals were obtained from Sigma-Aldrich, MO.

(9,10-Dihydroanthracen-10-yl)-*N*-methylmethanamine hydrochloride (2).[174] BH_3•THF complex (1.0 M in THF, 0.51 g, 6.0 mmol) was added in a dropwise manner to a stirred solution of **44 (**0.3 g, 1.2 mmol) in anhydrous THF (4 mL) under N_2 at 0 °C.

The mixture was slowly warmed to rt and heated at reflux (6 h). The reaction mixture was allowed to cool to rt, and HCl (6.0 M, 3 mL) was added with caution. The mixture heated at reflux (1 h) and allowed to cool to rt, and the solvent was removed under reduced pressure. Water was added and the residue was extracted with ether (25 mL). The aqueous portion was made basic with 10% NaOH and extracted with CH_2Cl_2 (3 × 25 mL). The organic layer was washed with water, brine and dried ($MgSO_4$). Removal of solvent under reduced pressure afforded **2**. It was then purified by medium pressure column chromatography, CH_2Cl_2/MeOH (9:1) (0.267g, 85%). HCl salt: mp 250 - 252 °C. ^{1}H NMR ($CDCl_3$): 2.44 (s, 3H), 3.07 (d, *J* = 7.2 Hz, 2H), 3.97 (d, *J* = 18.6 Hz, 1H), 4.16 (d, *J* = 18.6 Hz, 1H), 4.54 (t, *J* = 8.1 Hz, 1H), 7.27 - 7.50 (m, 8H); ^{13}C NMR ($CDCl_3$): δ 34.15, 35.01, 44.16, 52.91, 127.27, 127.92, 128.70, 129.08, 136.51, 137.57. Anal. Calcd for ($C_{16}H_{17}N$·HCl·0.25 H_2O) C, 72.71; H, 7.05; N, 5.29 Found: C, 72.77; H, 6.98; N, 5.30.

(9,10-Dihydroanthracen-10-yl)-*N*,*N*-dimethylmethanamine hydrochloride (3).[174] BH_3•THF complex (1.0 M in THF, 0.51 g, 6.0 mmol) was added in a dropwise manner to a stirred solution of **45 (**0.3 g, 1.19 mmol) in anhydrous THF (4 mL) under N_2 at 0 °C. The mixture was slowly warmed to rt and heated at reflux (6 h). The reaction mixture was allowed to cool to rt, and HCl (6.0 M, 3 mL) was added with caution. The mixture heated at reflux (1 h) and allowed to cool to rt, and the solvent was removed under reduced pressure. Water was added and the residue was extracted with ether (25 mL). The aqueous portion was made basic with 10% NaOH and extracted with CH_2Cl_2 (3 × 25

mL). The organic layer was washed with water and brine, dried ($MgSO_4$), and concentrated under reduced pressure to give **3.** It was then purified by medium pressure column chromatography, CH_2Cl_2/MeOH (9:1) (0.248 g, 88%). HCl salt: mp 248 - 250 °C ^{1}H NMR (DMSO): 2.72 (s, 6H), 3.36 (d, *J* = 7.5 Hz 2H), 3.96 (d, *J* = 18.3 Hz, 1H), 4.21 (d, *J* = 18.3 Hz, 1H), 4.67 (t, *J* = 8.1 Hz, 1H); ^{13}C NMR (DMSO): δ 35.21, 43.06, 44.20, 60.73, 127.23, 128.01, 128.76, 129.08, 136.87, 138.05. Anal. Calcd for ($C_{17}H_{19}N$·HCl· 0.25 H_2O) C, 74.57; H, 7.36, N; 5.11 Found: C, 73.36; H, 7.42; N, 5.03.

2-(9,10-Dihydroanthracen-9-yl)ethanamine oxalate (4).[174] Anhydrous ammonia (15 mL) was added to a well stirred solution of compound **48** (0.2 g, 0.9 mmol) dissolved in THF (5 mL) by using a cold finger under N_2 at -78 °C. Sodium metal (0.05 g) was then added in pieces and the reaction was stirred for 25 min. The mixture was then allowed to cool to rt and poured into a large excess of NH_4Cl solution, then extracted with EtOAc (3 × 25 mL). The combined EtOAc extracts were washed with water, brine and dried ($MgSO_4$). The solvent was removed under reduced pressure to yield the amine **4** that was purified by medium pressure column chromatography, CH_2Cl_2/MeOH (9:1) (0.1 g, 50.0%). Oxalate salt: mp 193-195 °C. ^{1}H NMR ($CDCl_3$): 2.02 (q, *J* = 7.8 Hz, 2H), 2.7 (t, *J* = 7.8 Hz, 2H), 4.02 (t, *J* = 7.2 Hz, 1H), 3.89 (d, *J* = 18.3 Hz, 1H) 4.0 (d, *J* = 18.3 Hz, 1H), 7.1 - 7.3 (m, 8H). ^{13}C NMR ($CDCl_3$): δ 34.8, 39.5, 40.1, 45.6, 126.3, 128.1, 136.4, 140.6. Anal Calcd for ($C_{16}H_{17}N$·$C_2H_2O_4$) C, 68.99; H, 6.11; N, 4.47 Found C, 68.72; H, 6.26; N; 4.45.

2-(9,10-Dihydroanthracen-9-yl)-*N*-methylethanamine oxalate (5). BH_3•THF complex (1.0 M in THF, 0.33 g, 3.96 mmol) was added in a dropwise manner to a stirred solution of **54 (**0.25 g, 0.99 mmol) in anhydrous THF (4 mL) under N_2 at 0 °C. The mixture was slowly warmed to rt and heated at reflux (6 h). The reaction mixture was allowed to cool to rt, and HCl (6.0 M, 3 mL) was added with caution. The mixture heated at reflux (1 h) and allowed to cool to rt, and the solvent was removed under reduced pressure. Water was added and the residue was extracted with ether (25 mL). The aqueous portion was made basic with 10% NaOH and extracted with CH_2Cl_2 (3 × 25 mL). The organic layer was washed with water and brine, dried ($MgSO_4$), and concentrated under reduced pressure to give the amine as an oil. The oil obtained was purified by medium pressure column chromatography, CH_2Cl_2/MeOH (9:1) to yield **17** as an oil (0.2 g, 85%). Oxalate salt: mp 202 - 205 °C. ^{1}H NMR ($CDCl_3$): 1.81 (q, *J* = 7.5 Hz, 2H), 2.38 (s, 3H), 2.56 (t, *J* = 7.5 Hz, 2H), 3.99 (d, *J* = 18.3 Hz, 1H), 4.09 (d, *J* = 18.3 Hz, 1H), 4.0 (t, *J* = 7.8 Hz, 1H), 7.16 - 7.3 (m, 8H). ^{13}C NMR ($CDCl_3$): δ 35.3, 36.7, 37.4, 45.4, 50.2, 126.4, 128.1, 136.4, 140.6. Anal Calcd for ($C_{17}H_{19}N{\cdot}C_2H_2O_4{\cdot}0.25\ H_2O$) C, 68.76; H, 6.52; N, 4.22 Found: C, 68.43, H, 6.35, N, 4.22.

2-(9,10-Dihydroanthracen-9-yl)-*N*,*N*-dimethylethanamine oxalate (6). To a stirred solution of triethylamine (0.18 g, 1.79 mmol) in absolute ethanol was added dimethylamine hydrochloride (0.14 g, 1.79 mmol), titanium isopropoxide (0.51 g, 1.79 mmol) and compound **57** (0.2 g, 0.89 mmol). The reaction mixture was stirred at rt for 12 h. Sodium borohydride (0.1 g, 2.68 mmol) was added to this mixture and stirring was

continued for a further 12 h. The reaction was quenched by pouring the mixture into aqueous ammonia (20 mL, 2 N) and the resulting precipitate was filtered and washed with CH_2Cl_2 (3 × 20 mL). The filtrate was collected and the mixture was extracted with CH_2Cl_2. The CH_2Cl_2 portion was dried ($MgSO_4$) and concentrated under reduced pressure to obtain viscous yellow oil that was purified by medium pressure column chromatography, CH_2Cl_2/MeOH (9:1) to yield **6** (0.12 g, 55%). Oxalate salt: mp 184 - 186 °C. ^{1}H NMR ($CDCl_3$): 1.83 (q, *J* = 7.5 Hz, 2H), 2.26 (s, 6H), 2.33 (m, 2H), 3.94 (d, *J* = 18.6 Hz, 1H), 4.14 (d, *J* = 18.6 Hz, 1H), 4.1 (t, *J* = 7.2 Hz, 1H), 7.1 - 7.3 (m, 8H). ^{13}C NMR ($CDCl_3$): δ 32.3, 40.4, 45.3, 52.2, 56.2, 126.8, 128.7, 138.4, 140.1. Anal Calcd for ($C_{18}H_{21}N{\cdot}C_2H_2O_4{\cdot}0.5\ H_2O$) C, 68.55; H, 6.90; N, 3.99 Found: C, 68.76, H, 6.72, N, 3.96.

3-(9,10-Dihydroanthracen-9-yl)propan-1-amine oxalate (7). BH_3•THF complex (1.0 M in THF, 0.17 g, 1.98 mmol) was added in a dropwise manner to a stirred solution of **63** (0.1 g, 0.397 mmol) in anhydrous THF (4 mL) under N_2 at 0 °C. The mixture was slowly warmed to rt and heated at reflux (6 h). The reaction mixture was allowed to cool to rt, and HCl (6.0 M, 3 mL) was added with caution. The mixture heated at reflux (1 h) and allowed to cool to rt, and the solvent was removed under reduced pressure. Water was added and the residue was extracted with ether (25 mL). The aqueous portion was made basic with 10% NaOH and extracted with CH_2Cl_2 (3 × 25 mL). The organic layer was washed with water and brine, dried ($MgSO_4$), and concentrated under reduced pressure to give **7** as an oil. It was then purified by medium pressure column chromatography, CH_2Cl_2/MeOH (9:1) (0.07 g, 75%). Oxalate salt: mp 210 - 212 °C. ^{1}H NMR (DMSO):

1.49 (m, 2H), 1.56 (m, 2H), 2.69 (t, *J* = 7.2 Hz, 2H), 3.92 (t, *J* = 6.3 Hz, 1H), 3.89 (d, *J* = 18.6 Hz, 1H), 4.0 (d, *J* = 18.6 Hz, 1H), 7.1 - 7.3 (m, 8H). ^{13}C NMR (DMSO): δ 25.92, 34.35, 35.02, 35.08, 46.48, 50.1, 128.3, 128.5, 136.7, 140.6. Anal Calcd for ($C_{17}H_{19}N{\cdot}C_2H_2O_4$) C, 69.71; H, 6.47; N, 4.28 Found: C, 69.47; H, 6.35; N, 4.22

3-(9,10-Dihydroanthracen-9-yl)-*N*-methylpropan-1-amine oxalate (8). BH_3•THF complex (1.0 M in THF, 0.161 g, 1.88 mmol) was added in a dropwise manner to a stirred solution of **64 (**0.1 g, 0.376 mmol) in anhydrous THF (4 mL) under N_2 at 0 °C. The mixture was slowly warmed to rt and heated at reflux (6 h). The reaction mixture was allowed to cool to rt, and HCl (6.0 M, 3 mL) was added with caution. The mixture was heated at reflux (1 h) and allowed to cool to rt, and the solvent was removed under reduced pressure. Water was added and the residue was extracted with ether (25 mL). The aqueous portion was made basic with 10% NaOH and extracted with CH_2Cl_2 (3 × 25 mL). The organic layer was washed with water and brine, dried ($MgSO_4$), and concentrated under reduced pressure to give **8** as an oil. It was then purified by medium pressure column chromatography, CH_2Cl_2/MeOH (9:1) (0.075 g, 80%). Oxalate salt: mp 148 - 150 °C. ^{1}H NMR (DMSO): 1.53 (m, 4H), 2.44 (s, 3H), 2.78 (t, J = 7.2 Hz, 2H), 3.92 (t, J = 7.4 Hz, 1H), 4.02 (d, J = 18.6 Hz, 1H), 3.8 (d, J = 18.6 Hz, 1H), 7.1-7.3 (m, 8H). ^{13}C NMR (DMSO): δ 24.3, 33.1, 34.25, 35.01, 46.37, 48.66, 128.38, 128.55, 136.72, 140.5. Anal Calcd for ($C_{18}H_{21}N{\cdot}C_2H_2O_4$) C, 70.36; H, 6.79; N, 4.10 Found: C, 70.44; H, 6.87; N, 4.11.

3-(9,10-Dihydroanthracen-9-yl)-*N*,*N*-dimethylpropan-1-amine oxalate (9). BH_3•THF complex (1.0 M in THF, 0.15 g, 1.75 mmol) was added in a dropwise manner to a stirred solution of **65 (**0.1 g, 0.35 mmol) in anhydrous THF (4 mL) under N_2 at 0 °C. The mixture was slowly warmed to rt and heated at reflux (6 h). The reaction mixture was allowed to cool to rt, and HCl (6.0 M, 3 mL) was added with caution. The mixture was heated at reflux (1 h) and allowed to cool to rt, and the solvent was removed under reduced pressure. Water was added and the residue was extracted with ether (25 mL). The aqueous portion was made basic with 10% NaOH and extracted with CH_2Cl_2 (3 × 25 mL). The organic layer was washed with water and brine, dried ($MgSO_4$), and concentrated under reduced pressure to give **9** as an oil. It was then purified by medium pressure column chromatography, CH_2Cl_2/MeOH (9:1) (0.078g, 85%). Oxalate salt: mp ^{1}H NMR (CD_3OD): 1.63 (s, 4H), 2.71 (s, 6H), 2.94 (s, 2H), 3.87 (d, *J* = 18.6 Hz, 1H), 3.89 (t, *J* = 7.2 Hz, 1H), 4.1 (d, *J* = 18.6 Hz, 2H), 7.14 -7.28 (m, 8H). ^{13}C NMR (CD_3OD): δ 22.5, 33.8, 34.7, 42.1, 57.5.2, 126.2, 127.8, 136.3, 139.9. Anal Calcd for ($C_{19}H_{23}N{\cdot}C_2H_2O_4$) C, 70.96; H, 7.09; N, 3.94 Found: C, 70.77; H, 7.05; N, 4.04.

***N*-Methyl-2,2-diphenylethanamine oxalate (11)**. Sodium cyanoborohydride (0.5 g, 8 mmol) was added to a stirred solution of 2,2-diphenylethanamine **66** (1 g, 5.0 mmol) and 37% aqueous formaldehyde (2.0 mL, 25 mmol) in acetonitrile (15 mL). A vigorous exothermic reaction followed and a dark residue was separated. The reaction mixture was stirred for 15 min, and then glacial acetic acid was added dropwise until the solution tested neutral on wet pH paper. Stirring was continued for an additional 45 min, glacial

acetic acid being added occasionally to maintain the pH near neutrality. The solvent was evaporated at reduced pressure, and 2 N KOH (20 mL) was added to the residue. The resulting mixture was extracted with ether (3 × 20 mL). The combined ether extracts were washed with 0.5 N KOH (20 mL) and then extracted with 1N HCl (3 × 10 mL). The acid extracts were combined and neutralized with solid KOH and then extracted with ether (3 × 20 mL). The combined ether extracts were dried ($MgSO_4$) and evaporated in vacuum to provide yellow oil. The resulting yellow oil was purified using medium pressure chromatography, CH_2Cl_2/MeOH (9:1) to yield **11** (0.45 g, 40%). Oxalate salt: mp 150 - 152 °C. ^{1}H NMR ($CDCl_3$): 2.36 (s, 3H), 3.01 (d, *J* = 8.1 Hz, 2H), 4.28 (t, *J* = 8.1 Hz, 1H), 7.2 - 7.4 (m, 10H). ^{13}C NMR ($CDCl_3$): δ 40.3, 51.8, 62.3, 123.0, 123.8, 124.2, 141.5. Anal Calcd for ($C_{15}H_{17}N{\cdot}C_2H_2O_4$) C, 68.29; H, 6.67; N, 4.50 Found: C, 67.89; H, 6.35; N, 4.64.

3,3-Diphenylpropan-1-amine hydrochloride (13). Commercially available 3,3-diphenylpropan-1-amine (0.1 g) was dissolved in anhydrous acetone (4 mL). Anhydrous HCl (1.2 mL) was added to this solution and refrigerated. The solution was filtered and dried under vacuum to yield **13** (0.08 g, 90%). HCl salt: mp 216 - 218 °C. (lit[246] 218 - 219 °C). ^{1}H NMR ($CDCl_3$): 2.36 (q, *J* = 7.8 Hz, 2H), 2.63 (t, *J* = 8.4 Hz, 2H), 4.13 (t, *J* = 7.8 Hz, 1H), 7.17 - 7.30 (m, 10H). ^{13}C NMR ($CDCl_3$): δ 33.1, 38.37, 48.0, 127.0, 128.2, 129.2, 144.6. Anal Calcd for ($C_{15}H_{17}N{\cdot}HCl$) C, 72.71; H, 7.32; N, 5.65 Found: C, 72.75; H, 7.36; N, 5.60.

***N,N*-Dimethyl-3,3-diphenylpropan-1-amine oxalate (15)**. To a solution of triethylamine (0.96 g, 9.5 mmol) in absolute ethanol (10 mL) was added dimethylamine hydrochloride (0.77 g, 9.5 mmol), titanium isopropoxide (2.69 g, 9.5 mmol), and compound **68** (1 g, 4.7 mmol). Reaction mixture was stirred at rt for 12 h. To this mixture $NaBH_4$ (0.266 g, 7.05 mmol) was added and stirring was continued for 12 h. The reaction was quenched by pouring the mixture into ammonia (30 mL, 2 N) solution. The resulting precipitate was filtered and washed with CH_2Cl_2 (3 × 20 mL). The filtrate was collected and the mixture was extracted. The CH_2Cl_2 portion was dried ($MgSO_4$) and concentrated under reduced pressure to give viscous yellow oil. The resulting yellow oil was purified using medium pressure chromatography, CH_2Cl_2/MeOH (9:1) to obtain **15** (0.25 g, 22%). Oxalate salt: mp 150 - 152 °C. ^{1}H NMR ($CDCl_3$): 2.52 (m, 2H), 2.85 (s, 6H), 3.0 (m, 2H), 4.2 (t, *J* = 7.4 Hz, 1H), 7.2 - 7.4 (m, 10H). ^{13}C NMR ($CDCl_3$): δ 32.2, 45.8, 50.6, 58.3, 126.3, 128.2, 129.1, 143.1. Anal. Calcd for ($C_{17}H_{21}N{\cdot}C_2H_2O_4{\cdot}0.25\ H_2O$) C, 67.43; H, 7.14; N, 4.13 Found: C, 67.73; H, 6.97; N, 4.11.

4,4-Diphenylbutan-1-amine hydrochloride (16).[247] A 1.0 M solution of BH_3•THF complex (0.386 g, 4.5 mmol) was added at 0 °C to a well stirred solution of compound **71** (0.2 g, 0.9 mmol) in anhydrous THF (5 mL). The solution was brought to rt and then heated to reflux (8 h) and cooled. 6.0 M HCl (2 mL) solution was added cautiously to the reaction mixture, and continued to reflux (1 h). The reaction mixture was cooled and the solvent was removed under reduced pressure resulting in a white residue. Water (10 mL) was added to this residue followed by extraction with EtOAc (2 × 15 mL). The aqueous

phase was made basic with 10% NaOH and extracted with CH_2Cl_2 (3 × 25 mL). The combined CH_2Cl_2 extracts were washed with water, brine and dried ($MgSO_4$). The solvent was removed under reduced pressure to give the amine **16** (0.17 g, 85%) as oil. HCl salt: mp 198 - 200 °C. ^{1}H NMR ($CDCl_3$): 1.45 (m, 2H), 2.1 (m, 2H), 2.7 (t, *J* = 7.8 Hz, 2H), 4.0 (t, *J* = 7.8 Hz, 1H), 7.1 - 7.3(m, 10H). ^{13}C NMR ($CDCl_3$): δ 31.2, 36.2, 42.5, 53.5, 126.5, 128.3, 129.3, 143.0. Anal Calcd for ($C_{16}H_{19}N$·HCl) C, 73.40; H, 7.70; N, 5.35 Found: C, 72.30; H, 7.51; N, 5.24.

***N*-Methyl-4,4-diphenylbutan-1-amine oxalate (17).** BH_3•THF complex (1.0 M in THF, 0.335 g, 3.9 mmol) was added in a dropwise manner to a stirred solution of **75 (**0.2 g, 0.78 mmol) in anhydrous THF (4 mL) under N_2 at 0 °C. The mixture was slowly warmed to rt and heated at reflux (6 h). The reaction mixture was allowed to cool to rt, and HCl (6.0 M, 3 mL) was added with caution. The mixture heated at reflux (1 h) and allowed to cool to rt, and the solvent was removed under reduced pressure. Water was added and the residue was extracted with ether (25 mL). The aqueous portion was made basic with 10% NaOH and extracted with CH_2Cl_2 (3 × 25 mL). The organic layer was washed with water and brine, dried ($MgSO_4$), and concentrated under reduced pressure to give **17** as an oil. It was then purified by medium pressure column chromatography, CH_2Cl_2/MeOH (9:1) (0.148 g, 80%). Oxalate salt: mp 163 - 165 °C. (lit[247] mp 162 - 164 ^{o}C. ^{1}H NMR ($CDCl_3$): 1.49 (q, *J* = 7.8 Hz, 2H), 2.1 (q, *J* = 8.1 Hz, 2H), 2.4 (s, 3H), 2.61 (t, *J* = 7.5 Hz, 2H) 3.9 (t, *J* = 7.5 Hz, 1H), 7.1 - 7.31 (m, 10H). ^{13}C NMR ($CDCl_3$): δ

27.2, 36.2, 36.8, 50.8, 51.1, 126.2, 128.2, 129.3, 143.0. Anal Calcd for ($C_{17}H_{21}N \cdot C_2H_2O_4$) C, 69.28; H, 7.03; N, 4.25; Found: C, 69.02; H, 7.11; N, 4.26.

***N,N*-Dimethyl-4,4-diphenylbutan-1-amine oxalate (18)**.[247] BH_3•THF complex (1.0 M in THF, 0.317 g, 3.7 mmol) was added in a dropwise manner to a stirred solution of **76** (0.2 g, 0.74 mmol) in anhydrous THF (4 mL) under N_2 at 0 °C. The mixture was slowly warmed to rt and heated at reflux (6 h). The reaction mixture was allowed to cool to rt, and HCl (6.0 M, 3 mL) was added with caution. The mixture was heated at reflux (1 h) and allowed to cool to rt, and the solvent was removed under reduce pressure. Water was added and the residue was extracted with ether (25 mL). The aqueous portion was made basic with 10% NaOH and extracted with CH_2Cl_2 (3 × 25 mL). The organic layer was washed with water and brine, dried ($MgSO_4$), and concentrated under reduced pressure to give **18** as an oil. It was then purified by medium pressure column chromatography, CH_2Cl_2/MeOH (9:1) (0.155 g, 83%). Oxalate salt. mp 149 - 151 °C. (lit[247] mp 152 – 154 °C). ^{1}H NMR ($CDCl_3$): 1.54 (q, *J* = 7.5 Hz 2H), 2.1 (q, *J* = 7.8 Hz, 2H), 2.3 (s, 6H), 2.49 (t, *J* = 7.8 Hz, 2H), 3.9 (t, *J* = 7.5 Hz, 1H), 7.1-7.3 (m, 10H). ^{13}C NMR ($CDCl_3$): δ 24.7, 36.3, 44.8, 51.6, 59.3, 126.3, 128.2, 129.1, 143.1. Anal Calcd for ($C_{18}H_{23}N \cdot C_2H_2O_4 \cdot 0.25 H_2O$) C, 69.04; H, 7.38; N, 4.02 Found: C, 69.32, H, 7.20, N, 4.12.

***N*-((9,10-Dihydroanthracen-10-yl)methyl)-2-phenylethanamine hydrochloride (20).** BH_3•THF complex (1.0 M in THF, 1.0 g 12.2 mmol) was added in a dropwise manner to a stirred solution of **77** (0.8 g, 2.44 mmol) in anhydrous THF (4 mL) under N_2 at 0 °C.

The mixture was slowly warmed to rt and heated at reflux (6 h). The reaction mixture was allowed to cool to rt, and HCl (6.0 M, 3 mL) was added with caution. The mixture was heated at reflux (1 h) and allowed to cool to rt, and the solvent was removed under reduce pressure. Water was added and the residue was extracted with ether (25 mL). The aqueous portion was made basic with 10% NaOH and extracted with CH_2Cl_2 (3 × 25 mL). The combined CH_2Cl_2 extracts were washed with water and brine, dried ($MgSO_4$), and concentrated under reduced pressure to give the amine as an oil. It was then purified by medium pressure column chromatography, CH_2Cl_2/MeOH (9:1) to yield **20** (0.57 g, 75%). HCl salt: mp 188 – 190 °C. ^{1}H NMR ($CDCl_3$): 2.4 (m, 2H), 2.93 (m, 2H), 3.07 (d, *J* = 8.1 Hz, 2H), 3.95 (d *J* = 18.6 Hz, 1H), 4.09 (d, *J* = 18.6 Hz, 1H), 4.5 (t, *J* = 7.8 Hz, 1H), 7.1 - 7.4 (m, 13H). ^{13}C NMR ($CDCl_3$): δ 36.6, 40.3, 48.7, 50.5, 57.5, 126.2, 126.8, 127.7, 128.7, 138.2, 138.6, 139.7. Anal Calcd for ($C_{23}H_{23}N$·HCl·0.25 H_2O) C, 77.94; H, 6.96; N, 3.95; Found: C, 78.19; H, 6.87; N, 4.0.

***N*-((9,10-Dihydroanthracen-10-yl)methyl)-3-phenylpropan-1-amine oxalate** (**21**). BH_3•THF complex (1.0 M in THF, 0.25 g 2.92 mmol) was added in a dropwise manner to a stirred solution of **78 (**0.2 g, 0.58 mmol) in anhydrous THF (4 mL) under N_2 at 0 °C. The mixture was slowly warmed to rt and heated at reflux (6 h). The reaction mixture was allowed to cool to rt, and HCl (6.0 M, 3 mL) was added with caution. The mixture heated at reflux (1 h) and allowed to cool to rt, and the solvent was removed under reduced pressure. Water was added and the residue was extracted with ether (25 mL). The aqueous portion was made basic with 10% NaOH and extracted with CH_2Cl_2 (3 × 25

mL). The combined CH_2Cl_2 extracts were washed with water and brine, dried ($MgSO_4$), and concentrated under reduced pressure to give amine as an oil. It was then purified by medium pressure column chromatography, CH_2Cl_2/MeOH (9:1) to yield **57** (0.15 g, 80%). Oxalate salt: mp 208 - 210 °C. ^{1}H NMR ($CDCl_3$): 1.94 (m, 2H), 2.63 (t, *J* = 7.5Hz, 2H), 2.9 (m, 2H), 3.1 (d, *J* = 8.1 Hz, 2H), 3.97 (d, *J* = 18.6 Hz, 4.1 (d, *J* = 18.6 Hz, 2H), 4.3 (t, *J* = 8.1 Hz, 2H), 7.1 - 7.4 (m, 13H). ^{13}C NMR ($CDCl_3$): δ 29.6, 30.3, 35.7, 40.5, 49.5, 49.2, 58.6, 126.1, 126.8, 128.1, 128.7, 128.9, 138.2, 138.6, 139.7. Anal Calcd ($C_{24}H_{25}N{\cdot}HCl{\cdot}0.25\ H_2O$) C, 73.99; H, 6.59; N, 3.31 Found: C, 74.11; H, 6.49; N, 3.33.

***N*-((9,10-Dihydroanthracen-9-yl)methyl)-4-phenylbutan-1-amine hydrochloride (22)**. BH_3•THF complex (1.0 M in THF, 0.6 g 7.0 mmol) was added in a dropwise manner to a stirred solution of **79 (**0.5 g, 1.4 mmol) in anhydrous THF (4 mL) under N_2 at 0 °C. The mixture was slowly warmed to rt and heated at reflux (6 h). The reaction mixture was allowed to cool to rt, and HCl (6.0 M, 3 mL) was added with caution. The mixture heated at reflux (1 h) and allowed to cool to rt, and the solvent was removed under reduced pressure. Water was added and the residue was extracted with ether (25 mL). The aqueous portion was made basic with 10% NaOH and extracted with CH_2Cl_2 (3 × 25 mL). The combined CH_2Cl_2 extracts were washed with water and brine, dried ($MgSO_4$), and concentrated under reduced pressure to give amine as an oil. It was then purified by medium pressure column chromatography, CH_2Cl_2/MeOH, (9:1) to yield **22** (0.38 g, 80%). HCl salt: mp 198 - 200 °C. ^{1}H NMR ($CDCl_3$): 1.63 (m, 4H), 2.61 (m, 2H), 2.9 (m, 2H), 3.1 (m, 2H), 3.97 (d, *J* = 18.2 Hz, 1H), 4.1 (d, *J* = 18.2 Hz, 1H), 4.4 (t, *J* =

8.1 Hz, 2H), 7.1 - 7.4 (m, 13H). ^{13}C NMR ($CDCl_3$): δ 28.6, 30.1, 35.7, 40.4, 49.5, 50.2, 58.6, 126.0, 126.8, 128.1, 128.6, 128.7, 138.2, 138.6, 139.7. Anal Calcd for ($C_{25}H_{27}N{\cdot}HCl{\cdot}0.25\ H_2O$) C, 77.59; H, 7.55; N, 3.61 Found: C, 77.75; H, 7.56; N, 3.62.

[(9,10-Dihydro-9-anthryl)methyl]trimethyl ammonium iodide (23).[248] To a solution of compound **3** (0.2 g, 0.79 mmol**)** in anhydrous CH_2Cl_2 (4 mL) was added iodomethane (0.168 g, 3.95 mmol). The reaction mixture was stirred at rt for 3 h. Ethyl acetate (3 mL) was then added to the mixture in a dropwise manner resulting in the formation of white turbid solution. The reaction mixture was then cooled, refrigerated to obtain a white solid. The solid was then purified by medium pressure column chromatography, CH_2Cl_2/MeOH (10:1) to obtain **23** (0.22 g, 70%). mp 148 - 150 °C. ^{1}H NMR (DMSO): 3.04 (s, 9H), 3.54 (d, *J* = 7.2 Hz, 2H), 4.79 (t, *J* = 7.2 Hz), 3.97 (d, *J* = 18.3 Hz, 1H), 4.01 (d, *J* = 18.3 Hz, 1H), 4.28 (m, 8H). ^{13}C NMR (DMSO): δ 35.5, 42.6, 53.5, 68.5, 127.2, 127.9, 138.1, 138.6. Anal Calcd for ($C_{18}H_{22}N$) C, 56.33; H, 5.90; N, 3.64 Found: C, 56.15, H, 5.87; N, 3.63.

(7,12-Dihydrotetraphen-12-yl)methanamine fumarate (24). Methanesulfonic acid (20 ml) was added to compound **84** (0.5 g, 1.8 mmol) and was stirred for 1 h. The reaction mixture was allowed to cool and then added to a cold solution of 10% NaOH until basic. The mixture was then extracted with CH_2Cl_2 (75 ml). Combined extracts were washed with brine, water, and dried ($MgSO_4$). Evaporation of solvent gave a mixture of **24** (major) and **25** (minor) as the products. Further purification was carried out by medium

pressure column chromatography, CH_2Cl_2/MeOH (10:1) to obtain product as a light brown oil (0.040 g, 20%). However, the final mixture obtained was mixture of **24** and **25**. Fumarate salt: mp 148 – 150 °C. ^{1}H NMR ($CDCl_3$): 3.1 (m, 1H), 3.18 (m, 1H), 4.1 (d, *J* = 18.6 Hz, 2H), 4.21 (d, *J* = 18.6 Hz, 2H), 4.6 (t, *J* = 7.2 Hz), 7.2 - 8.1 (m, 9H); ^{13}C NMR ($CDCl_3$): δ 37.2, 44.1, 47.84, 105.3, 117.8, 125.2, 134.7, 157.1. Anal.Calcd ($C_{19}H_{17}NO{\cdot}C_4H_6O_4$) C, 73.58; H, 5.63; N, 3.73.

(7,12-Dihydro-3-methoxytetraphen-12-yl)methanamine fumarate (26).

Methanesulfonic acid (20 ml) was added to the compound **85** (0.5 g, 1.62 mmol) and was stirred for 1 h. The reaction mixture was allowed to cool and then added to a cold solution of 10% NaOH until basic, and extracted with CH_2Cl_2 (75 ml). Combined extracts were washed with brine, water, and dried ($MgSO_4$). Evaporation of solvent gave a mixture of **26** (major) and **27** (minor) as the products. Further purification was carried out by medium pressure column chromatography, CH_2Cl_2/MeOH (10:1). Only the major product was separated (0.040 g, 26%) as light brown oil. Fumarate salt: mp 132 – 135 °C. ^{1}H NMR ($CDCl_3$): 2.97 (m, 1H,) 3.05 (m, 1H) 3.94 (s, 3H), 3.98 (d, *J* = 18.6 Hz, 2H), 4.24 (d, *J* = 18.6 Hz, 2H), 4.75 (t, *J* = 7.2 Hz), 7.17 - 8.1 (m, 9H); ^{13}C NMR ($CDCl_3$): δ 35.99, 45.9, 47.84, 55.53, 106.3, 118.8, 125.6, 134.7, 156.4. Anal. Calcd for ($C_{20}H_{19}NO{\cdot}C_4H_6O_4{\cdot}0.5\ H_2O$) C, 68.0; H, 5.95; N, 3.30 Found: C, 67.49, H, 5.54; N, 3.52.

4-(4-(Dimethylamino)-1-phenylbutyl)benzoic acid (29).[249] Compound **89** (0.4 g, 1.35 mmol) was dissolved in a solution of MeOH:CH_2Cl_2 (5:1) (10 mL). Pd/C (0.2 g 10%) was added and the mixture was stirred overnight under a hydrogen atmosphere. The reaction mixture was filtered with celite and the filtrate was concentrated under reduced pressure. The residue was triturated with diethyl ether and the precipitate was collected by filtration to obtain product. Recrystallization from ethanol and petroleum ether afforded **29** as a faint yellow powder (0.38 g, 95%). mp 233 – 235 °C. ^{1}H NMR (DMSO): 1.56 (m, 2H), 2.13 (m, 2H), 2.6 (s, 6H), 3.05 (t, *J* = 7.2 Hz, 2H), 4.07 (t, *J* = 7.2 Hz, 1H), 7.22 -7.88 (m, 9H); ^{13}C NMR (DMSO): δ 23.07, 32.11, 42.6, 50.9, 56.8, 127.0, 128.4, 129.6, 144.7, 150.4, 167.89. Anal Cacld for ($C_{19}H_{23}NO_2 \cdot HCl \cdot H_2O$) C, 64.85; H, 7.44; N, 3.98 Found: C, 64.18; H, 7.08; N, 3.70. (ESIMS (-ve) calcd for $C_{19}H_{23}NO_2$ [$(M-H)^-$] 298.17 Found 298.22.

6,11-Dihydro-11-oxo-dibenz[*b,e*]oxepin-2-acetic acid (31).[237] A mixture of compound **93** (1.43 g, 5.0 mmol), polyphosphoric acid (9.0 g) and 7 mL of acetic acid was stirred at 80 °C for 6 h. After hydrolyzing the mixture with 75 mL of water, 10% NaOH was added until basic and the aqueous mixture was extracted with ether. Acidification of the ice-cooled aqueous phase with concentrated HCl provided a solid which was purified by medium pressure column chromatography, CH_2Cl_2/MeOH (10:1) to obtain **31** (0.53 g, 40%). mp 134 - 136 °C. (lit[237] 135 - 136 °C). ^{1}H NMR($CDCl_3$): 3.70 (s, 2H), 5.21 (s, 2H), 7.0 - 8.1 (m, 7H); ^{13}C NMR($CDCl_3$): δ 39.48, 73.19, 120.74, 124.69, 126.65, 127.39, 128.86, 129.07, 132.17, 132.38, 135.04, 135.98, 139.96, 160.16, 176.77, 190.45;

Anal Calcd for ($C_{16}H_{12}O_4$) C, 71.63; H, 4.50; O, 23.85 Found: C, 71.18; H, 4.46; O, 23.58.

6,11-Dihydrodibenz[*b,e*]oxepin-2-acetic acid (32).[237] To a stirred solution of compound **31** (0.1 g, 0.37 mmol) in acetic acid (3 mL) was added Zn powder (0.3 g, 4.46 mmol) and the mixture was refluxed for 2 h, cooled and filtered. The filtrate was concentrated in vacuum to obtain syrupy residue. After addition of water to the syrupy residue, the mixture was extracted with $CHCl_3$ (3 × 25 mL) which was washed with water, dried ($MgSO_4$) and concentrated. The residue obtained was purified by crystallization from benzene to yield product **32** (0.055 g 60%). mp 156 - 158 °C. (lit[237] 155 – 157 °C). ^{1}H NMR($CDCl_3$): 3.57 (s, 2H), 4.24 (s, 2H), 5.32 (s, 2H), 6.8 - 7.3 (m, 7H); ^{13}C NMR($CDCl_3$): δ 38.47, 39.69, 70.27, 119.68, 125.27, 125.40, 125.64, 126.65, 127.58, 127.65, 127.81, 128.20, 128.28, 128.46, 128.63, 131.32, 135.26, 139.32, 155.74, 179.21. Anal. ($C_{16}H_{14}O_3 \cdot 0.75\ H_2O$) C, 71.76; H, 5.83 Found: C, 71.87; H, 5.45.

11-Methylene-6,11-dihydrodibenz[*b,e*]oxepin-2-acetic acid (33). To a solution of compound **94** (0.1 g) in absolute ethanol was added 10% NaOH and refluxed for 3 h. The reaction mixture was then cooled and concentrated. HCl was added to the mixture and extracted with CH_2Cl_2 (3 × 25 mL). The solvent was concentrated in vacuum to obtain the product **33** as a pale white solid (0.085 g, 90%). mp 162 - 164 °C. ^{1}H NMR($CDCl_3$): 3.62 (s, 2H), 5.2 (s, 2H), 5.32 (s, 1H), 5.74 (s, 1H), 6.86 (d, *J* = 8.4 Hz 1H), 7.14 (d, *J* = 8.4 Hz 1H), 7.33 - 7.38 (m, 4H); ^{13}C NMR($CDCl_3$): δ 39.72, 70.39,

117.20, 119.62, 125.41, 126.48, 127.11, 127.71, 128.73, 130.14, 130.65, 133.69, 143.36, 147.53, 154.85, 177.62. Anal Calcd for ($C_{17}H_{14}O_3 \cdot H_2O$) C, 69.61; H, 5.84 Found: C, 69.87; H 5.84. ESIMS (-ve) *m*/*z* calcd for $C_{17}H_{13}O_3$ [$(M-H)^-$] 265.09, Found 264.963.

(*E*,*Z*)-(11-[4-Methylpentylidene]-6,11-dihydrobenz[*b*,*e*]oxepin-2-acetic acid (34). In a two-necked round-bottomed flask equipped with a stirrer was added compound **101** (0.1 g, 0.31 mmol), acetonitrile (4 mL), TEMPO (2,2,6,6-tetramethyl-1-piperidinyloxy free radical (0.0339 g, 0.0217 mmol), sodium chlorite (0.056 g, 0.62 mmol) and 0.67 M sodium phosphate buffer (1.2 mL) and kept for stirring. A dilute bleach solution (0.15 mL) was added to this mixture in a dropwise manner. The resultant mixture was heated to 35 °C and stirring was continued until reaction was completed (6 h). After cooling the reaction mixture to 25 °C, water (5 mL) was added and the pH was adjusted to 8.0 by addition of 2N NaOH. The reaction mixture was than poured into ice-cold sodium sulfite solution (30 mL) maintained below 20 °C. After stirring for 30 min at rt, methyl t-butyl ether (MTBE) was added and the rapidly stirred mixture was acidified with 2 N HCl to pH 3-4. The organic layer was separated and washed with water, brine, dried ($MgSO_4$) and concentrated to give **34** as a mixture of geometrical isomers (*E*/*Z* = 3/7) as an oil (0.041 g, 40%). ^{1}H NMR($CDCl_3$): 0.91 (d, *J* = 6.6 Hz, 6H), 1.40 (q, *J* = 7.2 Hz, 2H), 1.62 (m, 1H), 2.42 (q, *J* = 7.2 Hz, 2H), 3.58 (s, 2H), 5.71 (t, *J* = 7.8 Hz, 1H), 6.1 (t, *J* = 7.8 Hz, 1H), 6.8 - 7.3 (m, 7H); ^{13}C NMR($CDCl_3$): δ 22.07, 27.06, 27.29, 38.63, 39.68, 69.95, 119.31, 123.60, 124.43, 125.86, 126.92, 127.04, 128.68, 129.42, 131.91, 133.21, 133.54,

137.84, 145.44, 154.28, 177.43; Anal Calcd for ($C_{22}H_{24}O_3$) C, 78.54, H, 7.19 Found: C, 78.1; H, 9.7. ESIMS (-ve) calcd for $C_{22}H_{24}O_3$ [$(M-H)^-$] 335.16, found 335.23.

6,11-Dihydro-11-oxo-dibenz[*b,e*]oxepin-2-acetic acid ethyl ester (**35**).[237] A mixture of compound **31** (1.0 g), absolute ethanol (10 mL) and concentrated sulfuric acid (2 mL) was refluxed for 6 h. The solution was then cooled and concentrated. The crude product obtained was dissolved in ether, washed with 5% NaOH solution, water and dried ($MgSO_4$) to yield solid. The solid was purified by medium pressure column chromatography, CH_2Cl_2/MeOH (9:1) to obtain **35** (0.99 g, 90%). mp 90 - 92 °C. (lit[237] 89 – 91 °C). ^{1}H NMR($CDCl_3$): 1.26 (t, *J* = 7.2 Hz, 3H), 3.60 (s, 2H), 4.14 (q, *J* = 7.2 Hz, 2H), 5.17 (s, 2H), 7.0 - 7.57 (m, 7H); ^{13}C NMR($CDCl_3$): δ 14.44, 40.48, 61.22, 73.84, 121.26, 125.33, 128.04, 128.17, 129.49, 129.70, 132.65, 133.0, 135.77, 136.60, 140.69, 160.67, 171.69, 191.11.

11-Oxo-2-[4,4-dimethyl-2-oxazolin-2-yl)methyl]-6,11-dihydrobenz[*b,e*]oxepin (**36**). To a solution of compound **31** (0.3 g, 1.18 mmol) in CH_2Cl_2 (8 mL) and pyridine (1 mL) was added $SOCl_2$ (0.214 g, 1.8 mmol) at 0 °C, and the mixture was stirred at rt for 2 h. The reaction mixture was concentrated and the residue obtained was treated with 2-amino-2-methylpropanol (0.77 g, 8.73 mmol) in toluene (5 mL) at 50 °C for 3 h. The reaction mixture was then diluted with EtOAc, washed with brine, dried ($MgSO_4$) and concentrated. The residue obtained was recrystallized from toluene to obtain carboxamide (0.2 g, 0.58 mmol) which was suspended in CH_2Cl_2 (8 mL). To this

suspension was added $SOCl_2$ (0.082 g 0.69 mmol) at 0 °C, and the mixture was stirred at rt for 1 h. The reaction mixture was diluted with CH_2Cl_2, washed with brine, dried ($MgSO_4$) and concentrated to obtain product which was purified by medium pressure column chromatography, hexane/EtOAc (2:1) to yield **36** as an oil (0.05g, <5%). ^{1}H NMR($CDCl_3$): 1.31 (s, 6H), 3.63 (s, 2H), 3.95 (s, 2H), 5,21 (s, 2H), 7.0 - 8.1 (m, 7H); ^{13}C NMR($CDCl_3$): δ 27.94, 33.51, 66.72, 73.17, 78.94, 120.67, 124.72, 127.34, 128.63, 128.81, 129.04, 131.55, 132.29, 135.09, 135.30, 140.06, 157.81, 159.91, 163.57, 175.87, 186.23, 190.42.

(*E*,*Z*)-(11-[4-Methylpentylidene]-6,11-dihydrobenz[*b*,*e*]oxepin-2-acetic acid methyl ester (37). To a suspension of 4-(methylpentane) triphenylphosphonium bromide (0.79 g, 1.86 mmol) in anhydrous THF (5 mL) under N_2 atmosphere at 0 °C was added a 2.5 M solution of *n*-BuLi (0.35 g, 5.58 mmol) in hexane. The solution was stirred under the same condition for 1 h. A solution of **31** (0.1 g, 0.37 mmol) in THF (2 mL) was added and the resulting mixture was stirred at rt for 2 h. After being concentrated, the reaction mixture was diluted with water, washed with ether, and than neutralized. The resulting solution was concentrated and the residue obtained was dissolved in methanol (10 mL) containing *p*-TsOH·H_2O (0.1 g, 0.55 mmol) and refluxed for 2 h. The reaction mixture was concentrated, diluted with EtOAc (50 mL) and washed with water. The organic layer was dried ($MgSO_4$) and concentrated in vacuum to obtain product which was purified by medium pressure column chromatography, CH_2Cl_2/MeOH (9:1) to yield **37** as an oil. The product obtained was in very low yield (<5%). 1H NMR($CDCl_3$): 0.91 (d, 6H), 1.28 (m,

2H), 1.65 (m, 2H), 2.44 (m, 1H), 3.5 (s, 2H), 3.71 (s, 3H), 5.17 (bs, 2H), 5.67 (t, *J* = 7.5 Hz, 1H), 6.0 (t, *J* = 7.5 Hz 1H), 6.7 - 7.3 (m, 7H).

9,10-Dihydroanthracene-10-carboxylic acid (43). To a well-stirred suspension of 9,10-dihydroanthracene **42** (4.5 g, 25.0 mmol) in anhydrous ether (40 mL) was added *n*-BuLi (1.6 g, 25 mmol) under N_2 at 0 °C. The resulting dark solution was stirred at rt for 2 h and then heated to reflux for 45 min. The reaction mixture was then poured over an excess of dry ice slurry, extracted with water and acidified with HCl. The precipitate obtained was collected by vacuum filtration and recrystallized from 2-propanol to yield **43** (2.5 g, 45%) as white solid. mp 200 - 202 °C. (lit[243] 200 - 207 °C). ^{1}H NMR ($CDCl_3$): 3.9 (s, 1H), 4.2 (s, 1H), 4.9 (s, 1H), 7.26 (s, 4H), 7.42 (s, 4H).

2-(9,10-Dihydroanthracen-10-yl)-*N*-methylacetamide (44). Thionyl chloride (2.65 g, 22.2 mmol) was added under N_2 to a stirred solution of compound **43** (l.0 g, 4.45 mmol) in anhydrous benzene (4 mL). The solution was heated at reflux (2 h), allowed to cool and the excess benzene and thionyl chloride were removed under reduced pressure to provide an oil. The oil obtained was dissolved in anhydrous THF (4 mL) and cooled in an ice bath (0 °C). Methylamine/THF (2 M, 0.276 g, 8.9 mmol) solution was added dropwise into the stirred solution, and the mixture was stirred at rt (2 h). The solvent was removed under reduced pressure to give a white solid. Water (20 mL) was added, and the suspension was extracted with EtOAc (3 × 25 mL). The combined extracts were washed with water, brine and dried ($MgSO_4$). Removal of solvent under reduced pressure gave

crude amide as viscous oil. The resulting amide was purified using medium pressure chromatography, petroleum ether/EtOAc (6:4) to yield **44** (0.756 g, 72%). ^{1}H NMR ($CDCl_3$): 2.65 (s, 3H), 3.95 (d, *J* = 18.3 Hz, 1H), 4.12 (d, *J* = 18.3 Hz, 1H), 4.85 (s, 1H), 7.25 - 7.46 (m, 8H).

2-(9,10-Dihydroanthracen-10-yl)-*N*,*N*-dimethylacetamide (45).[243] Thionyl chloride (2.65 g, 22.3 mmol) was added under N_2 to a stirred solution of compound **43** (1.0 g, 4.45 mmol) in anhydrous benzene (4 mL). The solution was heated at reflux (2 h), allowed to cool and the excess benzene and thionyl chloride were removed under reduced pressure to provide an oil. The oil obtained was dissolved in anhydrous THF (4 mL) and cooled in an ice bath (0 °C). Dimethylmethylamine/THF (2 M, 0.4 g, 8.9 mmol) solution was added dropwise into the stirred solution, and the mixture was stirred at rt (2 h). The solvent was removed under reduced pressure to give a white solid. Water (20 mL) was added, and the suspension was extracted with EtOAc (3 × 25 mL). The combined extracts were washed with water, brine and dried ($MgSO_4$). Removal of solvent under reduced pressure gave crude amide as oil. The resulting oil was purified using medium pressure chromatography, petroleum ether/EtOAc (6:4) to yield **45** (0.83 g, 75%). ^{1}H NMR ($CDCl_3$): 3.06 (s, 6H), 4.0 (d, *J* = 18.6 Hz, 1H), 4.51 (d, *J* = 18.6 Hz, 1H), 5.34 (s, 1H), 7.20 - 7.37 (m, 8H).

9-(2-Nitrovinyl)anthracene (47).[191] Ammonium acetate (0.56 g, 7.27 mmol) was added to a well stirred solution of nitromethane (30 mL) and 9-anthraldehyde **46** (1.5 g, 7.27

mmol). The reaction mixture was heated to reflux for 40 min. The red solution obtained was evaporated under reduced pressure to remove nitromethane. The oily red solid was then dissolved in EtOAc and washed with water and brine. The EtOAc was removed under reduced pressure to yield nitrostyrene product **47** (95%). ^{1}H NMR ($CDCl_3$): 7.5 - 7.6 (m, 4H), 7.68 (s, 1H), 7.7 - 7.8 (m, 4H), 7.78 (d, *J* = 14 Hz, 1H) 7.9 (d, *J* = 14 Hz, 1H).

2-(Anthracen-9-yl)ethanamine (48). Compound **47** (0.5 g, 2.2 mmol) was added to an ice-cold solution of THF (25 mL) and $LiAlH_4$ (0.22 g, 6.0 mmol). The reaction was heated to reflux for 5 h and then cooled. To this was added 1 ml water and 1 mL 10% NaOH. Celite was then added to the mixture and filtered. The mixture was washed with CH_2Cl_2. The filtrate was washed with water, dried ($MgSO_4$), and the solvent was removed under reduced pressure to yield crude product as oil that was purified by medium pressure column chromatography, CH_2Cl_2/MeOH (9:1) to obtain **48** (0.3 g, 80%). ^{1}H NMR ($CDCl_3$): 2.8 (t, *J* = 7.8 Hz, 2H), 3.0 (t, *J* = 7.8 Hz, 2H), 7.4 - 7.5 (m, 4H), 7.56 (s, 1H), 7.6 - 7.7(m, 4H).

9-Bromomethylanthracene (50).[193] A suspension of 9-hydroxymethylanthracene **(49,** 1.5 g, 7.2 mmol) in toluene (40 mL) was cooled to 0 ^{o}C followed by addition of phosphorus tribromide (0.8 mL, 8.4 mmol) *via* syringe. The mixture was stirred at 0 °C for 1 h and then warmed to rt, during which the reaction became homogeneous. Saturated Na_2CO_3 solution (15 mL) was added slowly and the reaction was stirred until it cooled to

rt. The phases were separated, and the organic phase was washed with water (10 mL), brine (10 mL) and dried over $MgSO_4$. The yellow filtrate was concentrated to minimum volume, and then stored at 0 °C for crystallization. The yellow needle-like solid was collected and dried in vacuum (1.24 g). The mother liquid was concentrated and purified using medium pressure column chromatography (0.6 g). The two parts were combined to give the product **50** (total 1.84 g, 94%) as yellow needles. mp 145 -148 °C. ^{1}H NMR ($CDCl_3$): 5.5 (s, 2H), 7.2 - 8.4 (m, 9H).

2-(Anthracen-9-yl)acetonitrile (51). A solution of compound **50** (1.5 g, 5.53 mmol) in DMSO (15 mL) was added over 10 min to a rapidly stirred suspension of KCN (0.54 g, 8.29 mmol) in DMSO (30 mL) at 70 °C under N_2. The mixture was stirred for an additional 40 min, cooled to rt and then diluted with water. The aqueous layer was saturated with sodium chloride and then extracted with ether (3 × 25 mL). The combined extracts were washed with water, dried ($MgSO_4$,), filtered, and concentrated to yield product **51** (0.96 g, 80%) as a pale white solid. mp 154 - 156 °C. ^{1}H NMR ($CDCl_3$): 4.61 (s, 2H), 7.2 - 8.5 (m, 9H).

2-(Anthracen-9-yl)acetic acid (52). To a suspension of compound **51** (0.95 g, 4.37 mmol) in ethylene glycol (50 mL) was added KOH (0.97 g, 17.48 mmol) in 10 ml of water. The mixture was heated to reflux for 24 h until the entire solid was completely dissolved. The hot solution was filtered, and the filtrate was acidified with dilute HCl to

obtain precipitate of product **52** (1.08 g, 100%). mp 212 - 214 °C. (lit[244] 208 - 212 °C). ^{1}H NMR ($CDCl_3$): 4.63 (s, 2H), 7.4 - 8.5 (m, 9H).

2-(9,10-Dihydroanthracen-9-yl)acetic acid (53). To a refluxing solution of compound **52** (0.375 g, 1.58 mmol) in 1-pentanol (10 mL) were added sodium pieces (0.36 g, 10 equiv) slowly. The reaction mixture was stirred for 10 min until all the sodium dissolved. Water (10 mL) was added to the cooled mixture and then made acidic with 5% HCl. The reaction mixture was dried under high vacuum and the oily solution obtained was extracted with chloroform, dried ($MgSO_4$) and concentrated to yield pure product **53** (0.3 g, 80%) as white solid. mp 168 - 170 °C. (lit[245] 167 - 169 °C) ^{1}H NMR ($CDCl_3$): 2.63 (s, 2H), 4.48 (t, *J* = 6.9 Hz, 1H), 3.91 (d, *J* = 18.6 Hz, 1H) 4.06 (d, *J* = 18.6 Hz, 1H), 7.4 - 8.4 (m, 9H).

2-(9,10-Dihydroanthracen-9-yl)-*N*-methylacetamide (54). Thionyl chloride (0.86 g, 7.3 mmol) was added under N_2 to a stirred solution of compound **53** (0.35 g, 1.45 mmol) in anhydrous benzene (4 mL). The solution was heated at reflux (2 h), allowed to cool and the excess benzene and thionyl chloride were removed under reduced pressure to provide an oil. The oil obtained was dissolved in anhydrous THF (4 mL) and cooled in an ice bath (0 °C). Methylamine/THF (2 M, 0.09 g, 2.9 mmol) solution was added dropwise into the stirred solution, and the mixture was stirred at rt (2 h). The solvent was removed under reduced pressure to give a white solid. Water (20 mL) was added, and the suspension was extracted with EtOAc (3 × 25 mL). The combined extracts were washed

with water, brine and dried ($MgSO_4$). Removal of solvent under reduced pressure gave the crude amide as yellow oil. The resulting amide was purified using medium pressure chromatography, CH_2Cl_2/Acetone to yield **54** (0.27g, 76%). ^{1}H NMR ($CDCl_3$): 2.16 (s, 3H), 2.41 (d, *J* = 7.5 Hz, 2H), 3.93 (d, *J* = 18.3 Hz, 1H), 4.05 (d, *J* = 18.3 Hz, 1H), 4.56 (t, *J* = 7.5 Hz, 1H), 7.1 -7.3 (m, 8H).

2,(9,10-Dihydroanthracene-9-yl)ethanol (56). Na_2K silica gel (2 g) was added to a well stirred solution of 2-(anthracen-9-yl)ethanol **55** (0.75 g, 4.4 mmol) in anhydrous THF (10 mL) under N_2 at rt. The reaction mixture was refluxed for 15 min then allowed to cool to rt and quenched with water (50 mL). The solid precipitate obtained was filtered and washed with EtOAc (3 × 25 mL). The filtrate was collected and the mixture was extracted. The EtOAc portion was dried ($MgSO_4$) and concentrated under reduced pressure to obtain viscous yellow oil. This was purified using medium pressure column chromatography, CH_2Cl_2/MeOH (9:1) to give **56** (0.65 g, 86%). ^{1}H NMR ($CDCl_3$): 1.76 (q, *J* = 6.3 Hz, 2H), 3.49 (t, *J* = 6.3 Hz, 2H), 3.93 (d, *J* = 18.2 Hz, 1H), 4.15 (d, *J* = 18.2 Hz, 1H), 4.08 (t, *J* = 7.2 Hz, 1H), 7.1 - 8.3 (m, 8H). ^{13}C NMR ($CDCl_3$): δ 31.5, 35.4, 38.5, 42.3, 60.1, 62.3, 130.1, 131.2, 136.2, 140.2.

2-(9,10-Dihydroanthracene-9-yl)acetaldehyde (57). A solution of compound **56** (0.50 g, 2.2 mmol) in anhydrous CH_2Cl_2 (10 mL) was added to a stirred mixture of Dess-Martin (periodinane) oxidant (1.39 g, 3.3 mmol) in CH_2Cl_2. The reaction mixture was stirred for 1h then diluted with ether (50 mL) and poured into 1.3 M NaOH (50 mL). The ether layer

was separated and extracted with 1.3 M NaOH (3 × 15 mL). The ether portion was washed with water (2 × 20 mL), brine (20 mL), dried ($MgSO_4$) and concentrated under reduced pressure to yield product as oil. The resulting oil was purified by medium pressure column chromatography, Petroleum ether/EtOAc (9:1) to give **57** (0.391 g, 80%) as an oil. ^{1}H NMR ($CDCl_3$): 2.76 (d, *J* = 7.5 Hz, 2H), 3.86 (d, *J* = 18.3 Hz, 1H), 4.05 (d, *J* = 18.3 Hz, 1H), 4.59 (t, *J* = 6.9 Hz, 1H), 7.0 - 7.2 (m, 8H), 9.7 (s, 1H). ^{13}C NMR ($CDCl_3$): 34.85, 40.77, 50.0, 126.19, 127.35, 137.21, 138.5, 200.0.

3-(Anthracen-9-yl)propanoic acid (61).[197] Anthrone **58** (3.0 g, 15.5 mmol) was added to a well stirred solution of potassium *t*-butoxide (2.17 g, 19.38 mmol) dissolved in anhydrous *t*-butyl alcohol (30 mL). The solution was stirred for 1h at rt. Acrylonitrile (0.9 g, 17.05 mmol) dissolved in 10 mL of anhydrous *t*-butyl alcohol was added dropwise over a period of 1 h to this reddish-brown solution of potassium anthranolate. During the addition of the nitrile a bright red precipitate separated. The reaction mixture was refluxed for 2 h and a clear deep red-colored solution was obtained. 5% HCl (2 mL) was added to the cooled mixture and *t*-butyl alcohol was removed under vacuum to yield a brown solid. Concentrated HCl (20 mL) was added to the residue which was refluxed for 12 h. After cooling, HCl was removed with the aid of a sintered glass filter and the solid remaining in the flask was washed with water. The solid acid was dissolved in a mixture of concentrated ammonium hydroxide (50 mL) and water (30 mL) and the resulting solution was heated at 90 °C for 4 h with 9.5 g of zinc dust. The cooled reaction mixture was filtered to remove excess zinc and the filtrate was extracted with ether. The aqueous

layer was acidified with HCl to yield a crude acid which was filtered and dried. Recrystallization of the crude acid with 2-propanol gave **61** (1.96 g, 51% yield) as pale yellow crystals. mp 194 - 195 °C. (lit[197] 194 – 195 °C). ^{1}H NMR ($CDCl_3$): 2.85 (t, *J* = 6.9 Hz, 2H), 4.01 (t, *J* = 6.9 Hz, 2H), 7.4 - 8.3 (m, 9H).

3-(9,10-Dihydroanthracen-9-yl)propanoic acid (62).[197] To a refluxing solution of compound **61** (0.5 g, 2.0 mmol) in 1-pentanol (15 mL) was added sodium pieces (0.46 g, 20 mmol) slowly. The reaction mixture was then stirred for 10 min until all the sodium dissolved. The reaction mixture was cooled, water (10 mL) was added to the mixture and made acidic with 5% HCl. The reaction mixture was dried under high vacuum and the oily solution obtained was extracted with chloroform, dried ($MgSO_4$,) and concentrated to give crude product. The crude product obtained was purified by medium pressure chromatography, CH_2Cl_2/MeOH (9:1) to give **62** (0.4 g, 85%) as a white solid. mp 138 - 140 °C. (lit[197] 137 - 140 °C). ^{1}H NMR ($CDCl_3$): 1.96 (q, *J* = 6.9 Hz, 2H), 2.32 (t, *J* = 7.2 Hz, 2H), 3.95 (t, *J* = 7.2 Hz, 1H), 3.9 (d, *J* = 18.6 Hz, 1H), 4.0 9 (d, *J* = 18.6 Hz, 1H), 7.1 - 7.29 (m, 8H).

3-(9,10-Dihydroanthracen-9-yl)propanamide (63). Thionyl chloride (0.14 g, 1.18 mmol) was added under N_2 to a stirred solution of compound **62** (0.15 g, 0.59 mmol) in anhydrous benzene (4 mL). The solution was heated at reflux (2 h), allowed to cool and the excess benzene and thionyl chloride were removed under reduced pressure to provide an oil. The brown oil obtained was dissolved in anhydrous THF (4 mL) and cooled in an

ice bath (0 °C). Anhydrous ammonia was slowly bubbled into the stirred solution for 0.5 h, and the mixture was stirred at rt (2 h). The solvent was removed under reduced pressure to give oil. Water (20 mL) was added, and the suspension was extracted with EtOAc (3 × 25 mL). The combined extracts were washed with water and brine and dried ($MgSO_4$). Removal of solvent under reduced pressure gave the crude amide. The resulting amide was purified using medium pressure chromatography, CH_2Cl_2/Acetone (9:1) to yield **63** (0.11 g, 75%). mp 131 - 133 °C. ^{1}H NMR ($CDCl_3$): 1.96 (t, *J* = 7.2 Hz, 2H), 2.18 (q, *J* = 7.2 Hz, 2H), 3.97 (t, *J* = 7.5 Hz, 1H), 3.90 (d, *J* = 18.2 Hz, 1H), 4.08 (d, *J* = 18.2 Hz, 1H), 7.2 - 8.3 (m, 8H).

3-(9,10-Dihydroanthracen-10-yl)-*N*-methylpropanamide (64). Thionyl chloride (0.14 g, 1.18 mmol) was added under N_2 to a stirred solution of compound **62** (0.15 g, 0.59 mmol) in anhydrous benzene (4 mL). The solution was heated at reflux (2 h), allowed to cool and the excess benzene and thionyl chloride were removed under reduced pressure to provide an oil. The oil obtained was dissolved in anhydrous THF (4 mL) and cooled in an ice bath (0 °C). Methylamine/THF (2 M, 0.036 g, 1.18 mmol) solution was added dropwise into the stirred solution, and the mixture was stirred at rt (2 h). The solvent was removed under reduced pressure to give a white solid. Water (20 mL) was added, and the suspension was extracted with EtOAc (3 × 25 mL). The combined extracts were washed with water, brine and dried ($MgSO_4$). Removal of solvent under reduced pressure gave crude amide. The resulting amide was purified using medium pressure chromatography, CH_2Cl_2/Acetone (9:1) to yield **64** (0.12 g, 78%). mp 148 - 150 °C. ^{1}H NMR ($CDCl_3$):

1.94 (t, *J* = 8.1 Hz, 2H), 2.12 (q, *J* = 7.2Hz, 2H), 2.73 (d, *J* = 4.8Hz, 3H), 3.95 (t, *J* = 7.5Hz, 1H), 3.89 (d, 18.6 Hz, 1H), 4.07 (d, *J* = 18.6 Hz, 1H), 7.1 - 7.3 (m, 8H). **^{13}C NMR ($CDCl_3$)**: δ 25.8, 32.5, 33.7, 34.7, 46.0, 125.8, 127.5, 135.6, 139.2, 172.6.

3-(9,10-Dihydroanthracen-10-yl)-*N*,*N*-dimethylpropanamide (65). Thionyl chloride (0.14 g, 1.18 mmol) was added under N_2 to a stirred solution of compound **62** (0.15 g, 0.59 mmol) in anhydrous benzene (4 mL). The solution was heated at reflux (2 h), allowed to cool and the excess benzene and thionyl chloride were removed under reduced pressure to provide an oil. The oil obtained was dissolved in anhydrous THF (4 mL) and cooled in an ice bath (0 °C). Dimethylmethylamine/THF (2 M, 0.053 g, 1.18 mmol) solution was added dropwise into the stirred solution, and the mixture was stirred at rt (2 h). The solvent was removed under reduced pressure to give a white solid. Water (20 mL) was added, and the suspension was extracted with EtOAc (3 × 25 mL). The combined extracts were washed with water, brine and dried ($MgSO_4$). Removal of solvent under reduced pressure gave the crude amide. The resulting amide was purified using medium pressure chromatography, CH_2Cl_2/Acetone (9:1) to yield **65** (0.124 g, 76%) as an oil. ^{1}H NMR ($CDCl_3$): 1.98 (t, *J* = 7.5 Hz, 2H), 2.26 (m, 2H), 2.87 (s, 3H), 2.92 (s, 3H), 4.04 (t, *J* = 7.2 Hz, 1H), 3.85 (t, *J* = 18.6 Hz, 1H), 4.11 (d, 18.6 Hz, 1H), 7.20 - 7.29 (m, 8H). ^{13}C NMR ($CDCl_3$): δ 25.5, 33.5, 32.2, 34.8, 45.7, 125.7, 127.4, 135.6, 139.5, 172.0.

3,3-Diphenylpropanal (68). A solution of 3,3-diphenylpropanol **67** (1.5 g, 7.0 mmol) in anhydrous CH_2Cl_2 (15 mL) was added to a stirred mixture of Dess-Martin (periodinane)

oxidant (3.2 g, 7.7 mmol) in CH_2Cl_2 (30 mL). After 50 min, the reaction mixture was diluted with ether (50 mL) and poured into 1.3 M aqueous NaOH (50 mL). The ether layer was separated and extracted with 1.3 M NaOH (30 mL). The ether layer was washed with water, dried ($MgSO_4$), and the solvent was removed under reduced pressure to give the **68** (1.11 g, 75%) as an oil. ^{1}H NMR ($CDCl_3$): 3.1 (m, 2H), 4.2 (t, *J* = 7.5 Hz, 1H), 7.1 - 7.3 (m, 10H), 9.2 (s, 1H). ^{13}C NMR ($CDCl_3$): δ 52.2, 55.8, 126.3, 128.2, 129.3, 143.1, 202.0.

4,4-Diphenylbutyronitrile (71). To a suspension of potassium metal (0.69 g, 17.76 mmol) and catalytic amount of ferric nitrate in liquid ammonia (50 mL, -70 °C) was added diphenylmethane **69** (2.5 g, 14.8 mmol) dissolved in ether (15 mL) over 15 min. The deep red suspension obtained was stirred for 30 min. To this reaction mixture was added bromopropionitrile **70** (1.98 g, 14.8 mmol) in ether. After the disappearance of deep red color, NH_3 was allowed to evaporate. The organic layer was separated and residue was extracted twice with ether (40 mL). The combined ether extracts were washed with 0.1 N HCl (2 × 30 mL) water (50 mL), brine (50 mL) and dried ($MgSO_4$). The solvent was removed under reduced pressure and resulting oil **71** (1.14 g, 35%) was purified by medium pressure chromatography, CH_2Cl_2/petroleum ether (2:3). ^{1}H NMR ($CDCl_3$): 2.27 (t, *J* = 7.5 Hz, 2H), 2.38 (q, *J* = 7.8 Hz, 2H), 4.06 (t, *J* = 7.8 Hz 1H), 7.1 - 7.3 (m, 10H).

4,4-Diphenylbutyric acid (73).[202] A solution of γ-phenyl-γ-butyrolactone **72** (1.62 g, 10.0 mmol) in anhydrous benzene (50 mL) was added in small proportions to anhydrous aluminum chloride (1.46 g, 11.0 mmol). The mixture was stirred at rt for 5 h, and then quenched with 2 N HCl. The benzene layer was extracted with ether (3 × 25 mL). Combined extracts were washed with water and dried ($MgSO_4$) after filtration, evaporation of the solvent afforded the compound **73** (2.0 g, 84%) as colorless crystals: mp 88 - 90 °C. (lit[202] mp 89 - 91 °C) ^{1}H NMR ($CDCl_3$): 2.3 (q, *J* = 7.8 Hz, 2H), 2.6 (t, *J* = 7.5 Hz, 2H), 4.1 (t, *J* = 7.8 Hz, 7.1 - 7.3 (m, 10H). ^{13}C NMR ($CDCl_3$): 25.1, 27.2, 50.2, 126.2, 128.3, 129.3, 143.0, 178.2.

***N*-Methyl-4,4-diphenylbutanamide (75).** Thionyl chloride (1.18 g, 10.0 mmol) was added under N_2 to a stirred solution of compound **73** (0.5 g, 2.0 mmol) in anhydrous benzene (4 mL). The solution was heated at reflux (2 h), allowed to cool and the excess benzene and thionyl chloride were removed under reduce pressure to provide an oil. The oil obtained was dissolved in anhydrous THF (4 mL) and cooled in an ice bath (0 °C). Methylamine/THF (2 M, 0.31 g, 10 mmol) solution was added dropwise into the stirred solution, and the mixture was stirred at rt (2 h). The solvent was removed under reduced pressure to give a white solid. Water (20 mL) was added, and the suspension was extracted with EtOAc (3 × 25 mL). The combined extracts were washed with water, brine and dried ($MgSO_4$). Removal of solvent under reduced pressure gave the crude amide. The resulting amide was purified using medium pressure chromatography, CH_2Cl_2/Acetone (9:1) to yield **75** (0.42 g, 80%). ^{1}H NMR ($CDCl_3$): 2.1 (t, *J* = 7.5 Hz,

2H), 2.38 (q, *J* = 7.8 Hz, 2H), 2.74 (d, *J* = 5.1Hz 3H), 3.9 (t, *J* = 7.8 Hz 1H), 7.1 - 7.3 (m, 10H).

***N,N*-Dimethyl-4,4-diphenylbutanamide (76)**[247]. Thionyl chloride (1.18 g, 10.0 mmol) was added under N_2 to a stirred solution of compound **73** (0.5 g, 2.0 mmol) in anhydrous benzene (4 mL). The solution was heated at reflux (2 h), allowed to cool and the excess benzene and thionyl chloride were removed under reduce pressure to provide an oil. The oil obtained was dissolved in anhydrous THF (4 mL) and cooled in an ice bath (0 °C). Dimethylmethylamine/THF (2 M, 0.45 g, 10.0 mmol) solution was added dropwise into the stirred solution, and the mixture was stirred at rt (2 h). The solvent was removed under reduced pressure to give a white solid. Water (20 mL) was added, and the suspension was extracted with EtOAc (3 × 25 mL). The combined extracts were washed with water, brine and dried ($MgSO_4$). Removal of solvent under reduced pressure gave crude amide as an oil. The resulting oil was purified using medium pressure chromatography, CH_2Cl_2/Acetone (9:1) to yield **76** (0.43 g, 85%). ^{1}H NMR ($CDCl_3$): 2.24 (t, *J* = 7.5 Hz, 2H), 2.39 (q, *J* = 7.2 Hz, 2H), 2.82 (d, *J* = 5.7 Hz, 3H), 3.97 (t, *J* = 7.2 Hz, 1H), 7.1 - 7.3 (m, 10H).

9,10-Dihydro-*N*-phenethylanthracene-10-carboxamide (77). Thionyl chloride (2.6 g, 22.0 mmol) was added under N_2 to a stirred solution of compound **43** (1g, 4.4 mmol) in anhydrous benzene (10 mL). The solution was heated at reflux (2 h), allowed to cool and the excess benzene and thionyl chloride were removed under reduce pressure to provide

an oil. The oil obtained was dissolved in anhydrous THF (4 mL) and cooled in an ice bath (0 °C). Phenylethylamine (1.0 g, 8.8 mmol) was added dropwise into the stirred solution, and the mixture was stirred at rt (2 h). The solvent was removed under reduced pressure to give a white solid. Water (20 mL) was added, and the suspension was extracted with EtOAc (3 × 25 mL). The combined extracts were washed with water, brine and dried ($MgSO_4$). Removal of solvent under reduced pressure gave a crude solid. The resulting amide was purified using medium pressure chromatography, CH_2Cl_2/Acetone (9:1) to yield **77** (1.05 g, 73%). mp 140 - 143 °C. ^{1}H NMR ($CDCl_3$): 2.63 (t, *J* = 7.2 Hz, 2H) 3.43 (q, *J* = 7.2 Hz, 2H), 3.85 (s, 2H), 4.82 (s, 1H), 6.9 - 7.4 (m, 13H). ^{13}C NMR ($CDCl_3$): δ 35.62, 39.70, 41.74, 54.53, 126.10, 127.8, 128.6, 138.2, 143.4, 170.9.

9,10-Dihydro-*N*-(3-phenylpropyl)anthracene-10-carboxamide (**78**). Thionyl chloride (2.6 g, 22.0 mmol) was added under N_2 to a stirred solution of compound **43** (1 g, 4.4 mmol) in anhydrous benzene (10 mL). The solution was heated at reflux (2 h), allowed to cool and the excess benzene and thionyl chloride were removed under reduced pressure to provide an oil. The oil obtained was dissolved in anhydrous THF (4 mL) and cooled in an ice bath (0 °C). Phenylpropylamine (1.0 g, 8.8 mmol) was added dropwise into the stirred solution, and the mixture was stirred at rt (2 h). The solvent was removed under reduced pressure to give a white solid. Water (20 mL) was added, and the suspension was extracted with EtOAc (3 × 25 mL). The combined extracts were washed with water, brine and dried ($MgSO_4$). Removal of solvent under reduced pressure gave a crude solid. The resulting amide was purified using medium pressure chromatography, CH_2Cl_2/Acetone

(9:1) to yield **78** (1.15 g, 75%). ^{1}H NMR ($CDCl_3$): 1.63 (m, 2H), 2.46 (t, *J* = 7.2Hz, 2H), 3.15 (q, *J* = 7.2 Hz, 2H), 3.96 (d, *J* = 18.6 Hz, 1H), 4.16 (d, *J* = 18.6 Hz, 1H), 4.82 (s, 1H), 6.9 - 7.4 (m, 13H). ^{13}CNMR ($CDCl_3$): δ 29.2, 33.2, 40.20, 41.7, 54.2, 126.1, 126.8, 128.1, 128.7, 128.9, 138.0, 138.2, 143.4, 170.9.

9,10-Dihydro-*N*-(4-phenylbutyl)anthracene-10-carboxamide (**79**). Thionyl chloride (2.6 g, 22.0 mmol) was added under N_2 to a stirred solution of compound **43** (1 g, 4.4 mmol) in anhydrous benzene (10 mL). The solution was heated at reflux (2 h), allowed to cool and the excess benzene and thionyl chloride were removed under reduced pressure to provide an oil. The oil obtained was dissolved in anhydrous THF (4 mL) and cooled in an ice bath (0 °C). Phenylbutylamine (1.0 g, 8.8 mmol) was added dropwise into the stirred solution, and the mixture was stirred at rt (2 h). The solvent was removed under reduced pressure to give a white solid. Water (20 mL) was added, and the suspension was extracted with EtOAc (3 × 25 mL). The combined extracts were washed with water, brine and dried ($MgSO_4$). Removal of solvent under reduced pressure gave a crude solid. The resulting amide was purified using medium pressure chromatography, CH_2Cl_2/Acetone, (9:1) to yield **79** (1.13 g, 72%). ^{1}H NMR ($CDCl_3$): 1.48 (m, 4H), 2.5 (t, *J* = 7.2 Hz, 2H), 2.7 (t, J = 6.9 Hz, 2H), 3.91 (d, *J* = 18.3 Hz, 1H), 4.12 (d, *J* = 18.3 Hz, 1H), 7.0 - 8.4 (m, 13H). ^{13}C NMR ($CDCl_3$): δ 28.2, 29.2, 35.7, 40.60, 41.7, 54.2, 126.1, 126.8, 128.1, 128.7, 128.6, 138.0, 138.2, 143.4, 170.9.

2-(Bromomethyl)benzaldehyde (81).[212] A solution of 2-(bromomethyl)benzonitrile **80** (5.0 g, 25.5 mmol) in dried CH_2Cl_2 (75 ml) was cooled in an ice-water bath and maintained under an inert atmosphere. A 1.0 M solution of diisobutyl aluminum hydride (26.0 mL, 26.0 mmol) in heptane was added in a dropwise manner over a period of 30 min. The resulting solution was then allowed to warm slowly to rt with stirring in a period of 3 h by removing the ice-water bath. The reaction mixture was cooled again with an ice-bath, and then directly poured into a 1000 mL beaker containing ice (100 g) and a precooled HBr aqueous solution (6.0 N, 100 mL). The resulting mixture was vigorously stirred for 1 h and then extracted with CH_2Cl_2. The combined extracts were washed with 1 N $NaHCO_3$, water, and dried ($MgSO_4$). Evaporation of solvent gave product **81** (4.9 g, 97% yield) as a clear brown liquid. ^{1}H NMR ($CDCl_3$): 4.91 (s, 2H), 7.45 (d, J = 5.4 Hz 1H), 7.52 (d, J = 5.7 Hz, 1H), 7.56 (d, J = 5.4 Hz, 1H), 7.83 (d, J = 5.7 Hz, 1H), 10.23 (s, 1H).

2-((Naphthalen-2-yl)methyl)benzaldehyde (82). 2-naphthylboronic acid (1.5 g, 8.7 mmol) was added to a well stirred solution of **81** (1.0 g, 5.0 mmol) with potassium phosphate (21.2 g, 10.0 mmol) and palladium tetrakistriphenyl (5mol % 0.288 g) in dry THF (20 ml). The reaction mixture was stirred for a while at rt and heated to reflux for 8 h. The reaction mixture was cooled to rt, filtered and washed with CH_2Cl_2 (50 ml). The filtrate was evaporated to obtain a brown oily liquid as product **82** which was further purified by medium pressure column chromatography, petroleum ether/EtOAc (9:1) to

give semi-solid **82** (0.85 g, 62%). ^{1}H NMR ($CDCl_3$): 4.0 (s, 2H), 7.1 - 7.8 (m, 10H), 10.3 (s,1H).

2-((6-Methoxynaphthalen-2-yl)methyl)benzaldehyde (83).

6-methoxy-2-napthylboronic acid (1.5 g, 7.5 mmol) was added to a well stirred solution of **81** (1.0 g, 5.0 mmol) with potassium phosphate (21.2 g, 10.0 mmol) and palladium tetrakistriphenyl (5mol % 0.288 g) in dry THF (20 ml). The reaction mixture was stirred for a 15 min at rt and heated to reflux for 8 h. The reaction mixture was cooled to rt, filtered and washed with CH_2Cl_2 (50 ml). The filtrate was evaporated to obtain a brown oily liquid as product **63** which was further purified by medium pressure column chromatography, petroleum ether/EtOAc (9:1) to give a pale yellow solid (0.9 g, 65%). mp 67 - 70 °C. ^{1}H NMR ($CDCl_3$): 3.9 (s, 3H), 4,58 (s, 2H), 7.1 - 7.9 (m, 10H), 10.3 (s,1H).

2-Amino-1-(2-((naphthalen-2-yl)methyl)phenyl)ethanol (84). Trimethylsilylcyanide (1.05 g, 10.6 mmol) was added dropwise to a well stirred solution of **82** (1.75 g, 7.1 mmol) and ZnI (0.054 g, 0.28 mmol) cooled in an ice bath. The reaction mixture was allowed to warm to rt and then heated to 60 °C for 30 min. The reaction mixture was cooled back to 0 °C and lithium aluminum hydride (0.96 g, 25.32 mmol) was added in a dropwise manner. The reaction mixture was further refluxed for 12 h, cooled to rt, and 1ml water and 1ml NaOH were added. The reaction mixture was then diluted with CH_2Cl_2 (50 ml) and filtered through celite. The filtrate evaporated under reduced pressure

to obtain a red oily liquid which was further purified by medium pressure column chromatography, CH_2Cl_2/MeOH (9:1) to get **84** (0.8 g, 45%). ^{1}H NMR ($CDCl_3$): 1.8 (bs, 2H), 2.64 (m, 2H), 4.1 (s, 2H), 4.7 (m, 1H), 7.0 - 7.8 (m, 10H).

2-Amino-1-(2-((6-methoxynaphthalen-6-yl)methyl)phenyl)ethanol (85).

Trimethylsilylcyanide (0.94 g, 9.49 mmol) was added dropwise to a well stirred solution of **83** (1.75 g, 6.33 mmol) and ZnI (0.048 g, 0.253 mmol) cooled in an ice bath. The reaction mixture was allowed to warm to rt and than heated to 60 °C for 30 min. The reaction mixture was cooled back to 0 °C and lithium aluminium hydride (0.96 g, 25.32 mmol) was added in a dropwise manner. The reaction mixture was further refluxed for 12 h, cooled to rt, and 1 ml water and 1ml NaOH were added. The reaction mixture was then diluted with CH_2Cl_2 (50 ml) and filtered using celite. The filtrate evaporated under reduced pressure to obtain red oily liquid which was further purified by medium pressure column chromatography, CH_2Cl_2/MeOH (9:1) to get **85** (0.75 g, 40%). mp 150 - 153 °C. ^{1}H NMR ($CDCl_3$): 1.75 (bs, 2H), 2.64 (m, 2H), 3.9 (s, 3H), 4.16 (s, 2H), 4.82 (m, 1H), 7.0 - 7.66 (m, 10H).

Methyl 4-benzoylbenzoate (87). To a solution of 4-benzoylbenzoic acid **86** (0.5 g, 2.2 mmol) in methanol (10 mL) was added 0.5 ml of concentrated H_2SO_4 and refluxed for 4 h. The reaction mixture was cooled to rt and solvent was evaporated under vacuum. Water was added to the residue which was extracted with EtOAc (3 × 20 mL). The combined EtOAc extracts were washed with water, brine, and dried ($MgSO_4$). The

solvent was evaporated under reduced pressure to give a yellow oil **87** (0.5 g, 95%). ^{1}H NMR($CDCl_3$): 3.97 (s, 3H), 7.23 - 7.81 (m, 9H); ^{13}C NMR($CDCl_3$): δ 51.8, 60.2, 128.2, 129.2, 130.2, 132.5, 165.8.

(*E,Z*)-Methyl 4-(4-(dimethylamino)-1-phenylbut-1-enyl)benzoate (88).

3-Dimethylaminopropyl triphenylphosphonium bromide (0.847 g, 1.9 mmol) was dissolved in 10 ml of THF and 1.6M *n*-butyllithium (0.133 g, 2.09 mmol) was added dropwise under cooling in a dry ice-acetone bath at -78 °C. The mixture was then stirred for 30 min under ice cooling. A solution of compound **87** (0.475 g, 1.9 mmol) in 10 ml THF was added to the mixture and stirring was continued for 30 min. The reaction mixture was brought to rt and was stirred for another 1h. Brine was added to the reaction mixture and extracted with EtOAc (3 × 20 mL). Extract was washed with water, brine and dried ($MgSO_4$). The solvent was evaporated under reduced pressure to give pale brown oily substance **88** as a mixture of geometrical isomers (*E*/*Z* = 1/2) which was further purified by medium pressure column chromatography, CH_2Cl_2/MeOH (9:1) to obtain **88** (0.53 g 90%). ^{1}H NMR($CDCl_3$): 2.3 (q, *J* = 7.8 Hz, 2H), 2.20 (s, 6H), 2.44 (t, *J* = 6.8 Hz, 2H), 3.92 (s, 3H), 6.19 (t, *J* = 7.8 Hz, 1H), 6.22 (t, *J* = 7.8 Hz, 1H), 7.17 - 7.8.0 (m, 9H); ^{13}C NMR($CDCl_3$): δ 25.06, 44.11, 51.8, 60.2, 126.4, 128.6, 129.2, 165.4.

(*E,Z*)-4-(4-(Dimethylamino)-1-phenylbut-1-enyl)benzoic acid (89).[249] Compound **88** (0.5 g, 1.6 mmol) was dissolved in methanol (5 mL), 1 N NaOH (3 mL) was added and resulting mixture was stirred overnight at rt. 1 N HCl was added to the reaction mixture

and concentrated to dryness. After a $CHCl_3$:MeOH (5:1) mixture (10 mL) was added to the residue, the resulting mixture was stirred for 30 min and filtered with celite. The filtrate was concentrated and purified by column chromatography to obtain a yellow gummy solid. The solid obtained was triturated with ether to yield precipitate of **89** (0.42 g, 89%) which was collected by filtration. ^{1}H NMR (CD_3OD): 1.86 (m, 2H), 2.13 (s, 6H), 2.52 (m, 2H), 6.19 (t, *J* = 7.2 Hz 1H), 6.24 (t, *J* = 7.2 Hz 1H), 7.17 - 7.8.0 (m, 9H); ^{13}C NMR(CD_3OD): δ 25.07, 48.11, 60.8, 115.3, 126.4, 128.6, 130.2, 169.4.

Ethyl 2-(bromomethyl)benzoate (91).[237] A mixture of ethyl 2-methylbenzoate **90** (1.0 g, 6.0 mmol), *N*-bromosuccinimide (1.12 g, 6.3 mmol) and benzoyl peroxide (0.145 g, 0.6 mmol) in 40 mL carbon tetrachloride was heated under reflux for 4 h. The reaction mixture was then cooled to rt with additional cooling using an ice bath for 1 h. The succinimide was separated by filtration and the filtrate was evaporated under vacuum to give **91**. The crude product (purity > 95%) obtained was in quantitative yield and was used as such in next step. ^{1}H NMR($CDCl_3$): 1.45 (t, *J* = 7.5 Hz, 3H), 4.40 (q, *J* = 7.5 Hz, 2H), 4.98 (s, 2H), (7.2 - 8.2 (m, 4H); ^{13}C NMR($CDCl_3$): δ 15.1, 30.9, 62.9, 129.2, 129.6, 130.3, 130.6, 133.8, 139.6, 170.2.

2-(3-Carboxybenzyloxy)phenylacetic acid (93).[237] A mixture of ethyl 2-(4-hydroxyphenyl) acetate (0.73 g, 4.1 mmol), compound **91** (1.0 g, 4.1 mmol), potassium carbonate (2.26 g, 16.4 mmol) and potassium iodide (0.068 g, 0.41 mmol) in 50 mL of butanone was refluxed for 16 h, cooled, and filtered and the filtrate concentrated to one

third its original volume. Water was added to the mixture which was extracted with ether (3 × 25 mL). The ether extract was washed with 5% NaOH and water, dried ($MgSO_4$), filtered and concentrated in vacuum to give an oil (**92**) which was refluxed with potassium hydroxide (3.67 g, 65.6 mmol) in 40 mL of ethanol for 12 h. The mixture was concentrated and the residue was dissolved in water and extracted with ether. Acidification of the aqueous layer provided a yellow solid which was purified by medium pressure column chromatography, Petroleum ether/EtOAc (9:1) to obtain product **93** (0.49 g, 58%). mp 176 - 178 °C. (lit[237] 176 – 178 °C). ^{1}H NMR($CDCl_3$): 3.51 (s, 2H), 5.44 (s, 2H), 6.9 - 8.0 (m, 8H); ^{13}C NMR($CDCl_3$): δ 39.8, 68.1, 114.6, 126.1, 126.1, 127.2, 127.4, 128.8, 130.2, 130.7, 132.2, 139.5, 158.0, 169.1, 174.8.

11-Methylene-6,11-dihydrodibenz[*b,e*]oxepin-2-acetic acid methyl ester (94).[236] To a suspension of methyltriphenylphosphonium bromide (0.6 g, 1.68 mmol) in anhydrous THF (2 mL) was added 2.5 N *n*-BuLi (0.023 g, 0.37 mmol) solution in hexane under N_2 atmosphere at 0 °C, and the mixture was stirred under same conditions for 1 h. A solution of compound **31** (0.1 g, 0.37 mmol) in THF (2 mL) was added and the resulting mixture was stirred at rt for 2 h. After being concentrated, the reaction mixture was diluted with water, washed with ether and then neutralized (10% HCl). The solution was concentrated and the residue was dissolved in MeOH (10 mL) containing *p*-TsOH·H_2O (0.091 g, 0.48 mmol) and refluxed for 2 h. After being concentrated, the reaction mixture was diluted with EtOAc, washed with water and dried ($MgSO_4$). The solvent was evaporated in vacuum to obtain **94** which was purified by medium pressure column chromatography,

hexane/EtOAc (2:1) to obtain **94** as an oil (0.045 g, 45%). ^{1}H NMR($CDCl_3$): 3.60 (s, 2H), 3.73 (s, 3H), 5.19 (s, 2H), 5.32 (s, 1H), 5.74 (s, 1H), 6.82 (d, *J* = 8.4 Hz, 1H), 7.11 (d, *J* = 8.4Hz, 1H), 7.31 - 7.39 (m, 5H); ^{13}C NMR($CDCl_3$): δ 39.85, 51.64, 70.39, 117.09, 119.52, 125.10, 126.14, 126.46, 127.09, 127.68, 128.70, 130.04, 130.48, 133.74, 143.38, 147.61, 154.70, 171.79.

2-[(4-(2-Hydroxyethyl)phenoxy)methyl]benzoic acid (96). A mixture of 4-(2-hydroxyethyl)phenol (3.12 g, 22.62 mmol), ethyl α-bromo-*o*-toluate **91** (5.0 g, 20.56 mmol), potassium carbonate (8.52 g, 61.68 mmol) and potassium iodide (0.34 g, 2.056 mmol) in 75 mL of butanone was refluxed for 16 h, cooled and then filtered. The filtrate was concentrated to one third its original volume. Water (50 mL) was added to the mixture and extracted with ether (3 × 25 mL). Ether extracts were washed with 5% NaOH, water and dried ($MgSO_4$). The ether layer was concentrated in vacuum to obtain the intermediate compound **95** which was refluxed with sodium hydroxide (0.79 g, 19.97 mmol) in 30 ml of methanol for 12 h. The resulting mixture was concentrated and the residue obtained was dissolved in water and extracted with ether (3 × 25 mL). Acidification of aqueous layer provided **96** as an oil (2.0 g, 57%). ^{1}H NMR($CDCl_3$): 2.76 (t, *J* = 7.2 Hz, 2H), 3.72 (t, 7.2 Hz 2H), 5.4 (s, 2H), 6.89 - 8.05 (m, 8H); ^{13}C NMR($CDCl_3$): δ 37.43, 62.50, 67.33, 113.83, 126.39, 126.62, 127.97, 129.02, 130.01, 130.68, 131.44, 138.99, 156.71, 168.34.

2-((4-(2-Acetoxyethyl)phenoxy)methyl)benzoic acid (97). Anhydrous acetyl chloride (0.034 g, 0.44 mmol) was added dropwise to a solution of compound **96** (0.1 g, 0.367 mmol) in anhydrous THF (4 mL). The reaction mixture was stirred at rt overnight. THF was evaporated and the residue obtained was washed with water and extracted with CH_2Cl_2 to obtain the acetylated product **97** (0.109 g, 95%). ^{1}H NMR($CDCl_3$): 2.09 (s, 3H), 2.92 (t, *J* = 7.8 Hz, 2H), 4.29 (t, *J* = 7.8 Hz, 2H), 5.58 (s, 2H), 6.97 - 8.23 (m, 8H); ^{13}C NMR($CDCl_3$): δ 20.57, 33.81, 64.85, 67.82, 114.52, 114.63, 114.70, 126.10, 126.87, 126.91, 129.50, 129.79, 131.27, 133.14, 140.37, 157.01, 170.02, 171.75.

2-(6,11-Dihydro-11-oxo-dibenz[*b,e*]oxepin-2-yl)ethanol (98).[239] Compound **97** (0.2 g, 0.63 mmol) was dissolved in CH_2Cl_2 (4 mL) and trifluroacetic anhydride (0.2 g, 0.95 mmol) was added followed by a catalytic amount of borontrifluoride etherate. The reaction mixture was heated to 40 °C for 4 h and then washed with sat $NaHCO_3$ and water. The organic phase was dried ($MgSO_4$), filtered and concentrated in vacuum to oil. The crude product obtained was subjected to hydrolysis under basic conditions to get an oil that was purified by medium pressure column chromatography, CH_2Cl_2/CH_3OH (9:1) to obtain **98** as an oil (0.145 g, 90%). ^{1}H NMR($CDCl_3$): 2.90 (t, *J* = 6.6 Hz 2H), 3.89 (t, *J* = 6.6 Hz, 2H), 5.18 (s, 2H), 7.0 - 8.1 (m, 7H); ^{13}C NMR($CDCl_3$): δ 37.68, 63.02, 73.16, 120.44, 124.71, 127.36, 128.80, 129.01, 131.29, 131.94, 132.34, 135.19, 135.94, 140.0, 159.58, 190.77.

6,11-Dihydro-11-oxo-dibenz[*b,e*]oxepin-2-ethyloxy(tert-butyl)dimethylsilane (99). To a solution of compound **98** (0.1 g, 0.398 mmol) in DMF (4 mL) at 0 °C under N_2, tert-butyldimethylsilyl chloride (0.065 g, 0.437 mmol) and imidazole (0.040 g, 0.597 mmol) was added. The reaction mixture was then allowed to warm to rt and stirred overnight. Resulting mixture was diluted with an equal volume of chloroform, washed with water and brine. The organic layer was dried ($MgSO_4$), filtered and concentrated in vacuum to give the product **99**. The product obtained was purified by medium pressure column chromatography, 3%CH_3OH/CH_2Cl_2 to yield compound **99** as an oil (0.13 g, 90%). ^{1}H NMR($CDCl_3$): 0.04 (s, 6H), 0.92 (s, 9H), 2.88 (t, *J* = 6.6 Hz, 2H), 3.85 (t, *J* = 6.6 Hz, 2H), 5.2 (s, 2H), 7.0 - 8.1(m, 7H); ^{13}C NMR($CDCl_3$): δ -5.76, 17.91, 25.52, 38.07, 63.82, 73.20, 119.99, 124.57, 127.32, 128.77, 129.0, 131.44, 132.22, 132.66, 135.25, 136.23, 140.16, 159.45, 190.73.

(*E,Z*)-11-[4-Methylpentylidene]-6,11-dihydrobenz[*b,e*]oxepin-2-ethyloxy(tert-butyl)dimethylsilane (100). To a suspension of 4-(methylpentane) triphenylphosphonium bromide (0.927 g, 2.17 mmol) in anhydrous THF (5 mL) was added lithium bis(trimethylsilyl)amide (0.726 g, 4.34 mmol) in a dropwise manner. The resulting orange colored solution was stirred for 30 min at 0 °C and slowly brought to rt and stirring was continued for 1 h. To the deep orange colored solution was then added the compound **99** (0.4 g, 1.085 mmol) dissolved in THF (3 mL) and the reaction mixture was stirred for 12 h at rt. The reaction was then quenched by adding NH_4Cl solution to the mixture. The THF was evaporated and residue was extracted with ethyl acetate (3 ×

25 mL). The solvent was dried ($MgSO_4$), filtered and concentrated in vacuum to yield an oil. This was purified by medium pressure column chromatography, CH_2Cl_2/Petroleum ether (7:3) to give compound **100** as a mixture of geometrical isomers (*E*/*Z* = 3/7) as an oil (0.25 g, 53%). ^{1}H NMR($CDCl_3$): 0.06 (s, 6H), 0.93 (s, 9H), 1.44 (d, *J* = 7.8 Hz, 6H), 1.65 (m, 1H), 2.23 (q, *J* = 8.1 Hz, 2H), 2.48 (q, *J* = 8.1 Hz, 2H), 2.80 (t, *J* = 6.9 Hz, 2H), 3.83 (t, *J* = 6.9 Hz, 2H), 5.2 (s, 2H), 5.72 (t, *J* = 7.5 Hz, 0.7H), 6.06 (t, *J* = 7.5 Hz, 0.3H), 6.8 - 7.4 (m, 7H); ^{13}C NMR($CDCl_3$): δ -5.71, 17.99, 22.14, 25.59, 27.18, 27.32, 38.33, 38.69, 64.42, 70.01, 118.87, 123.54, 125.87, 127.11, 127.62, 128.30, 129.31, 131.45, 133.4, 136.83, 138.34, 145.45, 153.43.

(*E*,*Z*)-(11-[4-Methylpentylidene]-6,11-dihydrobenz[*b*,*e*]oxepin-2-ethyl alcohol (101). To a solution of Compound **100** (0.170 g, 0.389 mmol) in anhydrous THF (4 mL), *tert*-butyl ammonium fluoride (0.203 g, 0.778 mmol) was added in a dropwise manner at 0 °C under N_2. The resultant mixture was stirred for 1 h then allowed to warm to rt and stirring was continued for another 1 h. The reaction mixture was then concentrated in vacuum and the residue obtained was washed with water and extracted with EtOAc (3 × 25 mL) It was purified by medium pressure column chromatography, hexane/EtOAc (1:1) to yield product **101** as an oil (0.119 g, 95%). ^{1}H NMR($CDCl_3$): 0.92 (d, *J* = 6.6 Hz, 6H), 1.44 (q, *J* = 7.8 Hz, 2H), 2.21 (m, *J* = 7.5 Hz, 1H), 2.45 (q, *J* = 7.5 Hz, 2H), 2.81 (t, *J* = 6.3 Hz 2H), 3.84 (q, *J* = 6.3 Hz, 2H), 5.2 (bs, 2H), 5.7 (t, *J* = 7.8 Hz, 0.7H), 6.04 (t, *J* = 7.8 Hz, 0.3H), 6.7 - 7.3 (m, 7H); ^{13}C NMR($CDCl_3$): δ 22.10, 26.75, 27.30, 37.84, 38.43, 63.41, 69.98, 118.27, 123.76, 125.85, 127.01, 127.59, 127.97, 128.61, 129.12, 129.49, 131.43,

133.16, 138.12, 145.38, 153.66. Anal Calcd for ($C_{22}H_{26}O_2 \cdot 0.25\ H_2O$) C, 80.82; H, 8.16 Found: C, 80.49, H, 8.48. ESIMS (+ ve) calcd for $C_{22}H_{26}O_2$ [$(M+H)^+$] 323.19, found 323.26

7.2 Molecular Modeling

Molecular modeling investigations were conducted using the SYBYL 7.1 molecular modeling package (Tripos International, St. Louis, MO) on MIPS R14K- and R16K-based IRIX 6.5 Silicon Graphics Fuel and Tezro workstations. Molecular mechanics-based energy minimizations were performed using the Tripos Force Field with Gasteiger-Hückel charges, a distance-dependent dielectric constant $\varepsilon = 4$ D/Å and a non-bonded interaction cutoff = 8 Å and were terminated at an energy gradient of 0.05 kcal/(mol×Å). The H_1 (P35367) and 5-HT_{2A} (P28233) receptor sequences were retrieved from the ExPASy Proteomics Server (http://www.expasy.org/) and aligned with a profile of several related class A GPCRs (human, dopamine D_3 (P35462), muscarinic cholinergic M_1 (P11229), vasopressin V_{1a} (P37288), adrenergic β_2 (P07550), δ-opioid (P41143), 5-HT_{2A} (P28223), dopamine D_2 (P14416), bovine rhodopsin (P02699) using the ClustalX[159] program. Within ClustalX, the slow-accurate alignment algorithm was used, the BLOSUM matrix series was employed and the gap opening penalty was increased from 10.0 to 15.0 to help maintain the continuity of the transmembrane helical segments. The alignment was carried out in two separate steps as reported by Bissantz, *et al.*[250] Manual adjustment of the ClustalX alignment was required to properly align the disulfide-forming cysteine residues in the e2 loop. The result was an unambiguous alignment in the

transmembrane (TM) helical regions of both the H_1 and 5-HT_{2A} sequences with that of the β_2–adrenoceptor. This alignment, along with a file containing the atomic coordinates of the adrenergic β_2 receptor (PDB ID = 2RH1), was used as input to the MODELLER[162] software package to generate a population of 100 different H_1 or 5-HT_{2A} homology models. Each of these receptors was subsequently energy-minimized. An analogous method was used in the case of homology models generated from bovine rhodopsin as the template. In this case, atomic coordinates of the bovine rhodopsin receptor (PDB ID = 1U19), were used as input to the MODELLER software package.

The automated docking program GOLD version 3.01 (Cambridge Crystallographic Data Centre, Cambridge, UK) was then used to dock diphenhydramine, AMDA (**1**) and the high-affinity matrix compounds **9** and **18** into each of the 100 receptor models. In the case of modeling investigations for the carboxylate- substituted compounds, olopatadine and acrivastine were added to the above set of compounds. Based on the fitness function values, steric and electronic interactions of the docked poses and reported site-directed mutagenesis data, one receptor model was selected to represent the ligand binding site of the H_1 and 5-HT_{2A} receptors. These models were subsequently analyzed using PROCHECK[161] and the ProTable facility with in SYBYL to assess the geometric integrity of various structural elements (bond lengths, torsion angles, etc.) within each receptor. After checks for stereochemical integrity, the receptor models were used for the docking of all the target compounds. Ligand molecules were sketched using SYBYL and energy-minimized using the same parameters as were used for the receptor models. Basic amines were protonated to form ammonium ions. GOLD was

used to dock each ligand structure (using the parameter set defined by the "standard default settings" option) into the final receptor model. Each receptor-ligand complex was then energy-minimized with its best-ranked docking pose.

The HINT scoring function (version 3.11S β) was utilized to explore and visualize hydropathic interactions by analyzing the ligand-receptor complexes generated by the automated docking program GOLD. The interaction scores were calculated for the energy-minimized highest-ranked ligand conformation. The receptors (5-HT_{2A} and H_1) and ligands were partitioned using the "dictionary" and "calculated" methods respectively. The 'All' hydrogen treatment option was employed in the H-bonding model, and hydrogen atoms at unsaturated positions as well as alpha to a heteroatom were considered to participate in H-bonding interactions. The inferred solvent model, which considers the partition of each residue based on its hydrogen count, was selected. The '+20 -NH- SASA' chain H-bond correction option was selected. Intermolecular HINT Tables were calculated for all (hydrophobic and polar) interactions with an interaction output cutoff value of 1.0. Finally, hydrophobic and polar interaction HINT maps were generated separately for a region extending 8 Å beyond the docked ligands.

Literature Cited

Literature Cited

1. Kroeze, W. K.; Roth, B. L. Molecular Biology and Genomic Organization of G Protein-Coupled Receptors. In *The Serotonin Receptors: From Molecular Pharmacology to Human Therapeutics*, Roth, B. L., Ed. Humana Press: 2006; pp 1-38.
2. Jonnakuty, C.; Gragnoli, C. What Do We Know About Serotonin? *J. Cell. Physiol.* **2008,** 217, 301-306.
3. Nichols, D. E.; Nichols, C. D. Serotonin Receptors. *Chem. Rev.* **2008,** 108, 1614-1641.
4. Glennon, R. A.; Dukat, M. Novel Serotonergic Agents: 5-HT_2 - Update 1997. *Serotonin ID Resesarch Alert* **1997,** 2, 107-113.
5. Westkaemper, R. B.; Runyon, S. P.; Bondarev, M. L.; Savage, J. E.; Roth, B. L.; Glennon, R. A. 9-(Aminomethyl)-9,10-dihydroanthracene is a Novel and Unlikely 5-HT_{2A} Receptor Antagonist. *Eur. J. Pharmacol.* **1999,** 380, R5-R7.

6. Nonaka, H.; Otaki, S.; Ohshima, E.; Kono, M.; Kase, H.; Ohta, K.; Fukui, H.; Ichimura, M. Unique Binding Pocket for KW-4679 in the Histamine H_1 Receptor. *Eur. J. Pharmacol.* **1998,** 345, 111-117.

7. Peroutka, S. J.; Howell, T. A. The Molecular Evolution of G Protein-Coupled Receptors: Focus on 5-Hydroxytryptamine Receptors. *Neuropharmacology* **1994,** 33, 319-324.

8. Whitaker-Azmitia, P. M. The Discovery of Serotonin and its Role in Neuroscience. *Neuropsychopharmacology* **1999,** 21, 2S.

9. Rapport, M. M.; Green, A. A.; Page, I. H. Crystalline Serotonin. *Science* **1948,** 108, 329-331.

10. Rapport, M. M.; Green, A. A.; Page, I. H. Serum Vasoconstrictor, Serotonin; Chemical Inactivation. *J. Biol. Chem.* **1948,** 176, 1237-1241.

11. Rapport, M. M. Serum Vasoconstrictor (Serotonin). V. The Presence of Creatinine in the Complex. A Proposed Structure of the Vasoconstrictor Principle. *J. Biol. Chem.* **1949,** 180, 961-969.

12. Rapport, M. M.; Green, A. A.; Page, I. H. Serum Vasoconstrictor (Serotonin). IV. Isolation and Characterization. *J. Biol. Chem.* **1948,** 176, 1243-1251.

13. Erspamer, V.; Asero, B. Identification of Enteramine, the Specific Hormone of the Enterochromaffin Cell System, as 5-Hydroxytryptamine. *Nature* **1952,** 169, 800-801.

14. Twarog, B. M.; Page, I. H. Serotonin Content of some Mammalian Tissues and Urine and a Method for its Determination. *Am. J. Physiol.* **1953,** 175, 157-161.

15. Fitzpatrick, P. F. Tetrahydropterin-Dependent Amino Acid Hydroxylases. *Annu. Rev. Biochem.* **1999,** 68, 355-381.

16. Boadle-Biber, M. C. Regulation of Serotonin Synthesis. *Prog. Biophys. Mol. Bio.* **1993,** 60, 1-15.

17. Molinoff, P. B.; Axelrod, J. Biochemistry of Catecholamines. *Annu. Rev. Biochem.* **1971,** 40, 465-500.

18. Gaddum, J. H.; Picarelli, Z. P. Two Kinds of Tryptamine Receptor. *Br. J. Pharmacol.* **1957,** 12, 323-328.

19. Peroutka, S. J.; Snyder, S. H. Multiple Serotonin Receptors: Differential Binding of [^{3}H]5-Hydroxytryptamine, [^{3}H]Lysrgic Acid Diethylamide and [^{3}H]Spiroperidol. *Mol. Pharmacol.* **1979,** 16, 687-699.

20. Bradley, P. B.; Engel, G.; Feniuk, W.; Fozard, J. R.; Humphrey, P. P.; Middlemiss, D. N.; Mylecharane, E. J.; Richardson, B. P.; Saxena, P. R. Proposals for the Classification and Nomenclature of Functional Receptors for 5-Hydroxytryptamine. *Neuropharmacology* **1986,** 25, 563.

21. Hannon, J.; Hoyer, D. Molecular Biology of 5-HT Receptors. *Behav. Brain. Res.* **2008,** 195, 198-213.

22. Glennon, R. A.; Dukat, M. Serotonin Receptor Subtypes. In *Psychopharmacology: The Fourth Generation of Progress*, Bloom, F. E.; Kupfer, D. J., Eds. Raven Press: New York, 1995; pp 415-429.

23. Glennon, R. A.; Dukat, M. Serotonin receptors and drug affecting serotonergic neurotransmission. In *Foye's principles of medicinal chemistry*, 5th ed.; Williams, D. A.; Lemke, T. L., Eds. Lippincott Wilkins: Baltimore, 2002; pp 315-337.

24. Westkaemper, R. B.; Roth, B. L. Structure and Function Reveals Insights in the Pharmacology of 5-HT Receptor Subtypes. In *The Serotonin Receptors: From Molecular Pharmacology to Human Therapeutics*, Roth, B. L., Ed. Humana Press: Totowa, NJ, 2006; pp 39-58.

25. Ballesteros, J. A.; Shi, L.; Javitch, J. A. Structural Mimicry in G Protein-Coupled Receptors: Implications of the High-Resolution Structure of Rhodopsin for Structure-Function Analysis of Rhodopsin-Like Receptors. *Mol. Pharmacol.* **2001,** 60, 1-19.

26. Suel, G.; Lockless, S. W.; Wall, M. A.; Ranganathan, R. Evolutionarily Conserved Networks of Residues Mediate Allosteric Communication in Proteins. *Nat. Struct. Biol.* **2003,** 10, 59-69.

27. Roth, B. L.; Lopez, E.; Patel, S.; Kroeze, W. Multiplicity of Serotonin Receptors: Useless Diverse Molecules or an Embarrassement of Riches. *The Neuroscientist* **2000,** 6, 252-262.

28. Etienne, N. The 5-HT_{2B} Receptor: A Main Cardio-Pulmonary Target of Serotonin. *J. Soc. Biol.* **2004,** 198, 22-29.

29. Nebigil, C. G. Serotonin 2B Receptor is required for Heart Development. *Proc. Nat. Acad. Sci. USA* **2000,** 97, 9508-9513.

30. Gershon, M. D. Serotonin and its Implication for the Management of Irritable Bowel Syndrome. *Rev. Gastroenterol. Disord.* **2003,** 3, S25-S34.

31. Crowel, M. D. Role of Serotonin in the Pathophysiology of the Irritable Bowel Syndrome. *Br. J. Pharmacol.* **2004,** 141, 1285-1293.

32. Roth, B. L.; Berry, S. A.; Kroeze, W. K.; Willins, D. L.; Kristiansen, K. Serotonin 5-HT_{2A} Receptors: Molecular Biology and Mechanisms of Regulation. *Crit. Rev. Neurobiol.* **1998,** 12, 319-338.

33. Meltzer, H. Y.; Li, Z.; Kaneda, Y.; Ichikawa, J. Serotonin Receptors: Their Key Role in Drugs to Treat Schizophrenia. *Prog. Neuro-Psychopharmacol. Biol. Psych.* **2003,** 27, 1159-1172.

34. Tsai, S. J. Association Study of Serotonin-6 Receptor Variant (C267T) with Schizophrenia and Agressive Behaviour. *Neurosci. Lett.* **1999,** 271, 135-137.

35. Hong, C. J. Association Analysis of the 5-HT(6) Receptor Polymorphism (C267T) in Mood Disorders. *Am. J. Med. Genet.* **1999,** 88, 601-602.

36. Holmes, C. Depression in Alzhimer's Disease: The Effect of Serotonin Receptor Gene Variation. *Am. J. Med. Genet.* **2003,** 119B, 40-43.

37. Tsai, S. J. Association Analysis of the 5-HT_6 Receptor Polymorphism C267T in Alzheimer's Disease. *Neurosci. Lett.* **1999,** 276, 138-139.

38. Buck. K. J. Serotonin 5-HT_2 Receptors and Alcohol: Reward, Withdrawal and Discrimination. *Alcohol. Clin. Exp. Res.* **2004,** 28, 211-216.

39. Heinz, A. Pharmacogenetic Insights to Monoaminergic Dysfunction in Alcohol Dependence. *Psychopharmacology* **2004,** 174, 561-570.

40. Dolan, M.; Anderson, I. M.; Deakin, J. F. Relationship between 5-HT Function and Impulsivity and Aggression in Male Offenders with Personality Disorders. *Br. J. Psychiat.* **2001,** 178, 352-359.

41. Krakowski, M. Violence and Serotonin: Influence of Impulse Control, Affect Regulation, and Social Functioning. *J. Neuropsych. Clin. Neurosci.* **2003,** 15, 294-305.

42. Roth, B. L.; Shapiro, D. A. Insights into the Structure and Function of 5-HT_2 Family Serotonin Receptors Reveal Novel Strategies for Therapeutic Target Development. *Expert Opin. Ther. Targets* **2001,** 5, 685-695.

43. Roth, B. L.; Meltzer, H. The role of Serotonin in Schizophrenia. In *Psychopharmacology: The fourth generation of progress*, Bloom, F.; Kupfer, D., Eds. Raven press: 1995; pp 1215-1227.

44. Miller, K. J. Serotonin 5-HT_{2C} receptor agonists: Potential for the treatment of obesity. *Mol. Interv* **2005,** 5, 282-291.

45. Tecott, L. H.; Sun, L. M.; Akana, S. F.; Strack, A. M.; Lowenstein, D. H.; Dallman, M. F.; Julius, D. Eating Disorders and Epilepsy in mice lacking 5-HT_{2C} Serotonin Receptors. *Nature* **1995,** 374, 542-546.

46. Ochi, T.; Goto, T. The antinociceptive effect induced by FR140423 is mediated through spinal 5-HT_{2A} and 5-HT_3 receptors. *Eur. J. Pharmacol.* **2000,** 409, 167-172.

47. Roth, B. L. *The Serotonin Receptors: From Molecular Pharmacology to Human Therapeutics*. Human Press Inc: 2006; pp 1-617.

48. Roth, B. L.; Williams, D. L.; Kristiansen, K.; Kroeze, W. K. 5-Hydroxytryptamine2 -Family Receptors (5-Hydroxytryptamine2A, 5-Hydroxytryptamine2B, 5-Hydroxytryptamine2C) Where Structure meets Function. *Pharmacol. Ther.* **1998,** 79, 3.

49. Leysen, J. E. 5-HT_2 Receptors. *Curr. Drug Targets CNS Neurol. Disord.* **2004,** 3, 11-26.

50. Sanders-Bush, E.; Fentress, H.; Hazelwood, L. Serotonin 5-HT_2 Receptors: Molecular and Genomic Diversity. *Mol. Interv.* **2003,** 3, 319-330.

51. Westkaemper, R. B.; Glennon, R. A. Application of Ligand SAR, Receptor Modeling and Receptor Mutagenesis to the Discovery and Development of a New Class of 5-HT_{2A} Ligands. *Curr. Top. Med. Chem.* **2002,** 2, 575-598.

52. Visiers, I.; Ebersole, B. J.; Dracheva, S.; Ballesteros, J. A.; Sealfon, S. C.; Weinstein, H. Structural Motifs as Functional Microdomains in G Protein-Coupled Receptors: Energetic Considerations in the Mechanism of Activation of the Serotonin 5-HT_{2A} Receptor by Disruption of the Ionic Lock of the Arginine Cage. *Int. J. Quantum Chem.* **2002,** 88, 65-75.

53. Westkaemper, R. B.; Hyde, E. G.; Choudhary, M. S.; Khan, N.; Gelbar, E. I.; Glennon, R. A.; Roth, B. L. Engineering a Region of Bulk Tolerance in the 5-HT_{2A} Receptor. *Eur. J. Med. Chem.* **1999,** 34, 441-447.

54. Wang, C. D.; Gallaher, T. K.; Shih, J. C. Site-Directed Mutagenesis of the Serotonin 5-Hydroxytryptamine Receptor: Identification of Amino Acids

Necessary for Ligand Binding and Receptor Activation. *Mol. Pharmacol.* **1993,** 43, 931-40.

55. Roth, B. L.; Shoham, M.; Choudhary, M. S.; Khan, N. Identification of Conserved Aromatic Residues Essential for Agonist Binding and Second Messenger Production at 5-HT_{2A} Receptors. *Mol. Pharmacol.* **1997,** 52, 259-266.

56. Braden, M. R.; Nichols, D. E. Assessment of the Roles of Serines 5.43(239) and 5.46(242) for Binding and Potency of Agonist Ligands at the Human Serotonin 5-HT_{2A} Receptor. *Mol. Pharmacol.* **2007,** 7, 1200-1209.

57. Kristiansen, K.; Kroeze, W. K.; Willins, D. L.; Gelber, E. I.; Savage, J. E.; Glennon, R. A.; Roth, B. L. A Highly Conserved Aspartic Acid (Asp 155) Anchors the Terminal Amine Moiety of Tryptamines and is Involved in Membrane Targeting of the 5-HT_{2A} Serotonin Receptor but does not Participate in Activation via a "Salt-bridge Disruption" Mechanism. *J. Pharmacol. Exp. Ther.* **2000,** 293, 735-746.

58. Popa, D.; Lena, C.; Fabre, V.; Prenat, C.; Gingrich, J.; Escourrou, P.; Hamon, M.; Adrian, J. Contribution of 5-HT_2 Receptor Subtypes to Sleep-Wakefulness and Respiratory Control, and Functional Adaptations in Knock-Out Mice Lacking 5-HT_{2A} Receptors. *J. Neurosci.* **2005,** 25, 11231-11238.

59. Fawcett, K. H. M. Anxiety Syndromes and their Relationship to Depressive Illness. *J. Clin. Psychiat.* **1983,** 44, 8-11.

60. Reed, K. The Functional Psychosis: The Schizophrenia and the Major Affective Disorders. In *Lectures in Psychiatry*, Warren, H., Ed. Green Publishers: St. Louis, MO, 1985; pp 182-200.

61. Mayberg, H. S.; Keightley, M.; Mahurin, R. K.; Brannan, S. K. Neuropsychiatric Aspects of Mood and Affective Disorders. In *Neuropsychiatry and Clinical Neurociences*, Yudotsky, S. C.; Hales, R. E., Eds. American Psychiatric Publishing: Wasington DC, 2002; pp 1021-1038.

62. Charnery, D. S. Monoamine Dysfunction and the Pathophysiology and Treatment of Depression. *J. Clin. Psychiat.* **1998,** 59, 11-14.

63. Delgado, P. L.; Moreno, F. A. Role of Norepinephrine in Depression. *J. Clin. Psychiat.* **2000,** 61, 5-12.

64. Stahl, S. M.; Grady, M. M.; Niculescu, R. Developments in Antidepressants. In *Advances in the Management and Treatment of Depression*, Potokar, J.; Thase, M. E., Eds. Informa Health Care: 2003; pp 87-104.

65. Wells, K. B.; Stewart, A.; Hays, R. D.; Burnam, M. A.; Rogers, W.; Daniel, M.; Berry, S.; Greenfield, S.; Ware, J. The Functioning and Wellbeing of Depressed Patients. Results from the Medical Outcomes study. *J. Am. Med. Assoc* **1989,** 262, 914-919.

66. Delgado, P. L.; Chaney, D. S.; Price, L. H.; Aghajanian, G. K.; Landis, H.; Heninger, G. R. Serotonin Function and the Mechanism of Antidepressant Action. Reversal of Antidepressant-Induced Remission by Rapid Depletion of Plasma Tryptophan. *Arch. Gen. Psychiat.* **1990,** 47, 411-418.

67. Kroeze, W. K.; Roth, B. L. The Molecular Biology of Serotonin Receptors: Therapeutic Implications for the Interface of Mood and Psychosis. *Biol. Psychiatry* **1998,** 44, 1128-1142.

68. Peroutka, S. J.; Snyder, S. H. Long-Term Antidepressant Treatment Decreases Spiroperidol-labeled Serotonin Receptor Binding. *Science* **1980,** 210, 88-90.

69. Wirshing, D. A.; Wirshing, W. C. Novel Antipsychotics: Comparison of Weight Gain Liabilities. *J. Clin. Psychol.* **1999,** 60, 358-363.

70. Langer, S. Z. 25 Years Since the Discovery of Presynaptic Receptors: Present Knowledge and Future Perspetives. *Trends Pharmacol. Sci.* **1997,** 18, 95-99.

71. Florella, D.; Rabin, R. A.; Winter, J. C. The Role of the 5-HT_{2A} and 5-HT_{2C} Receptors in the Stimulus Effects of m-Chlorophenylpiperazine. *Psychopharmacology* **1995,** 119, 222-230.

72. Peroutka, S. J.; Snyder, S. H. [3H] Mianserin: Differential Labeling of Serotonin and Histamine Receptors in rat Brain. *J. Pharmacol. Exp. Ther.* **1981,** 216, 142-148.

73. Esposito, E. Serotonin-Dopamine Interaction as a Focus of Novel Antidepressant Drugs. *Curr. Drug Targets* **2006,** 7, 177-185.

74. Nocjar, C.; Roth, B. L.; Pehek, E. A. Localization of 5-HT_{2A} Receptors on Dopamine Cells in Subnuclei of the Midbrain A10 Cell Group. *Neuroscience* **2002,** 111, 163-176.

75. Boess, F. G.; Martin, I. L. Molecular biology of 5-HT Receptors. *Neuropharmacology* **1994,** 33, 275-317.

76. Kennett, G. A.; Wood, M. D.; Bright, F.; Trail, B.; Riley, G.; Holland, V.; Avnella, K. Y.; Stean, T.; Uptona, N.; Bromidge, S.; Forbes, I. T.; Brown, A. M.; Middlemissa, D. N.; Blackburn, T. P. SB 242084, a Selective and Brain Penetrant 5-HT_{2C} Receptor Antagonist. *Neuropharmacology* **1997,** 36, 609-620.

77. Meltzer, H. Y.; Matsubara, S.; Lee, J. C. Classification of Typical and Atypical Antipsychotic Drugs on the Basis of Dopamine D-1, D-2 and Serotonin2 pK_i values. *J. Pharmacol. Exp. Ther.* **1989,** 251, 238-246.

78. Janssen, P. A.; Nimegeers, C. J.; Amouters, F.; Schellenkens, K. H.; Megens, A. A.; Meert, T. F. Pharmacology of Risperidione (R 64,766) A New Antipsychotic with Serotonin-S_2 and Dopamine-D_2 Antagonistic Properties. *J. Pharmacol. Exp. Ther.* **1988,** 244, 685-693.

79. Meltzer, H. Y. Mechanism of Action of Atypical Antipsychotic Drugs. In *Neuropsychopharmacology: The Fifth Generation of Progress*, Davis, K. L.; Charney, D.; Coyle, J. T.; Nemeroff, C., Eds. Raven Press: 2002; pp 819-832.

80. Sanchez, C.; Arnt, J. In Vivo Assesement of 5-HT_{2A} and 5-HT_{2C} Antagonistic Properties of Newer Antipsychotics. *Behav. Pharmacol.* **2000,** 11, 291-298.

81. Sorensen, S. M.; Kehne, J. H.; Fadayel, G. M.; Humphreys, T. M.; Ketteler, H. J.; Sullivan, C. K.; Taylor, V. L.; Schmidt, C. J. Characterization of the 5-HT_2 Receptor Antagonist MDL100907 as a Putative Atypical Antipsychotic: Behavioral, Electrophysiological and Neurochemical Studies. *J. Pharmacol. Exp. Ther.* **1993,** 266, 684-691.

82. Luisa, A. D. 5-HT_{2A} Antagonists in Psychiatric Disorders. *Curr. Opin. Invest. Drugs* **2002,** 3, 106-112.

83. Lieberman, J. A.; Mailman, R. B.; Duncan, G.; Sikich, L.; Chakos, M.; Nichols, D. E.; Kraus, J. E. A Decade of Serotonin Research: Role of Serotonin in treatment of Psychosis. Serotonergic Basis of Antipsychotic Drug Effects in Schizophrenia. *Biol. Psychiatry* **1998,** 44, 1099-1117.

84. Freedman, R. Schizophrenia. *New. Engl. J. Med* **2003,** 349, 1738-1749.

85. Martina, B. C.; Miller, L. S.; Kotzan, J. A. Antipsychotic Prescription Use and Costs for Persons with Schizophrenia in the 1990s: Current Trends and Five year time Series Forecasts. *Schizophr. Res.* **2001,** 47, 281-292.

86. Meltzer, H. Y.; Matsubara, S.; Lee, J., C. Classification of Typical and Atypical Antipsychotic Drugs on the Basis of Dopamine D-1, D-2 and Serotonin2 pK_i values. *J. Pharmacol. Exp. Ther.* **1989,** 251, 238-246.

87. Roth, B. L.; Sheffler, D. J.; Kroeze, W. K. Magic Shotguns Versus Magic Bullets: Selectively Non-Selective Drugs for Mood Disorders and Schizophrenia. *Nat. Rev. Drug Discovery* **2004,** 3, 353-359.

88. Holmes, A.; Lachowich, J. E.; Sibley, D. Phenotypic Analysis of Dopamine Receptor Knockout Mice; Recent Insights into the Functional Specificity of Dopamine Receptor Subtypes. *Neuropharmacology* **2004,** 47, 1117-1134.

89. Meltzer, H. Y. Dopamine and Negative Symptoms in Schizophrenia: Critique of type1- type2- Hypothesis. In *Controversies in Schizophrenia: Changes and Constancies*, Alpert, M., Ed. Guilford press: Newyork, 1985; pp 110-136.

90. Spurlock, G.; Heils, A.; Holmans, P.; Williams, J.; D'souza, U. M.; Cardno, A.; Murphy, K. C.; Jones, L.; Buckland, P. R.; McGuffin, P.; Lesch, K. P.; Owen, M. J. A Family Based Association Study of the T102C Polymorphism in 5-HT_{2A} and Schizophrenia plus Identification of New Polymorphisms in the Promoter. *Mol. Psychiatry* **1998,** 3, 42-49.

91. Sharpley, A. L.; Attenburrow, M. J.; Cowen, P. J. Slow Wave Sleep in Humans: Role of 5-HT_{2A} and 5-HT_{2C} Receptors. *Neuropharmacology* **1994,** 33, 467-471.

92. Gray, J. A.; Roth, B. L. Paradoxical Trafficking and Regulation of 5-HT(2A) Receptors by Agonists and Antagonists. *Brain Res. Bull.* **2001,** 56, 441-451.

93. Di Pietro, N. C.; Seamans, J. K. Dopamine and Serotonin Interactions in the Prefrontal Cortex: Insights on Antipsychotic Drugs and their Mechanism of Action. *Pharmacopsychiatry* **2007,** 40, S27-S33.

94. Garzya, V.; Forbes, I. T.; Gribble, A. D.;Hadley, M. S.; Lightfoot, A. P.; Payne, A. H.; Smith, A. B.; Douglas, S. E.; Cooper, D. G.; Stansfield, I. G.; Meeson, M.; Dodds, E. E.; Jones, D. N. C.; Wood, M.; Reavill, C.; Scorer, C. A.; Worby, A.; Riley, G.; Eddershaw, P.; Ioannou, C.; Donati, D.; Hagana, J. J.; Ratti, E. A. Studies towards the Identification of a New Generation of Atypical Antipsychotic Agents. *Bioorg. Med. Chem. Lett.* **2007,** 17, 400-405.

95. Abrams, J. K.; Johnson, P. L.; Hay-Schmidt, A. Serotonergic Systems Associated with Arousal and Vigilance Behaviours following Administration of Anxiogenic Drugs. *Neuroscience* **2005,** 133, 983-987.

96. Dugovic, C.; Waquier, A.; Leysen, J. E.; Marrannes, R.; Janssen, P. A. J. Functional Role of 5-HT_2 Receptors in the Regulation of Sleep and Wakefulness in the Rat. *Psychopharmacology* **1989,** 97, 436-442.

97. Francon, D.; Decobert, M.; Herve, B.; Griebel, G.; Avenet, P.; Scatton, B.; Fur, G. L. Eplivanserin Promotes Sleep Maintainance in Rats. *Sleep Biol Rhythms* **2007,** 5, A3.

98. Morairity, S. R.; Headley, L.; Flores, J.; Martin, B.; Kilduff, T. S. Selective $5HT_{2A}$ and $5HT_6$ Recptor Antagonists Promote Sleep in Rats. *Sleep* **2008,** 31, 34-44.

99. Adrien, J. The Serotonergic System and Sleep-Wakefulness Regulation. In *Pharmacology of Sleep*, Kales, A., Ed. Springer- Verlag: 1995; pp 91-111.

100. Repka-Ramirez, M. S.; Baraniuk, J. N. Histamine in Health and Disease. In *Histamine and H_1 Antihitamines in Allergic Disease*, second ed.; Simons, F. E., Ed. Marcel Dekker, Inc: New York, 2002; pp 1-26.

101. Macglashan, D. Histamine: A Mediator of Inflammation. *J. Allergy Clin. Immunol.* **2003,** 112, S53-S59.

102. Thurmond, R. L. Gelfand, E. W.; Dunford, P. J. The Role of Histamine H_1 and H_4 Receptors in Allergic Inflammation: The Search for New Antihistamines. *Nat. Rev. Drug. Discovery* **2008,** 7, 41-53.

103. Assanasean, P.; Naclerio, R. M. Antiallergic Anti-Inflammatory Effects of H_1-Antihistamines in Humans. In *Histamine and H_1-Antihistamines in Allergic Disease*, Simons, F. E., Ed. Marcel Dekker, Inc: 2002; Vol. 17, pp 101-139.

104. Akdis, C. A.; Blaser, K. Histamine in the Immune Regulation of Allergic Inflammation. *J. Allergy Clin. Immunol.* **2003,** 112, 15-22.

105. Fung-Leung, W. P.; Thurmond, R. L.; Ling, P.; Karlsson, L. Histamine H_4 Receptor Antagonists: The New antihistamines? *Curr. Opin. Invest. Drugs* **2004,** 5, 1174-1183.

106. Passalacqua, G.; Canonica, G. W. Structure and Classification of H_1-Antihistamines and Overview of their Actvities. In *Histamine and H_1-Antihistamines in Allergic Disease*, Simmons, F. E., Ed. Marcel Dekker, Inc: 2002; Vol. 17, pp 65-100.

107. Timmerman, H. Histamine H_1 Blockers: From Relative Failures to Blockbusters within Series of Analogues. In *Analogue-Based Drug Discovery*, Fischer, J.; Ganellin, C. R., Eds. Wiley-VCH: Weinheim, 2006; pp 401-418.

108. Sangalli, B. C. Role of the Central Histaminergic Neuronal System in the CNS Toxicity of the First Generation H_1-Antagonists. *Prog. Neurobiol.* **1997,** 52, 145-157.

109. Welch, M. J.; Meltzer, E. O.; Simons, F. E. H_1-Antihistamines and the Central Nervous System. In *Histamine and H_1-Antihistamines in Allergic Disease*, 2nd ed.; Simons, F. E., Ed. Marcel Dekker, Inc.: New York, 2002.

110. Walsh, G. M.; Annunziato, L.; Frossard, N.; Knol, K.; Levander, S.; Nicolas, J. M.; Taglialatela, M.; Tharp, M. D.; Tillement, J. P.; Timmerman, H. New Insights into the Second Generation Antihistamines. *Drugs* **2001,** 61, 207-236.

111. Simons, F. E. R.; Simons, K. J. Clinical Pharmacology of New Histamine H_1 Receptor Antagonists. *Clin. Pharmacokinet.* **1999,** 36, 329-352.

112. Fugner, A.; Bechtel, W.; Mierau, J. In Vitro and In Vivo Studies of the Non-Sedating Antihistamine Epinastine. *Arzneium-Forsch. Drug Res.* **1988,** 38, 1446-1453.

113. Singh, H.; Becker, P. M. Novel Therapeutic Usuage of Low-Dose Doxepin Hydrochloride. *Expert Opin. Invest. Drugs* **2007,** 16, 1295-1305.

114. Cusack, B.; Nelson, A.; Richelson, E. Binding of Antidepressant to Human Brain Receptors: Focus on Newer Generation Compounds. *Psychopharmacology* **1994,** 114, 559-565.

115. Sharif, N. A.; Xu, S. X.; Miller, S. T.; Gamache, D. A.; Yanni, J. M. Characterization of the Ocular Antiallergic and Antihistaminic Effects of Olopatadine (AL-4943A), a Novel Drug for Treating Ocular Allergic Diseases. *J.Pharmacol. Exp. Ther.* **1996,** 278, 1252-1261.

116. Brogden, R. N.; McTavish, D. Acrivastine. A Review of its Pharmaclogial Properties and Therapeutic Efficacy in Allergic Rhinitis, Urticaria, and Related Disorders. *Drugs* **1991,** 41, 927-940.

117. Markham, A.; Wagstaff, A. J. Fexofenadine. *Drugs* **1998,** 55, 269-274.

118. Ursin, R. Serotonin and Sleep. *Sleep Med. Rev.* **2002,** 6, 57-69.

119. Jouvet, M. Biogenic Amines and the States of Sleep. *Science* **1969,** 163, 32-41.

120. Teegarden, B. R.; Shamma, H. A.; Xiong, Y. 5-HT_{2A} Inverse-Agonists for the Treatment of Insomnia. *Curr. Top. Med. Chem.* **2008,** 8, 969-976.

121. Dursun, S. M.; Patel, J. K.; Burke, J. G.; Reveley, M. A. Effects of Typical Antipsychotic Drugs and Resperidone on the Quality of Sleep in Patients with Schizophrenia: A Pilot Study. *J. Psychiatry Neurosci.* **1999,** 24, 333-337.

122. Monti, J. M. Pharmacology of the Histaminergic System. In *Pharmacology of sleep*, Kales, A., Ed. Springer-Verlag Berlin Heidelberg: 1995; pp 117-142.

123. Press release from Hypnion, I.; Lexiington, M.

124. Kroeze, W. K.; Hufeisen, S. J.; Popadak, B. A.; Renock, S. M.; Steinberg, S.; Ernsberger, P.; Jayathilake, K.; Meltzer, H. Y.; Roth, B. L. H_1-Histamine Receptor Affinity Predicts Short-Term Weight Gain for Typical and Atypical Antipsychotic Drugs. *Neuropharmacology* **2003,** 28, 519-526.

125. Glennon, R. A.; Westkaemper, R. B.; Bartyzel, P. Medicinal Chemistry of Serotonergic Agents. In *Serotonin Receptor Subtypes*, Peroutka, S. J., Ed. Wiley-Liss: New York, 1991; pp 19-64.

126. Glennon, R. A.; Dukat, M.; El-Burmawy, M.; Law, H.; De Los Angeles, J.; Teitler, M.; King, A.; Herrick-Davis, K. Influence of Amine Substituents on 5-HT_{2A} Versus 5-HT_{2C} Binding of Phenylalkyl- and Indolylalkylamines. *J. Med. Chem.* **1994,** 37, 1929-1935.

127. Glennon, R. A.; Metwally, K.; Dukat, M.; Ismael, A. M.; De Los Angeles, J.; Herndon, J.; Teitler, M.; Khorana, N. Ketanserin and Spiperone as Templates for Novel Serotonin 5-HT_{2A} Antagonists. *Curr. Top. Med. Chem.* **2002,** 2, 539-558.

128. Zhang, W.; Bymaster, F. P. The In Vivo Effects of Olanzapine and other Antipsychotic Agents on Receptor Occupancy and Antagonism of Dopamine D_1,

D_2, D_3, $5HT_{2A}$ and Muscarinic Receptors. *Psychopharmacology* **1999,** 141, 267-278.

129. Kitson, L. S. 5-Hydroxytryptamine (5-HT) Receptor Ligands. *Curr. Pharm. Des.* **2007,** 13, 2621-2637.

130. Rasmussen, S. G. F.; Choi, H. G.; Rosenbaum, D. M.; Kobilka, T. S.; Thian, F. S.; Edwards, P. C.; Burghammer, M.; Ratnala, V. R. P.; Sanishvili, R.; F., F. R.; Scheretler, G. F. X.; Weis, W. I.; Kobilka, B. K. Crystal Structure of the Human β_2Adrenergic G Protein-Coupled Receptor. *Nature* **2007,** 450, 383-387.

131. Rosenbaum, D. M.; Cherezov, V.; Hanson, M. A.; Rasmussen, S. G. F.; Thian, F. S.; Kobilka, T. S.; Choi, H. J.; Yao, X. J.; Weis, W. I.; Stevens, R. C.; Kobilka, B. K. GPCR Engineering Yields High-Resolution Structural Insights into β_2-Adrenergic Receptor Function. *Science* **2007,** 318, 1266-1273.

132. Hopkins, A. L.; Groom, C. R. The Druggable Genome. *Nat. Rev. Drug. Discovery* **2002,** 1, 727-730.

133. Fredriksson, R. L.; Lundin, M. C.; Schioth, H. B. The G Protein-Coupled Receptors in the Human Genome form Five Main Families Phylogenetic Analysis, Paalogon groups, and Fingerprints. *Mol. Pharmacol.* **2003,** 63, 1256-1272.

134. Lagerstrom, M. C.; Schioth, H. B. Structural Diversity of G Protein-Coupled Receptors and Significance for Drug Discovery. *Nat. Rev. Drug. Discovery* **2008,** 7, 339-357.

135. Howard, A. D.; McAllister, G.; Feighner, S. D.; Liu, Q.; Nargund, R. P.; Van der Ploeg, L. H. T.; Patchett, A. A. Orphan G Protein-Coupled Receptors and Natural Ligand Discovery. *Trends Pharmacol. Sci.* **2001,** 22, 132-140.

136. Hermans, E. Biochemical and Pharmacological Control of the Multiplicity of Coupling at G Protein-Coupled Receptors. *Pharmacol. Ther* **2003,** 99, 25-44.

137. Vauquelin, G.; Mentzer, B. V., G Protein-Coupled Receptors. In *G Protein-Coupled Receptors*: *Molecular Pharmacology*, Vauquelin. G. and Mentzer, B., Ed. John Wiley & Sons Ltd: 2007, Ch 4, pp 77-226.

138. Ji, T. H.; Grossman, M.; Ji, I. G Protein-Coupled Receptors I: Diversity of Receptor-Ligand Interactions. *J. Biol. Chem.* **1998,** 273, 17299-17302.

139. Park, P. S.; Lodowski, D. T.; Palczewski, K. Activation of G Protein-Coupled Receptors: Beyond Two-State Models and Tertiary Conformational Changes. *Annu. Rev. Pharmacol. Toxicol.* **2008,** 48, 107-141.

140. Unger, V. M.; Hargrave, P. A.; Baldwin, J. M.; Schertler, G. F. X. Arrangement of Rhodopsin Transmembrane α-helices. *Nature* **1997,** 389, 203-206.

141. Teller, D. C.; Okada, T.; Behnke, C. A.; Palczewski, K.; Stenkamp, R. E. Advances in Determination of a High-Resolution Three-Dimensional Structure of Rhodopsin, a Model of G Protein-Coupled Receptors (GPCRs). *Biochemistry* **2001,** 40, 7761-7772.

142. Palczewski, K.; Kumasaka, T.; Hori, T.; Behnke, C. A.; Motoshima, H.; Fox, B. A.; Le Trong, I.; Teller, D. C.; Okada, T.; Stenkamp, R. E.; Yamamoto, M.;

Miyano, M. Crystal Structure of Rhodopsin: A G Protein-Coupled Receptor. *Science* **2000,** 289, 739-745.

143. Kobilka, B. G Protein-Coupled Receptor Structiure and Activation. *Biochimica et Biophysica Acta.* **2007,** 1768, 794-807.

144. Kobilka, B.; Deupi, X. Conformational Complexity of G Protein-Coupled Recpetors. *Trends Pharmacol. Sci.* **2007,** 28, 387-406.

145. Pin, J. P.; Galvez, T.; Prezeau, L. Evolution, Structure, and Activation Mechanism of Family 3/C G Protein-Coupled Receptors. *pharmacol. Ther.* **2003,** 98, 325-354.

146. Cherezov, V. R.; Rosenbaum, D. M.; Hanson, M. A.; Rasmussen, S. G. F.; Thian, F. S.; Kobilka, T. S.; Choi, H. J.; Kuhn, P.; Weis, W. I.; Kobilka, B. K.; Stevens, R. C. High-Resolution Crystal Structure of an Engineered Human β_2-Adrenergic G Protein-Coupled Receptor. *Science* **2007,** 318, 1258-1265.

147. Parrill, A. L. Crystal Structures of a Second G Protein-Coupled Receptor: Triumphs and Implications. *Chem. Med. Chem.* **2008,** 3, 1021-1023.

148. Helenius, A.; Simons, K. Solubilization of Membrane Proteins by Detergents. *Biochim. Biophys. Acta.* **1975,** 415, 29-79.

149. Ostermier, C.; Michel, H. Crystallization of Membrane Proteins. *Curr. Opin. Struct. Biol.* **1997,** 7, 697-701.

150. Reggio, P. H. Computational Methods in Drug Design: Modelling G Protein-Coupled Receptor Monomrs, Dimers, Oligomers. *AAPS J.* **2006,** 8, E322-336.

151. Patny, A.; Desai, P. V.; Avery, M. A. Homology Modeling of G Protein-Coupled Receptors and Implications in Drug Design. *Curr. Med. Chem.* **2006,** 13, 1667-1691.

152. Stenkamp, R. E.; Teller, D. C.; Palczewski, K. Rhodopsin: A Structural Primer for G Protein-Coupled Receptors. *Arch. Pharm. Chem. Life Sci.* **2005,** 338, 209-216.

153. Ballesteros, J. A.; Weinstein, H. Integrated Methods for the Construction of Three Dimensional Models and Computational Probing of Structure-function Relationships in G Protein-Coupled Receptors. *Methods Neurosci.* **1995,** 25, 366-428.

154. Flanagan, C. A.; Zhou, W.; Chi, L.; Yuen, T.; Rodic, V.; Robertson, D.; Johnson, M.; Holland, P.; Millar, R. P.; Weinstein, H.; Mitchell, R.; Sealfon, S. C. The Functional Microdomain in Transmembrane Helices 2 and 7 Regulates Expression, Activation, and Coupling Pathways of the Gonadotropin-Releasing Hormone Receptor. *J. Biol. Chem.* **1999,** 274, 28880-28886.

155. Ballesteros, J. A.; Jensen, A. D.; Liapakis, G.; Rasmussen, S. G. F.; Shi, L.; Gether, U.; Javitch, J. A. Activation of the β_2-Adrenergic Receptor Involves Disruption of an Ionic Lock between the Cytoplasmic Ends of Transmembrane Segments 3 and 6. *J. Biol. Chem.* **2001,** 276, 29171-29177.

156. Lin, S. W.; Sakmar, T. P. Specific Tryptophan UV-Absorbance Changes are Probes of the Transition of Rhodopsin to Its Active State. *Biochemistry* **1996,** 35, 11149-11159.

157. Shi, L.; Liapakis, G.; Xu, R.; Guarnieri, F.; Ballesteros, J. A.; Javitch, J. A. β_2 Adrenergic Receptor Activation: Modulation of the Proline Kink in Transmembrane 6 by a Rotamer Toggle Switch. *J. Biol. Chem.* **2002,** 277, 40989-40996.

158. Fritze, O.; Filipek, S.; Kuksa, V. P. K.; Hofmann, K. P.; Ernst, O. P. Role of the Conserved NPxxY(x)5, 6F Motif in the Rhodopsin Ground State and during Activation. *Proc. Nat. Acad. Sci. USA* **2003,** 100, 2290-2295.

159. Chenna, R.; Sugawara, H.; Koike, T.; Lopez, R.; Gibson, T. J.; Higgins, D. G.; Thompson, J. D. Multiple Sequence Alignment with the Clustal Series of Programs. *Nucleic Acids Res.* **2003,** 31, 3497-3500.

160. Buck, F.; Meyerhof, W.; Werr, H.; Richter, D. Characterization of N- and C-Terminal Deletion Mutants of the Rat Serotonin HT_2 Receptor in Xenopus Lavis oocytes. *Biochem. Biophys. Res. Comm.* **1991,** 178, 1421-1428.

161. Laskowski, R. A.; MacArthur, M. W.; Moss, D. S.; Thornton, J. M. PROCHECK: A Program to Check the Stereochemical Quality of Protein Structures. *J. Appl. Cryst.* **1993,** 26, 283-291.

162. Fiser, A.; Šali, A. MODELLER: Generation and Refinement of Homology-Based Protein Structure Models. In *Methods in Enzymology: Macromolecular Crystallography: Part D*, Carter, C. W. J.; Sweet, R. M., Eds. 2003; Vol. 374, pp 461-491.

163. Kellogg, G., E.; Semus, S., F.; Abraham, D. J. HINT: A New Method of Empirical Hydrophobic Field Calculation for CoMFA. *J. Comput.-Aided Mol. Des.* **1991,** 5, 545-552.

164. Jones, G.; Willett, P.; Glen, R. C.; Leach, A. R.; Taylor, R. Development and Validation of a Genetic Algorithm for Flexible Docking. *J. Mol. Biol.* **1997,** 267, 727-748.

165. Mooij, W. T. M.; Verdonk, M. L. General and Targeted Statistical Potentials for Protein-Ligand Interactions. *Proteins: Struc. func.Bioinf.* **2005,** 61, 272-287.

166. Hougha, L. B. Cellular Localization and Possible Functions for Brain Histamine: Recent Progress. *Prog. Neurobiol.* **1988,** 30.

167. Blaazer, A. R.; Smid, P.; Kruse, C. G. Structure-Activity Relationships of Phenylalkylamines as Agonist Ligands for 5-HT(2A) Receptors. *Chem. Med. Chem* **2008,** 3, 1299-1309.

168. Bubar, M. J.; Cunningham, K. A. Serotonin 5-HT_{2A} and 5-HT_{2C} Receptors as Potential Targets for Modulation of Psychostimulant use and Dependence. *Curr. Top. Med. Chem.* **2006,** 6, 1971-1985.

169. Sanger, D. J.; Soubrane, C.; Scatton, B. New Perspectives for the Treatment of Disorders of Sleep and Arousal. *Ann. Pharm. Fr.* **2007,** 65, 268-274.

170. Runyon, S. P.; Mosier, P. D.; Roth, B. L.; Glennon, R. A.; Westkaemper, R. B. Potential Modes of Interaction of 9-Aminomethyl-9,10-dihydroanthracene (AMDA) Derivatives with the 5-HT_{2A} Receptor: A Ligand Structure-Affinity

Relationship, Receptor Mutagenesis and Receptor Modeling Investigation. *J. Med. Chem.* **2008,** 51, 6808-6828.

171. Shapiro, D. A.; Kristiansen, K.; Kroeze, W. K.; Roth, B. L. Differential Modes of Agonist Binding to 5-Hydroxytryptamine$_{2A}$ Serotonin Receptors Revealed by Mutation and Molecular Modeling of Conserved Residues in Transmembrane Region 5. *Mol. Pharmacol.* **2000,** 58, 877-886.

172. Westkaemper, R. B.; Dukat, M.; Glennon, R. A. Molecular Modeling of Drug-Receptor Interactions using a 5-HT$_2$ Receptor Model. *Med. Chem. Res.* **1992,** 1, 401-408.

173. Westkaemper, R. B.; Runyon, S. P.; Savage, J. E.; Roth, B. L.; Glennon, R. A. Exploring the Relationship Between Binding Modes of 9-(Aminomethyl)-9,10-dihydroanthracene and Cyproheptadine Analogues at the 5-HT$_{2A}$ Serotonin Receptor. *Bioorg. Med. Chem. Lett.* **2001,** 11, 563-566.

174. Runyon, S. P.; Savage, J. E.; Taroua, M.; Roth, B. L.; Glennon, R. A.; Westkaemper, R. B. Influence of Chain Length and *N*-Alkylation on the Selective Serotonin Receptor Ligand 9-(Aminomethyl)-9,10-dihydroanthracene. *Bioorg. Med. Chem. Lett.* **2001,** 11, 655-658.

175. Peddi, S.; Roth, B. L.; Glennon, R. A.; Westkaemper, R. B. Structural Determinants for high 5-HT$_{2A}$ Receptor Affinity of Spiro[9,10-dihydroanthracene]-9,30-pyrrolidine (SpAMDA). *Bioorg. Med. Chem. Lett.* **2004,** 14, 2279-2283.

176. Parmentier, R.; Ohtsu, H.; Djebbara-Hannas, Z.; Valatx, J.-L.; Watanabe, T.; Lin, J.-S. Anatomical, Physiological, and Pharmacological Characteristics of Histidine Decarboxylase Knock-Out Mice: Evidence for the Role of Brain Histamine in Behavioral and Sleep–Wake Control. *J. Neurosci.* **2002,** 22, 7695-7711.

177. Harms, A. F.; Hespe, W.; Nauta, W. T.; Rekker, R. F.; Timmerman, H.; de Vries, J. Diphenhydramine Derivatives: Through Manipulation toward Design. In *Drug Design*, Ariëns, E. J., Ed. Academic Press: New York, 1975; Vol. 6, pp 1-80.

178. Zhang, M.-Q.; Leurs, R.; Timmerman, H. Histamine H_1-Receptor Antagonists. In *Burger's Medicinal Chemistry and Drug Discovery*, 5th ed.; Wolff, M. E., Ed. John Wiley & Sons: New York, 1997; Vol. 5, pp 495-559.

179. Casy, A. F. Chemistry and Structure-Activity Relationships of Synthetic Anti-Histamines. In *Histamine and Anti-Histaminics*, Rocha e Silva, M., Ed. Springer: Berlin, 1978; Vol. 18 pt. 2, pp 215-228.

180. Nauta, W. T.; Rekker, R. F. Structure-Activity Relationships of H_1 Receptor Antagonists. In *Histamine and Anti-Histaminics*, Rocha e Silva, M., Ed. Springer: Berlin, 1978; Vol. 18 pt. 2, pp 234-239.

181. Duarte, C. D.; Barreiro, E. J.; Fraga, C. A. M. Privileged Structures: A Useful Concept for the Rational Design of New Lead Drug Candidates. *Mini-Rev. Med. Chem.* **2007,** 7, 1108-1119.

182. Allaby, R. G.; Woodwark, M. Phylogenomic Analysis Reveals Extensive Phylogenetic Mosaicism in the Human GPCR Superfamily. *Evol. Bioinform.* **2007,** 3, 155-168.

183. The Ballesteros-Weinstein residue index (see Ballesteros, J. A.; Weinstein, H. Methods Neurosci. 1995, 25, 366) is used throughout this work to identify residues at specific positions within the transmembrane helical (TM) regions. Individual amino acids are specified by their one-letter residue abbreviation and primary sequence position followed by the Ballesteros-Weinstein index as a superscript.

184. Javitch, J. A.; Ballesteros, J. A.; Weinstein, H.; Chen, J. A Cluster of Aromatic Residues in the Sixth Membrane-Spanning Segment of the Dopamine D_2 Receptor is Accessible in the Binding-Site Crevice. *Biochemistry* **1998,** 37, 998-1006.

185. Barton, G. J. ALSCRIPT: A Tool to Format Multiple Sequence Alignments. *Protein Eng.* **1993,** 6, 37-40.

186. Kellogg, G., E.; Abraham, D., J. Hydrophobicity: is $LogP_{O/W}$ more than the Sum of its Parts? *Eur. J. Med. Chem.* **2000,** 35, 651-661.

187. Jongejan, A.; Leurs, R. Delineation of Receptor-Ligand Interactions at the Human Histamine H_1 Receptor by a Combined Approach of Site-Directed Mutagenesis and Computational Techniques - or -How to Bind the H_1 Receptor. *Arch. Pharm. Chem. Life Sci.* **2005,** 338, 248-259.

188. Kiss, R.; Kovári, Z.; Keseru, G. M. Homology Modelling and Binding Site Mapping of the Human Histamine H_1 Receptor. *Eur. J. Med. Chem* **2004,** 39, 959-967.

189. Wieland, K.; Ter Laak, A. M.; Smit, M. J.; Kühne, R.; Timmerman, H.; Leurs, R. Mutational Analysis of the Antagonist-Binding Site of the Histamine H_1 Receptor. *J. Biol. Chem.* **1999,** 274, 29994-30000.

190. Almaula, N.; Ebersole, B. J.; Zhang, D.; Weinstein, H.; Sealfon, S. C. Mapping the Binding Site Pocket of the Serotonin 5-Hydroxytryptamine$_{2A}$ Receptor. Ser$^{3.36(159)}$ Provides a Second Interaction Site for the Protonated Amine of Serotonin but not of Lysergic Acid Diethylamide or Bufotenine. *J. Biol. Chem.* **1996,** 271, 14672-14675.

191. Becker, H. D.; Soerensen, H. S., K. Photochemical Isomerization and Dimerization of 1-(9-anthryl)-2-nitroethylene. *J. Org. Chem.* **1986,** 51, 3223-3226.

192. Rabideau, P. W., Wetzel, D. M., Young, D.M. Metal-Ammonia Ring Reduction of Aromatic Carboxylic Acid Esters. *J. Org. Chem.* **1984,** 49, 1544-1549.

193. Lan, P.; Berta, D.; Porco, J. A., Jr.; South, M. S.; Parlow, J. J. Polymer-Assisted Solution-Phase (PASP) Suzuki Couplings Employing an Anthracene-Tagged Palladium Catalyst. *J. Org. Chem.* **2003,** 68, 9678-9686.

194. Lee, H.; Harvey, R. G. Synthesis of Cyclopentanobenz[*a*]anthracene Compounds Related to Carcinogenic Benz[*a*]anthracene and Cholanthrene Hydrocarbons. *J. Org. Chem.* **1990,** 55, 3787-3791.

195. Bhattacharyya, S. Reductive Alkylations of Dimethylamine Using Titanium (IV) Isopropoxide and Sodium Borohydride: An Effecient, Safe, and Convinient

Method for the Synthesis of *N*,*N*-Dimethylated Tertiary Amines. *J. Org. Chem.* **1995,** 60, 4928-4929.

196. Becker, H. M.; Hansen, L.; Anderson, K. Synthesis and Photochemical Isomerization of 1,2-Di-9-anthrylethanol and 1,2-Di-9-anthylethanone. *J. Org. Chem.* **1986,** 51, 2956-2961.

197. Daub, G. H.; Doyle, W. C. The Monocyanoethylation of Anthrone. An Improved Synthesis of -9-(Anthranyl)-propionic Acid and -(9,10-Dihydro-9-anthranyl)-propionic acid. *J. Org. Chem.* **1952,** 74, 4449-4450.

198. Borch, R. F.; Hassid, A. I. A New Method for the Methylation of Amines. *J. Org. Chem.* **1972,** 37, 1673-1674.

199. Jones, G.; Maisey, R. F.; Somerville, A. R.; Whittle, B. A. Substituted 1,1-Diphenyl-3-aminoprop-1-enes and 1,1-Diphenyl-3-aminopropanes as Potential Antidepressant Agents. *J. Med. Chem.* **1971,** 14, 161-164.

200. Clausen, R. P.; Moltzen, E. K.; Perregaard, J.; Lenz, S. M.; Sanchez, C.; Falch, E.; Frølund, B.; Bolvig, T.; Sarup, A.; Larsson, O. M.; Schousboe, A.; Krogsgaard-Larsen, P. Selective Inhibitors of GABA Uptake: Synthesis and Molecular Pharmacology of 4-*N*-Methylamino-4,5,6,7-tetrahydrobenzo[*d*]isoxazol-3-ol Analogues. *Bioorg. Med. Chem.* **2005,** 13, 895-908.

201. Elz, S. K., K.; Pertz, H. H. D., H.; TerLaak, A. M.; Khne, R. S., W. Histaprodifens: Synthesis, Pharmacological in Vitro Evaluation, and Molecular

Modeling of a New Class of Highly Active and Selective Histamine H_1-Receptor Agonists. *J. Med. Chem.* **2000,** 43, 1071-1084.

202. Miyano, S.; Tatsuoka, T.; Suzuki, K.; Imao, K.; Satoh, F.; Ishihar, T.; Hirotsu, I.; Kihara, T.; Hatta, M.; Horikawa, Y.; Sumoto, K. The Synthesis and Antilipidperoxidation Activity of 4,4-Diarylbutylamines and 4,4-Diarylbutanamides. *Chem. Pharm. Bull* **1990,** 38, 1570-1574.

203. Rashid, M.; Manivet, P. Identification of Binding Sites and Selectivity of Sarprogrelate, a novel 5-HT_2 Antagonist, to Human 5-HT_{2A}, 5-HT_{2B} and 5-HT_{2C} Receptor Subtypes by Molecular Modeling. *Life sciences* **2003,** 73, 193-207.

204. Dewkar, G. K.; Peddi, S.; Mosier, P. D.; Roth, B. L.; Westkaemper, R. B. Methoxy-substituted 9-Aminomethyl-9,10-dihydroanthracene (AMDA) Derivatives Exhibit Differential Binding Affinities at the 5-HT_{2A} Receptor. *Bioorg. Med. Chem. Lett.* **2008,** 18, 5268-5271.

205. Shah, J. R.; Mosier, P. D.; Westkaemper, R. B. A Synthesis, Structure-Affinity Relationship and Modeling of AMDA Analogs at 5-HT_{2A} and H_1 Receptors: Structural Factors Contributing to Selectivity. *Bioorg. Med. Chem* **2009,** submitted.

206. Rekker, R. F. The Predective Merits of Antihistamine-QSAR studies. In *Strategy in Drug Research*, Keverling Buisman, J., Ed. 1982; pp 315-336.

207. Zhong, W. G., J. P.; Zhang, Y.;Li, L.; Lester, H. A.; Dougherty, D. A. From ab initio quantum Mechanics to Molecular Neurobiology: A cation-Π binding site in the Nicotinic Receptor. *Proc. Nat. Acad. Sci. USA* **1998,** 95, 12088-12093.

208. Scopes, D. I.; Barrio, J. R.; Leonard, N. J. Defined Dimensional Changes in Enzyme Cofactors: Fluroscent "Stretched-Out" Analogs of Adenine Nucleotides. *Science* **1977,** 195, 296-298.

209. Reddy, S.; Pachaiyappan, B.; Nural, H. F.; Cheng, X.; Yuan, H.; Lankin, D. V.; Abdul-Hay, S. A.; Thatcher, R. J.; Shen, Y.; Kozikowski, A. P.; Petukhov, P. A. Molecular Modeling, Synthesis, and Activity Studies of Novel Biaryl and Fused-Ring BACE1 Inhibitors. *Bioorg. Med. Chem. Lett.* **2009,** 19, 264-274.

210. Campiani, G.; Ramunno, A.; Fiorini, I.; Nacci, V.; Morelli, E.; Novellino, E.; Goegan, M.; Mennini, T.; Sullivan, S.; Zisterer, D. M.; Williams, C. D. Synthesis of New Molecular Probes for Investigation of Steroid Biosynthesis Induced by Selective Interaction with Peripheral Type Benzodiazepine Receptors (PBR). *J. Med. Chem.* **2002,** 45, 4276-4281.

211. Besada, P.; Mamedova, L.; Thomas, C. J.; Costanzia, S.; Jacobson, K. A. Design and Synthesis of New Bicyclic Diketopiperazines as Scaffolds for Receptor Probes of Structurally Diverse Functionality. *Org. Biomol. Chem* **2005,** 3, 2016-2025.

212. Zhang, X.; Lippard, J. S. Synthesis of PDK, A Novel Porphyrin-Linked Dicarboxylate Ligand. *J. Org. Chem.* **2000,** 65, 5298-5305.

213. Glennon, R. A. Strategies for the Development of Selective Serotonergic Agents. In *The Serotonin Receptors: From Molecular Pharmacology to Human Therapeutics*, Roth, B. L., Ed. Humana press: Totawa, NJ, 2006; pp 91-142.

214. Zhang, J.; Xiong, B.; Zhen, X.; Zhang, A. Dopamine D_1 Receptor Ligands: Where are we now and Where are we Going. *Med. Res. Rev.* **2009,** 29, 272-294.

215. Fredholm, B. B.; Hokfelt, T.; Milligan, G. G Protein-Coupled Receptors: An update. *Acta. Physiol* **2007,** 190, 3-7.

216. Jacoby, E. Designing Compound Libraries Targeting GPCRs. *Ernst Schering Found Symp Proc.* **2006,** 2, 93-103.

217. Schwartz, T.; Rosenkilde, M. M. Is there a 'Lock' for all Agonist 'Keys' in 7TM Recptors? *Trends Pharmacol. Sci.* **1996,** 17, 213-216.

218. Strader, C. D.; Sigal, I. S.; Register, R. B.; Candelor, M. R.; Rands, E.; Dixon, R. A. Identification of Residues required for Ligand Binding to the β_2-Adrenergic Receptor. *Proc. Nat. Acad. Sci. USA* **1987,** 84, 4384-4388.

219. Ohta, K.; Hayashi, H.; Mizguchi, H.; Kagamiyama, H.; Fujimoto, K.; Fukui, H. Site-Directed Mutagenesis of the Histamine H_1 receptor roles of Aspartic acid 107, Aspargine198, Threonine194. *Biochem. Biophys. Res. Comm.* **1994,** 203, 1096-1101.

220. Yan, F. M., P. D.; Westkaemper, R. B.; Stewart, J. Z., J. K.; Vortherms, T. A. S., D. J.; Roth, B. L. Identification of the Molecular Mechanisms by Which the Diterpenoid Salvinorin A Binds to k-Opioid Receptors. *Biochemistry* **2005,** 44, 8643-8651.

221. Ho, B. Y.; Karschin, A.; Branchek, T.; Davidson, N.; Lester, H. A. The Role of Conserved Aspartate and Serine Residues in ligand Binding and in function of the

5-HT_{1A} Receptor: A Site-Directed Mutation Study. *FEBS Lett.* **1992,** 312, 259-262.

222. Page, K. M.; Curtis, C. A.; Jones, P. G.; Hulme, E. C. The Functional Role of the Binding Site Aspartate in Muscarinic Acetylcholine Receptors, Probed by Site-Directed Mutagenesis. *Eur. J. Pharmacol.* **1995,** 289, 429-437.

223. Lavander, S.; Stahle-Backdahl, M.; Hagermark, O. Peripheral Antihistamine and Sedative Effects of Single and Continuous Doses of Cetrizine and Hydroxyzine. *Eur. J. Clin. Pharmacol.* **1991,** 41, 435-439.

224. Zhang, M. Q.; Ter Laak, A. M.; Timmerman, H. Structure-Activity Relationships within a Series of Analogues of the Histamine H_1-Antagonist Terfenadine. *Eur. J. Med. Chem.* **1993,** 28, 165-173.

225. Ter Laak, A. M.; Tsai, R. S.; Carrupt, P. A.; Testa, B.; Timmeman, H. Lipophilicity and Hydrogen Bonding Capacity of H_1-Antihistaminic Agents in Relation to their Central Sedative Side Effects. *Eur. J. Pharm. Sci.* **1994,** 2, 373-384.

226. Timmeman, H. Why are Non-Sedating Antihistamines Non-Sedating? *Clin. Exp. Allergy* **1999,** 29, 13-18.

227. Leurs, R.; Martine, J. S.; Tensen, C. P.; Ter Laak, A. M.; Timmerman, H. Site-Directed Mutagenesis of the Histamine H_1 Receptor Reveals a Selective Intercation of Asparagine207 with subclass of H_1 Receptor Agonists. *Biochem. Biophys. Res. Comm.* **1994,** 201, 295-301.

228. Leurs, R.; Smit, M. J.; Meeder, R.; Terlaak, A. M.; Timmerman, H. Lysine [200] located in the Fifth Transmembrane Domain of Histamine H_1 Receptor Interacts with Histamine but not with all H_1 Agonists. *Biochem. Biophys. Res. Comm.* **1995,** 214, 110-117.

229. Ter Laak, A. M.; Timmerman, H.; Leurs, R.; Nederkoorn, P. H. J.; Smith, J. M.; Kelder, G. M. D. Modelling and Mutation Studies on the Histamine H_1-Receptor Agonist Binding Site Reveal Different Binding Modes for H_1-Agonist: Asp116(TM3) has a Constitutive Role in Receptor Stimulation. *J. Comp. Aided. Mol. Des* **1995,** 9, 319-330.

230. GIillard, M.; Perren, V. C.; Moguilevsky, N.; Massingham, R.; Chatelainc, P.; Schunackb, W.; Timmerman, H.; Leurs, R. Binding Characteristics of Cetirizine and Levocetirizine to Human H_1 Histamine Receptors: Contribution of Lys[191] and Thr[194]. *Mol. Pharmacol.* **2002,** 61, 391-399.

231. Andrews, P. R.; Craik, D. J.; Martin, J. L. Functional Group Contributions to Drug-Receptor Interactions. *J. Med. Chem.* **1984,** 27, 1648-1657.

232. Jones, G.; Willett, P.; Glen, R. C. Molecular Recognition of Receptor Sites using a Genetic Algorithm with a Description of Desolvation. *J. Mol. Biol.* **1995,** 245, 43-53.

233. Ryouichi, N.; Izuka, T.; Ishii, T., (Japan). Amide Derivatives and the Synthesis of Intemediates Thereof. U.S. Patent 09/171521, 2000.

234. Wiktelius, D.; Luthman, K. Taking Control of P1, P1' and Double Bond Stereochemistry in the Synthesis of Phe-Phe (E)-Alkene Amide Isostere Dipeptidomimetics. *Org. Biomol. Chem.* **2007,** 5, 603-605.

235. Yoshioka, T.; Kitagawa, M.; Oki, M.; Kubo, S.; Tagawa, H.; Ueno, K. Non-Steroidal Antiinflammatory Agents. 2. Derivatives/Analogues of Dibenz[b,e]oxepin-3-acetic acid. *J. Med. Chem.* **1978,** 21, 633-639.

236. Ohshima, E.; Otaki, S.; Sato, H.; Kumazawa, T.; Obase, H.; Ishii, A.; Omori, K.; Hirayama, N. Synthesis and Antiallergic Activity of 11-(Aminoalkylidene)-6,11-dihydrodibenz[b,e]oxepin Derivatives. *J. Med. Chem.* **1992,** 35, 2074-2084.

237. Aultz, D. E.; Helsley, G. C.; Hoffmann, D.; Mcfadden, A. R. Dibenz[b,e]oxepinalkanoic Acids as Nonsteroidal Antiinflammatory Agents. 1. 6,11-Dihydro-11-oxodibenz[b,e]oxepin-2-acetic acids. *J. Med. Chem.* **1977,** 20, 66-70.

238. Meyers, A. I.; Temple, D. L.; Haidukewych, D.; Mihelich, E. D. Oxazolines. XI. Synthesis of Functional Aromatic and Aliphatic Acids. A Useful Protecting Group for Carboxylic acids against Grignard and Hydride Reagents. *J. Org. Chem.* **1974,** 39, 2787-2793.

239. Hamer, R. R.; Tegeler, J. J.; Kurtz, E. S.; Allen, R. C.; Bailey, S. C.; Elliott, M. M.; Hellyer, L.; Helsley, G. C.; Przekop, P.; Freed, B. S.; White, J.; Martin, L. L. Dibenzoxepinone Hydroxylamines and Hydroxamic acids: Dual Inhibitors of Cyclooxygenase and 5-Lipoxygenas with Potent Topical Antiinflammatory Activity. *J. Med. Chem.* **1996,** 39, 246-252.

240. Corey, E. J.; Venkateswarlu, A. Protection of Hydroxyl Groups as Tert-butyldimethylsilyl Derivatives. *J. Am. Chem. Soc.* **1972,** 94, 6190-6191.

241. Missio, L. J.; Comasseto, J. V. Enantioselective Synthesis of (−)-g-Jasmolactone. *Tetrahedron, Asymmetry* **2000,** 11, 4609-4615.

242. Zhao, M. M.; Li, J.; Mano, E.; Song, Z. J.; Tschaen, D. M. Oxidation of Primary Alcohols to Carboxylic Acids with Sodium Chlorite Catalyzed by Tempo and Bleach: 4-Methoxyphenylacetic acid. *Org. Syn* **2005,** 81, 195.

243. Gajewski, J. J.; Gortva, A. M. Bimolecular Reactions of 3-Methylene-l,4-cyclohexadiene (p-Isotoluene), 5-Methylene-l,3-cyclohexadiene (o-Isotoluene), 1 -Methylene-1,4-dihydronaphthalene (Benzo-p -isotoluene), and 9-Methylene-9,l0-dihydroanthracen (Dibenzo-p-isotoluene). *J. Org. Chem.* **1989,** 54, 373-379.

244. May, E. L., Mosettig, E. Studies in Anthracne Series. III. Amino Ketones derived from 9-Acetylanthracene. *J. Am. Chem. Soc.* **1948,** 70, 686-688.

245. Vaughan, W. R.; Yoshimine, M. Studies in the Dibenzobicyclo[2.2.2]octadiene system. *J. Org. Chem.* **1957,** 22, 528-532.

246. Gensler, W. J.; Rockett, J. C. Friedel-Crafts reaction of 1-benzenesulfonyl-2-bromomethylethyleneimine and benzene. *J. Am. Chem. Soc.* **1955,** 77, 3262-3264.

247. Blank, B.; Zuccarelo, W. A.; Cohen, S. R.; Frishmuth, G. J.; Scaricaciottoli, D. Synthesis and Adrenocortical Inhibiting Activity of Substituted Diphenylalkyamines. *J. Med. Chem.* **1969,** 12, 271-276.

248. Hulinska, H.; Polivka, C.; Jilek, J. Sindelar, K.; Holubek, J. Svatek, E.; Matousova, O. Budenski, M.; Frycova, H. Protiva, M. *Collect. Czech. Chem. Commun.* **1988,** 53, 1820.

249. Ryouichi, N.; Takao, I.; Takeo, I. Novel Amide Derivatives and Intermediates for the Synthesis Thereof. U. S. Patent 6069149, 1998.

250. Bissantz, C.; Bernard, P.; Hilbert, M.; Rognan, D. Protein-Based Virtual Screening of Chemical Databases. II. Are Homology Models of G-Protein Coupled Receptors Suitable Targets? *Proteins* **2003,** 50, 5-25.

VITA

Jitesh R Shah was born on 12th March, 1980 in Mumbai, India and is an Indian citizen. He obtained his Master's degree in Pharmaceutical Chemistry and Bachelor's degree in Pharmacy from K. M. Kundnani College of Pharmacy, University of Mumbai, India. He worked as an analytical research scientist at Johnson & Johnson Ltd, Mumbai, India between 2003 and 2004. He began graduate studies in the Department of Medicinal Chemistry at Virginia Commonwealth University, in Richmond, USA in August 2004.